

SELECTED  
NOV 13 1995  
F

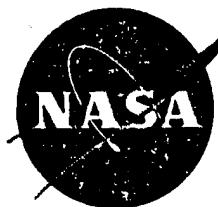
# Cornell University



IMPACT ON MULTILAYERED COMPOSITE PLATES

by

B.S. Kim and F. C. Moon



April, 1977

Final Report NASA CR 135247

19951109 069

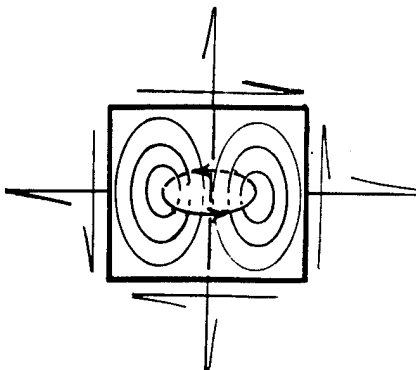
# Theoretical and Applied Mechanics

PLASTEC  
CLASSIFIED

2000  
BILL

DISTRIBUTION STATEMENT A  
Approved for public release  
Distribution Unlimited

Thurston Hall  
Ithaca, New York



DTIC QUALITY INSPECTED 5

IMPACT ON MULTILAYERED COMPOSITE PLATES

by

B.S. Kim and F. C. Moon



April, 1977

Final Report NASA CR 135247

Accession For	
NTIS	Classified <input checked="" type="checkbox"/>
DTIC	TAB <input type="checkbox"/>
Unclassified <input type="checkbox"/>	
Justification	
By DTIC AI memo	
Distribution / 11-2-95	
Availability Codes	
Dist	Avail and/or Special
A-1	

1. Report No. NASA CR135247	2. Government Accession No.	3. Recipient's Catalog No.	
4. Title and Subtitle Impact on Multi layered Composite Plates		5. Report Date 4/1977	
7. Author(s) B.S. KIM and F.C. MOON		6. Performing Organization Code	
9. Performing Organization Name and Address Department of Theoretical and Applied Mech. Cornell University Ithaca, N.Y. 14853		8. Performing Organization Report No.	
12. Sponsoring Agency Name and Address National Aeronautics and Space Administration Washington, D.C., 20546		10. Work Unit No.	
15. Supplementary Notes Project Manager: C.C. Chamis Materials and Structures Division NASA Lewis Research Center Cleveland, Ohio, 44135		11. Contract or Grant No. NSG-3080	
		13. Type of Report and Period Covered: Final Report 9/75-12/76	
		14. Sponsoring Agency Code	
16. Abstract <p>Stress wave propagation in a multilayer composite plate due to impact has been examined by means of the anisotropic elasticity theory. The plate is modelled as a number of identical anisotropic layers and the approximate plate theory of Mindlin is then applied each layer to obtain a set of difference-differential equations of motion. Dispersion relations for harmonic waves and correction factors are found. The governing equations are reduced to difference equations via integral transforms. With given impact boundary conditions these equations are solved for an arbitrary number of layers in the plate and the transient propagation of waves is calculated by means of a Fast Fourier Transform algorithm.</p> <p>The multilayered plate problem is extended to examine the effect of damping layers present between two elastic layers. A reduction of the interlayer normal stress is significant when the thickness of the damping layer is increased but it seems that the effect is mostly due to the softness of the damping layer. Finally the problem of a composite plate with a crack on the interlayer boundary has been formulated.</p>			
17. Key Words (Suggested by Author(s)) Multilayered Composite Plate, Approximate Plate Theory of Mindlin, Impact, Stress Wave, Dispersion Relation, Wave surface, Damping Layer, Crack, Fast Fourier Transform.		18. Distribution Statement Unclassified, unlimited	
19. Security Classif.(of this report) Unclassified	20. Security Classif. (of this page) Unclassified	21. No. of Pages	22. Price*

\* For sale by the National Technical Information Service, Springfield, Virginia 22151

Contents

	<u>Page</u>
Preface and Summary	ii
Symbols Used	iv
I Introduction	1
II Impact on Multilayer Elastic Plate	5
III Impact of a Composite Plate with an Interlaminar Damping Layer	30
IV Impact on a Plate with a Crack	37
V Conclusion and Recommended Research	43
Reference	44
Figures	47
Appendix A - Flow Chart	72
Appendix B - Sample Computer Deck	76
Appendix C - Program and Sample Output	77

### SYMBOLS USED

$\Delta$ : Plate thickness (Nondimensional length unit)

$b$ : A half of the layer thickness

$N$ : Layer number in the plate

$\rho$ : Density

$t_o$ : Impact time

$P_o(x_1, t)$ : Impact stress

\*  $x_1(\eta), x_2(\xi)$ : Coordinate variables

\*  $t(\tau)$ : Time variable

$T_o$ : Nondimensional time unit =  $a/\sqrt{c_{66}/\rho}$

\*  $\sigma_{ij}, \sigma(\Sigma), \tau(T), \sigma_{11}$ : Stress tensor and its components

\*  $u_i, u(U), v(V)$ : Displacement vector and its components

\*  $c_{ijkl}, c_{ij}(c_{ij})$ : Elastic Moduli ( $c_{11} = c_{11} - \frac{c_{12}}{c_{22}}$ )

$\lambda, \mu$ : Lame's constants

$\epsilon_{ij}, \epsilon_i$ : Infinitesimal strain tensor

$\hat{A}$ : Laplace transform (in  $\tau$ ) and Fourier transform (in  $\eta$ ) of  $A$

$P_n(\xi)$ : Legendre polynomial of  $\xi$

\*  $k(k)$ : Wave number

\*  $\omega(\bar{\omega})$ : Frequency

$\theta, \alpha, \beta$ : Phase shifts (wave number through the thickness)

$c_D, c_S$ : Dilatational and shear wave speed

$G^*(\omega) = G'(\omega) + iG''(\omega)$ : Complex modulus of elastomer

$D$ : Thickness of viscoelastic layer

$h$ : A half of the crack length

\* Quantities in ( ) are nondimensional quantities.

### Preface and Summary

This report is the last of a series on the response of composite plates to impact forces. The motivation for these studies has been an attempt to understand the damage to aircraft jet engine fan blades by foreign object impact such as ice balls, stones, and birds. In addition, the National Aeronautics and Space Administration, sponsors of this research, have sought to develop computer codes from these analyses which will aid the fan blade designer in locating potential failure modes and positions and thus assist in optimizing fan blade fabrication to create greater impact tolerance.

The basic approach of the principal investigator in these studies has been to use wave propagation techniques to model the early response of composite plates to impact type forces. In using the wave method, the plate can be simplified in the analyses by neglecting reflections from edge boundaries far from the impact point. Thus, while the overall geometry of the plate is no longer included in the analysis, more sophisticated mathematical models near the point of impact have been used.

The basic model for the composite plate studies has been the anisotropic plate theory as extended by Mindlin [1] to account for wave phenomena. The plate equations were used as an approximation of the exact theory of elasticity because they lead to simpler computational schemes for evaluating average stresses and displacements in the plate.

Fourier and Laplace transform techniques have been used throughout these studies and inversion of the transforms has been accomplished with a fast Fourier transform algorithm. This algorithm is an effective computational tool but requires careful scaling of the impact problem in both space and time

variables. When it is properly used it can lead to calculations of thousands of stress values in a fraction of the time of conventional finite element schemes.

In summary, the use of plate models for the fan blade impact has avoided the analytical complexities of the exact theory of elasticity as well as the computational difficulties of finite element methods.

In earlier reports both central and edge impact of an anisotropic plate were studied, [ 2-4 ]. In those reports only wave propagation in the plane of the plate was investigated. In another report [5] a multilayer plate model was developed in order to study impact induced wave propagation in both the thickness and inplane directions. In this final report further results are presented from the multilayer model. The composite plate has been modeled with as many as eight separate layers. Each layer may itself have several plies, so that effective anisotropic constants must be used for each layer in the analysis. The mathematical model exhibits wave propagation in both the thickness and inplane directions. Impact generated waves are shown to lead to interlaminar shear stresses and interlaminar tensile stresses during and after impact.

This report also presents an analysis of an impact damping mechanism. This consists of thin damping layer introduced between composite layers in the mathematical model. The resulting response due to impact shows that considerable reduction of stress can be achieved. However it appears that this stress reduction is linked to the lower elastic moduli of the damping sublayers and not the viscous nature of the sublayer.

Finally an attempt was made to analyze the impact of a plate with a crack. While the problem has been formulated, no progress was made on obtaining numerical answers to the crack problem.

## I. INTRODUCTION

The present research is a continuation of our previous work on the stress wave propagation in a laminated composite [2-5]. It has been motivated by the problem of the impact on jet engine fan blades caused by ingestions of foreign materials, such as birds and hailstones. The successful application of fiber-reinforced composite materials depends on the ability of these materials to withstand forces due to such impact.

The simplest approach to examine the dynamic behavior of a composite plate is based upon the work of White and Angona [6]. In their work, referred to as the effective modulus theory, the response of the composite plate to waves propagating normal to the laminate is predicted by a single constant wave speed, regardless of the internal structure of composites. Even though this theory is satisfactory for many problems, it fails in the case of some problems when the wave lengths become short. To overcome this limitation, Sun and et al. proposed a model which includes the effects of internal structure, such as the layer thickness [7]. In their work, referred to so the effective stiffness theory, displacements of both the reinforcing layer and the matrix layer are expressed as linear expansions about the midplanes of the layers and approximate equations of motion are derived for both layers. Then these approximate equations are required to satisfy the continuity conditions of displacement and stress components on every interface. Using this model the propagation of harmonic waves has been examined.

More recently a number of researchers have presented models for multilayer plates either by the discrete-continuum theory or the continuum mixture theory [8-14]. Many, however examined only the frequency-wave number dispersion relationship and stopped short of the transient

impact problem except for a few experimental or numerical works using the finite element method which sometimes show a considerable discrepancy from the experimental results.

In this report we present a new attempt to mathematically model the multilayer plate and develop a method by which we can examine the transient propagation of an impact wave in the plate, not only along the longitudinal direction but also through the thickness direction of the plate as well, using an inexpensive Fast Fourier Transform algorithm [3,15].

The composite plate under consideration for the first part of the present report is imagined to comprise  $N$  identical elastic layers. And each layer is made of a number of unidirectional plies lying alternately at a layup angle  $\pm\phi$  from the symmetry axis, as shown in Fig. 1. Then the elastic properties of the plate depend on the layup angle  $\phi$ . A key assumption for the first step of the work is that all the layers are identical. While restricting the application, this assumption allows us to formulate the problem using difference-differential equations due to a rather simple periodic structure of the plate. This technique for periodic structures has been widely used in the study of electrical transmission lines [16] and in the vibration of multistory buildings [17]. By means of an approximate plate theory of Mindlin [18], a set of approximate equations of motion is developed for a typical layer using the inter-laminar stresses as explicit variables. The relative motion of a layer to the adjacent layers is related by phase shifts which represent the solution of the difference parts of equations. In this way the number of the layers can be increased without increasing the size of matrix in the numerical process of invert to satisfy the boundary conditions.

It is also well understood that a thin viscoelastic layer present between elastic layers can reduce the elastic impact energy significantly by dissipating the strain energy into heat [19,20]. In our previous work [5] an elastomer layer is presented between a composite half space and a protection strip on the edge on which the impact is applied. Numerical results of the work showed an appreciable reduction in the normal stress. As an extension of this research and the first part of this report we now examine the wave propagation in a composite plate made of two elastic layers and an elastomer layer. Generalization of this problem is straightforward by assuming that our new periodic composite layer is now made of an elastic sublayer and a viscoelastic sublayer lying alternately. We can now develop the approximate theory which includes both sub-layers. For the second part of the present research we will examine the simplest case of this kind, i.e., an impact on a composite plate consisting of two elastic layers and an elastomer layer between them.

Another possible extension of the multilayer composite plate which can be found in frequent practice is discussed in the last part of this report. In this chapter a crack is introduced on the interface between two elastic layers which represent the final step before a failure occurs in the composite either by spalling or by excessive shear stress. Such crack problems constitute the main part of the study of fracture mechanics. A serious mathematical difficulty arises even in the static problems because of the mixed boundary conditions along the crack direction. The difficulty becomes more serious in the case of dynamic problems due to the diffraction of waves at the crack tip [21-24]. By employing the approximate equations of motion developed in the first part, the transient wave problem has been formulated and dual integral

equations are obtained after application of the mixed boundary conditions.

But the resulting dual integral equations are not easy to solve and are under investigation at this time.

In the results presented in this report only a line impact has been examined. This has simplified the calculations and saved computer time in testing the model. The technique, however, can be extended to the two-dimensional or central impact problem. Since the impact speed is very high (~450 m/sec) and the impact time is short (< 100  $\mu$ sec), the impact can be in the range of the elastic-plastic impact or even in the range of the hydraulic impact. But the initial transmission of impact energy is propagated by elastic waves, as if in an unbounded plate, and it is useful to investigate the problem by means of the linear theory of anisotropic elasticity in an infinite composite plate.

## II. IMPACT ON MULTILAYER ELASTIC PLATE

### 1. Formulation

#### Basic Theory of Linear Anisotropic Elasticity

Cauchy's equations of motion in cartesian tensor form without body forces are given by

$$\sigma_{ij,i} = \rho \ddot{u}_j \quad (II-1)$$

$$\sigma_{ij} = \sigma_{ji}$$

where the repeated index implies summation on that index. A comma represents a partial differentiation with respect to the index following the comma and a superposed dot denotes a time derivative.

tensor is related to the infinitesimal strain tensor  $\epsilon_{ij}$  by

$$\sigma_{ij} = c_{ijkl} \epsilon_{kl} \quad \text{or} \quad \sigma_i = c_{ij} \epsilon_j \quad (II-2)$$

The condensed elastic moduli  $c_{ij}$  has the following form for orthotropic materials

$$c_{ij} = \begin{bmatrix} c_{11}, c_{12}, c_{13}, 0, 0, 0 \\ c_{12}, c_{22}, c_{23}, 0, 0, 0 \\ c_{13}, c_{23}, c_{33}, 0, 0, 0 \\ 0, 0, 0, c_{44}, 0, 0 \\ 0, 0, 0, 0, c_{55}, 0 \\ 0, 0, 0, 0, 0, c_{66} \end{bmatrix}$$

Analysis of a Layer

For a layer shown in Fig. 1 we employ the approximate plate theory of Mindlin [18] and the displacement field  $\tilde{u}$  is expanded in terms of the Legendre polynomials as

$$\tilde{u}(x_1, x_2, x_3, t) = \sum_{n=0}^{\infty} \tilde{u}^{(n)}(x_1, x_3, t) \cdot P_n(\xi) \quad (II-3)$$

where  $\xi$  is the local coordinate along the thickness direction, normalized by  $b$ , a half layer thick.

Instead of solving Eq. (II-1) directly we solve a new approximate equation of motion which is obtained through a variational process by integration of Eq. (II-1) over the thickness  $\xi$  (see [1], [23]). The result is

$$b \cdot \sigma_{\alpha j \alpha}^{(n)} + [P_n(\xi) \cdot \sigma_{2j}]_{\xi=-1}^1 - \sigma_{2j}^{*(n)} = \frac{2\rho b}{2n+1} \ddot{u}_j^{(n)} : \quad j = 1, 2, 3 \\ \alpha = 1, 3 \quad (II-4)$$

where

$$\sigma_{\alpha j}^{(n)} = \int_{-1}^1 P_n(\xi) \cdot \sigma_{\alpha j} \, d\xi$$

$$\sigma_{2j}^{*(n)} = \int_{-1}^1 \frac{dP(\xi)}{d\xi} \sigma_{2j} \, d\xi$$

By substituting the constitutive relation (II-2) for the displacement expansion (II-3) into the above approximate equations of motion, we can find governing equations of motion in terms of  $u_1^{(0)}, u_2^{(0)}, u_3^{(0)}, u_1^{(1)}, \dots$

The accuracy of this approximate theory depends on how many terms of the

displacement field we retain. Since the complexity in formulation increases rapidly with the number of terms included we keep terms only up to second order. Furthermore, we will examine harmonic waves propagating along the  $x_1$  and  $x_2$  directions so that we drop  $u_3^{(n)}$  terms and set  $\frac{\partial}{\partial x_3} \{ \} = 0$ . Next to get rid of the undesired coupling with higher modes we set  $\ddot{u}_1^{(2)} = \ddot{u}_2^{(2)} = 0$ . Then the resulting equations are

$$2b(c_{11}u_{1,11}^{(0)} + \frac{1}{b}c_{12}u_{2,1}^{(1)}) + (\sigma_{21}^+ - \sigma_{21}^-) = 2b\rho\ddot{u}_1^{(0)}$$

$$2bc_{66}(\frac{1}{b}u_{1,1}^{(1)} + u_{2,11}^{(0)}) + (\sigma_{22}^+ - \sigma_{22}^-) = 2b\rho\ddot{u}_2^{(0)}$$

$$\frac{2b}{3}(c_{11}u_{1,11}^{(1)} + \frac{3}{b}c_{12}u_{2,1}^{(2)}) - 2c_{66}(\frac{u_1^{(1)}}{b} + u_{2,1}^{(0)}) + (\sigma_{21}^+ + \sigma_{21}^-) = \frac{2}{3}b\rho\ddot{u}_1^{(1)}$$

$$\frac{2b}{3}(c_{66}u_{2,11}^{(1)} + \frac{3}{b}c_{66}u_{1,1}^{(2)}) - 2(c_{12}u_{1,1}^{(0)} + \frac{1}{b}c_{22}u_{2,1}^{(1)}) + (\sigma_{22}^+ + \sigma_{22}^-) = \frac{2}{3}b\rho\ddot{u}_2^{(1)}$$

$$(\sigma_{22}^+ - \sigma_{22}^-) - 2(c_{12}u_{1,1}^{(1)} + \frac{3}{b}c_{22}u_{2,1}^{(2)}) = 0$$

(II-5)

$$(\sigma_{21}^+ - \sigma_{21}^-) - 2(c_{66}u_{2,1}^{(1)} + \frac{3}{b}c_{66}u_{1,1}^{(2)}) = 0$$

where the sign + and - represent the stress components on the top and bottom surfaces of the layer under examination, i.e., at  $\xi = \pm 1$ . Here we notice that the first, fourth, and last equations are written in terms of  $u_i^{(n)}$ , where  $(n+i)$  is an odd integer and represents the thickness stretching motion (or symmetric motion). In the rest of the equations in which  $(n+i)$  is an even integer the displacements represent the flexual motion (or antisymmetric motion). Hence, this process has decoupled the

stretching motion from bending motion\*. To get rid of the 2nd order modes from Eq. (II-5) we solve the last two equations for  $u_2^{(2)}$  and  $u_1^{(2)}$ , and insert them into the remaining equations. Then Eq. (II-5) can be reduced as follows:

$$2b(c_{11}u_{1,11}^{(0)} + \frac{1}{b}c_{12}u_{2,1}^{(1)}) + (\sigma_{21}^+ - \sigma_{21}^-) = 2b\rho\ddot{u}_1^{(0)}$$

$$2b c_{66}(\frac{1}{b}u_{1,1}^{(1)} + u_{2,11}^{(0)}) + (\sigma_{22}^+ - \sigma_{22}^-) = 2b\rho\ddot{u}_2^{(0)} \quad (II-6)$$

$$\frac{2b\hat{c}_{11}}{3}u_{1,1}^{(1)} - 2c_{66}\left(\frac{u_1^{(1)}}{b} + u_{2,1}^{(0)}\right) + \frac{c_{12}b}{3c_{22}}(\sigma_{22}^+ - \sigma_{22}^-),_1 + (\sigma_{21}^+ + \sigma_{21}^-) = \frac{2}{3}b\rho\ddot{u}_1^{(1)}$$

$$-2(c_{12}u_{1,1}^{(0)} + \frac{1}{b}c_{22}u_2^{(1)}) + (\sigma_{22}^+ + \sigma_{22}^-) = \frac{2}{3}b\rho\ddot{u}_2^{(1)}$$

where  $\hat{c}_{11} = c_{11} - c_{12}^2/c_{22}$ .

#### Plate Analysis

In view of the Legendre polynomial expansion, the displacements on the both sides of a layer can be written as  $u_i^{\pm} = u_i^{(0)} \pm u_i^{(1)}$  since the governing equations for a layer, Eq. (II-6), only include terms up to the first order of expansion, i.e., a linear expansion. Remembering that this analysis is valid for any arbitrary layer in a plate, say the nth layer, equation (II-6) can be immediately written as

---

\* These two motions are, of course, coupled through the boundary conditions.

$$\begin{aligned}
 \rho(\ddot{u}_n + \ddot{u}_{n-1}) &= c_{11}(u_n + u_{n-1})_{,11} + \frac{c_{12}}{b}(v_n - v_{n-1})_{,1} + \frac{1}{b}(\tau_n - \tau_{n-1}) \\
 \rho(\ddot{v}_n - \ddot{v}_{n-1}) &= -\frac{3}{b}c_{12}(u_n + u_{n-1})_{,1} - \frac{3}{b^2}c_{22}(v_n - v_{n-1}) + \frac{3}{b}(\sigma_n + \sigma_{n-1}) + (\tau_n - \tau_{n-1})_{,1} \\
 \rho(\ddot{u}_n - \ddot{u}_{n-1}) &= \hat{c}_{11}(u_n - u_{n-1})_{,11} - \frac{3c_{66}}{b^2}(u_n - u_{n-1}) - \frac{3}{b}c_{66}(v_n + v_{n-1})_{,1} \\
 &\quad + \frac{c_{12}}{c_{22}}(\sigma_n - \sigma_{n-1})_{,1} + \frac{3}{b}(\tau_n + \tau_{n-1}) \\
 \rho(\ddot{v}_n + \ddot{v}_{n-1}) &= c_{66}\left\{\frac{1}{b}(u_n - u_{n-1})_{,1} + (v_n + v_{n-1})_{,11}\right\} + \frac{1}{b}(\sigma_n - \sigma_{n-1})
 \end{aligned} \tag{III-7}$$

where  $\sigma$  and  $\tau$  are used to represent  $\sigma_{22}$  and  $\sigma_{12}$  and  $u$  and  $v$  denote  $u_1$  and  $u_2$ , respectively. These equations are the approximate equations of motion of a layer written in the form of a difference-differential equation. For a plate made of  $N$  layer, the above equations contain  $4(N+1)$  unknowns  $(u_0, v_0, \tau_0, \sigma_0, \dots, u_N, v_N, \tau_N, \sigma_N)$  and offer  $4N$  equations. Since the additional four conditions are supplied by boundary conditions on the top and bottom surfaces, solutions of these equations can be found.

In Eq. (III-7) we notice some important points. The first point is that the longitudinal coordinate  $x_1$  and the time variable are continuous variables while the thickness coordinate  $x_2$  is now discrete. This enables us to use integral transforms in  $x_1$  and time variables so that we can arrive at pure difference equations after integral transforms. The second point concerns the continuity conditions of stress and displacement. We note that  $u$ ,  $v$ ,  $\sigma_{22}$ , and  $\sigma_{12}$  have to be continuous across the layer boundary and these conditions are identically satisfied by

Eq. (II-7). But the normal stress tangential to the layer boundary is not necessarily continuous and Eq. (II-7) allows such a possibility. One can retain higher order terms in the displacement expansion given by Eq. (II-3) to give more accurate results. This can be achieved more easily by using Eq. (II-7) and increasing the number of layers in a plate under consideration. This process does not give any additional difficulties except a little more computer time.

## 2. Dispersion Relationships of Harmonic Waves

### Harmonic Waves

Before we examine the transient propagation of stress wave due to an impact we first investigate dispersion relations of harmonic waves in a composite plate governed by approximate equations of motion (II-7). For harmonic waves propagating along the  $x_1$  axis we assume

$$\{u_n, v_n, \sigma_n, \tau_n\} = \{U_n, V_n, \Sigma_n, T_n\} e^{i(kx_1 - \omega t)} \quad (II-8)$$

Substituting this into the approximate equations of motion (II-7) we obtain

$$\begin{aligned} (\omega^2 - c_{11}^2) (U_n + U_{n-1}) + c_{12} i \kappa (V_n - V_{n-1}) + b (T_n - T_{n-1}) &= 0 \\ -3c_{12} i \kappa (U_n + U_{n-1}) + (\omega^2 - 3c_{22}^2) (V_n - V_{n-1}) + i \kappa b (T_n - T_{n-1}) + 3b (\Sigma_n + \Sigma_{n-1}) &= 0 \end{aligned} \quad (II-9)$$

$$3c_{66} i \kappa (U_n - U_{n-1}) + (\omega^2 - c_{66}^2) (V_n + V_{n-1}) + b (\Sigma_n - \Sigma_{n-1}) = 0 \quad (II-9)$$

$$(\omega^2 - \hat{c}_{11}^2 - 3c_{66}^2) (U_n - U_{n-1}) - 3c_{66} i \kappa (V_n + V_{n-1}) + 3b (T_n + T_{n-1})$$

$$+ \frac{c_{12}}{c_{12}} i \kappa b (\Sigma_n - \Sigma_{n-1}) = 0$$

for  $n = 1, 2 \dots N$ . Here we set

$$\kappa = bk = k\left(\frac{\Delta}{2N}\right), \quad \Delta = 2bN$$

$$\omega^2 = \rho b^2 \omega^2 = \rho \omega^2 \left(\frac{\Delta}{2N}\right)^2$$

and  $\Delta$  is the total thickness of the plate. For a plate consisting of  $N$  layers, the boundary conditions require traction free surfaces, namely,  $T_o = \Sigma_o = T_N = \Sigma_N = 0$ . When these conditions are applied to equation (II-9) we obtain  $4N$  equations in terms of  $4N$  unknowns  $(U_o, V_o; U_n, V_n, T_n, \Sigma_n)$  with  $n = 1, \dots, N-1$ ;  $U_N, V_N$ . By setting the coefficient matrix to be singular, required dispersion relationships can be obtained.

#### One-layer Plate

The dispersion relationship for a plate made of a single layer can be found by setting  $N = 1$  in equation (II-9) with  $\Sigma_o = T_o = \Sigma_1 = T_1 = 0$ . The resulting equations are now written in matrix form as follows:

$$\begin{bmatrix} (\omega^2 - c_{11}\kappa^2) & c_{12}i\kappa & 0 & 0 \\ -c_{12}i\kappa & \frac{1}{3}(-3c_{22} + \omega^2) & 0 & 0 \\ 0 & 0 & c_{66}i\kappa & c_{66}\kappa^2 - \omega^2 \\ 0 & 0 & \hat{c}_{11}\kappa^2 + 3c_{66}\kappa^2 - \omega^2 & 3c_{66}i\kappa \end{bmatrix} \begin{bmatrix} U_1 + U_o \\ V_1 - V_o \\ U_1 - U_o \\ V_1 + V_o \end{bmatrix} = \begin{bmatrix} 0 \\ 0 \\ 0 \\ 0 \end{bmatrix} \quad (II-10)$$

Then by setting the determinant of the coefficient matrix to zero we obtain

$$c_{11}k^2 - \frac{1}{3}(\bar{\omega}^2 - 3c_{22})(\bar{\omega}^2 - c_{11}k^2) = 0 \quad (II-11)$$

$$c_{66}k^2 - \frac{1}{3}(\bar{\omega}^2 - c_{11}k^2 - 3c_{66})(\bar{\omega}^2 - c_{66}k^2) = 0 .$$

Here we notice that the first relationship corresponds to the state of deformation of  $U_1 = U_o$  and  $V_1 = -V_o$ , which represents the thickness extension of the plate (or the symmetric mode), and the second describes the flexual deformation (or antisymmetric mode). The exact theory of plates gives an infinite number of dispersion relationships, but because this model only has two inertia points (namely  $n = 0, 1$ ), each of them having two components of displacement, we only have the first four relationships.

Dispersion relationships and corresponding phase velocities for an isotropic plate with Poisson's ratio  $1/4$  (namely  $\lambda = \mu$ ) are given in Fig. 2a and 2b up to the range where the wave length becomes equal to the plate thickness. Solid lines represent the symmetric modes and dotted lines the antisymmetric modes. As predicted by Mindlin and Medick the optical branch of the symmetric mode approaches the dilatation wave [18]. The acoustic branch of the antisymmetric mode starts from the bending motion and approaches the shear wave when the wave number  $k$  becomes larger and larger\*. Similar relationships for an anisotropic plate made of 55% graphite fiber-epoxy matrix with a layup angle of  $45^\circ$  are shown in Fig. 3a and 3b.

---

\* See section 5 for discussion about the large wave number limit.

Two-layer Plate

In this case we obtain eight equations by putting  $n = 1$  and  $2$  in equation (II-9). Boundary conditions require  $T_0 = \Sigma_0 = T_2 = \Sigma_2 = 0$ . By following the same procedure we find the dispersion relations as

$$\{(\bar{\omega}^2 - c_{11}^2)(\bar{\omega}^2 - 3c_{22}^2) - 3c_{12}^2\kappa^2\}(\bar{\omega}^2 - \hat{c}_{11}^2\kappa^2 - 3c_{66}^2 + \frac{c_{66}c_{12}}{c_{22}}\kappa^2)$$
$$+ 3(\bar{\omega}^2 - c_{11}^2)\{(\bar{\omega}^2 - c_{66}^2\kappa^2)(\bar{\omega}^2 - \hat{c}_{11}^2\kappa^2 - 3c_{66}^2) - 3c_{66}^2\kappa^2\} = 0 \quad (II-12)$$

$$\{(\bar{\omega}^2 - c_{66}^2\kappa^2)(\bar{\omega}^2 - \hat{c}_{11}^2\kappa^2 - 3c_{66}^2) - 3c_{66}^2\kappa^2\}$$
$$+ 3(\bar{\omega}^2 - c_{66}^2\kappa^2)\{(\bar{\omega}^2 - c_{11}^2\kappa^2)(\bar{\omega}^2 - 3c_{22}^2) - 3c_{12}^2\kappa^2\} = 0$$

Again the first equation represents the symmetric mode and is shown as solid lines in Fig. 4 and 5. The second equation is plotted with dotted lines representing the antisymmetric mode.

As expected we have six relationships since the this two-layer model is equivalent to a three-mass system with two degrees of freedom for each mass. When the wave number  $k\Delta$  increases the following are observed: for the symmetric mode the upper optical branch approaches the dilatation wave, whereas for the antisymmetric mode the lower optical branch approaches the shear wave <sup>\*</sup>.

---

\* See section 5 for discussions about the large wave number limit.

N-Layer Plate

In general, we can obtain a  $2(N+1)$  order polynomial of  $\bar{\omega}^2$  by expanding a  $(4N) \times (4N)$  determinant and finding  $2(N+1)$  dispersion relationships. But, unfortunately, this process involves considerably complicated algebra and it may be necessary to develop a computer technique to find roots of an equation in determinant form (not in polynomial form).

A difference equation approach can be used to solve the  $N$  set of four simultaneous first order difference equations given by Eq. (II-9). This procedure is neat and can be generalized for any number of layers as discussed in the next section; but the last step of this approach, where a long polynomial is to be solved again, is not any simpler than the previous direct method.

### 3. Impact on an Elastic Composite Plate

#### Normalization and Integral Transforms of Governing Equations

The governing equations given by (II-7) are first nondimensionalized as follows:

$$\{U_n, V_n, \eta\} = \{u_n/\Delta, U_n/\Delta, x_1/\Delta\}$$

$$\{C_{ij}, T_n, \Sigma_n\} = \{c_{ij}/c_{66}, \tau_n/c_{66}, \sigma_n/c_{66}\}$$

$$\tau = t/T_o$$

where  $\Delta$  is the total thickness of the plate and  $T_o$  is the time required for the quasi-shear wave to travel the impact radius. Next we apply a Laplace transform in  $\tau$  and a Fourier transform in  $\eta$ , i.e.,

$$\hat{g}(s) = \int_0^\infty g(\tau) e^{-s\tau} d\tau$$

$$\hat{g}(k) = \frac{1}{\sqrt{2\pi}} \int_{-\infty}^{\infty} g(\eta) e^{ik\eta} d\eta .$$

Then the resulting equations are

$$-(fs^2 + \frac{c_{11}}{2N} k^2) (\hat{U}_n + \hat{U}_{n-1}) - c_{12} ik (\hat{V}_n - \hat{V}_{n-1}) + (\hat{T}_n - \hat{T}_{n-1}) = 0$$

$$c_{12} ik (\hat{U}_n + \hat{U}_{n-1}) - (\frac{fs^2}{3} + 2Nc_{22}) (\hat{V}_{n-1} - \hat{V}_{n-1}) + (\hat{\Sigma}_n + \hat{\Sigma}_{n-1}) - \frac{ik}{6N} (\hat{T}_n - \hat{T}_{n-1}) = 0$$

(II-13)

$$-c_{66} ik (\hat{U}_n - \hat{U}_{n-1}) - (fs^2 + \frac{c_{66}}{2N} k^2) (\hat{V}_n + \hat{V}_{n-1}) + (\hat{\Sigma}_n - \hat{\Sigma}_{n-1}) = 0$$

$$-(\frac{fs^2}{3} + \frac{c_{11} k^2}{6N} + 2Nc_{66}) (\hat{U}_n - \hat{U}_{n-1}) + c_{66} ik (\hat{V}_n + \hat{V}_{n-1}) - \frac{c_{12} ik}{6Nc_{22}} (\hat{\Sigma}_n - \hat{\Sigma}_{n-1}) + (\hat{T}_n - \hat{T}_{n-1}) = 0$$

where the normalization factor  $f$  is given as

$$f = \frac{1}{2N} \frac{\Delta^2 \rho}{c_{66} T_o^2} = \frac{b \Delta \rho}{c_{66} T_o^2} .$$

Solution of Difference Equations

Since the simultaneous difference equations given are linear and all the coefficients are constants the solution [26] has to be

$$\{\hat{U}_n, \hat{V}_n, \hat{T}_n, \hat{\Sigma}_n\} = \{A, B, C, D\} e^{2i\theta n} \quad (\text{II-14})$$

where the phase shift  $\theta$  is complex, in general, and propagation through the thickness direction in the plate is characterized by  $\theta$ . Namely,  $\theta$  is the wave number in the thickness direction. By substituting solution (II-14) into the difference equation (II-13) we obtain a set of four simultaneous homogeneous equations through which the relationships among the constants  $A, B, C$ , and  $D$  have to be determined. If we set the resulting coefficient matrix of  $A, B, C$ , and  $D$  to be singular we obtain the following equation for phase shift  $\theta$ :

$$\begin{aligned} & \cos^4 \theta \left( fs^2 + \frac{c_{11} k^2}{2N} \right) \left( fs^2 + \frac{c_{66}}{2N} k^2 \right) \\ & + \sin^4 \theta \left( \frac{fs^2}{3} + 2N c_{22} - \frac{c_{12} k^2}{6N} \right) \cdot \left( \frac{fs^2}{3} + \frac{\hat{c}_{11}}{6N} k^2 + 2N c_{66} - \frac{c_{66} c_{12}}{6N c_{22}} k^2 \right) \\ & + \cos^2 \theta \sin^2 \theta \left[ \left( fs^2 + \frac{c_{11} k^2}{2N} \right) \left\{ \frac{k^2}{6N} c_{66} + \frac{fs^2}{3} + 2N c_{22} - \left( \frac{k}{6N} \right)^2 \frac{c_{66}}{c_{22}} \left( fs^2 + \frac{c_{66} k^2}{2N} \right) \right\} \right. \\ & \left. - \left( c_{12} + c_{66} \right)^2 k^2 + \left( fs^2 + \frac{c_{66} k^2}{2N} \right) \left( \frac{fs^2}{3} + \frac{\hat{c}_{11} k^2}{6N} + 2N c_{66} + \frac{c_{12} k^2}{6N c_{22}} \right) \right] \\ & = a_1 \cos^4 \theta + a_2 \cos^2 \theta + a_3 = 0 . \end{aligned} \quad (\text{II-15})$$

This equation implies that for a given wave number  $k$  along  $x_1$  and a frequency  $s$  ( $s$  represents the frequency for the case of harmonic waves), an infinite value of wave numbers exists for propagation through the thickness direction, but only four of them are sufficient to give all linearly independent solutions of the form of Eq. (II-14). If we denote the solution of the phase shift equation as

$$\cos^2 \beta = \frac{-a_2 + \sqrt{a_2^2 - 4a_1 a_3}}{2a_1} \quad (II-16)$$

$$\cos^2 \alpha = \frac{-a_2 - \sqrt{a_2^2 - 4a_1 a_3}}{2a_1}$$

the complete general solutions of difference equation (II-13) are

$$\begin{bmatrix} \hat{U}_n \\ \hat{V}_n \\ \hat{T}_n \\ \hat{\Sigma}_n \end{bmatrix} = \begin{bmatrix} A_1 \\ B_1 \\ C_1 \\ D_1 \end{bmatrix} e^{2i\beta n} + \begin{bmatrix} A_2 \\ B_2 \\ C_2 \\ D_2 \end{bmatrix} e^{-2i\beta n} + \begin{bmatrix} A_3 \\ B_3 \\ C_3 \\ D_3 \end{bmatrix} e^{2i\alpha n} + \begin{bmatrix} A_4 \\ B_4 \\ C_4 \\ D_4 \end{bmatrix} e^{-2i\alpha n} \quad (II-17)$$

Next, by substituting the above solutions into the original difference equations (II-13) we find the relationships among  $A_i$ ,  $B_i$ ,  $C_i$ , and  $D_i$ . The results are

$$\begin{bmatrix} \hat{U}_n \\ \hat{V}_n \\ \hat{T}_n \\ \hat{\Sigma}_N \end{bmatrix} = \begin{bmatrix} X_1(\beta) E_1 \\ X_2(\beta) E_2 \\ X_3(\beta) E_3 \\ E_1 \end{bmatrix} \cdot \cos 2n\beta + i \begin{bmatrix} X_1(\beta) E_2 \\ X_2(\beta) E_1 \\ X_3(\beta) E_1 \\ E_2 \end{bmatrix} \cdot \sin 2n\beta$$

(II-18)

$$+ \begin{bmatrix} Y_1(\alpha) E_4 \\ Y_2(\alpha) E_3 \\ E_3 \\ Y_3(\alpha) E_4 \end{bmatrix} \cdot \cos 2n\alpha + i \begin{bmatrix} Y_1(\alpha) E_3 \\ Y_2(\alpha) E_4 \\ E_4 \\ Y_3(\alpha) E_3 \end{bmatrix} \cdot \sin 2n\alpha$$

where  $E_1 = D_1 + D_2$ ,  $E_2 = D_1 - D_2$ ,  $E_3 = C_3 + C_4$ ,  $E_4 = C_3 - C_4$  and

$$X_i(\beta) = - \frac{\Delta_i(\beta)}{\Delta(\beta)}$$

$$\Delta(\beta) = (fs^2 + \frac{C_{11}k^2}{2n})(fs^2 + \frac{C_{66}k^2}{2n})\cos^3\beta$$

$$+ \{(fs^2 + \frac{C_{66}k^2}{2n})(\frac{fs^2}{3} + \frac{\hat{C}_{11}k^2}{6n} + 2nC_{66}) - C_{66}C_{12}k^2 - C_{66}^2k^2\}\sin^2\beta \cdot \cos\beta$$

$$\Delta_1(\beta) = ik \sin^2\beta \cos\beta \{ \frac{C_{12}}{6nC_{22}}(fs^2 + \frac{C_{66}k^2}{2n}) - (C_{12} + C_{66}) \} \quad (II-19)$$

$$\Delta_2(\beta) = i \sin^3\beta \{ \frac{C_{66}C_{12}k^2}{6nC_{22}} - (\frac{fs^2}{3} + \frac{\hat{C}_{11}k^2}{6n} + 2nC_{66}) \} - \cos^2\beta \sin\beta (fs^2 + \frac{C_{11}k^2}{2n})$$

$$\begin{aligned}
 \Delta_3(\beta) &= k \sin^3\beta \{ (\frac{fs^2}{3} + \frac{\hat{C}_{11}k^2}{6n} + 2nC_{66})C_{12} - \frac{C_{12}^2k^2}{6nC_{22}}C_{66} \} \\
 &+ k \sin\beta \cos^2\beta \{ \frac{C_{12}}{6nC_{22}}(fs^2 + \frac{C_{11}k^2}{2n}) \cdot (fs^2 + \frac{C_{66}k^2}{2n}) - (fs^2 + \frac{C_{11}k^2}{2n})C_{66} \}
 \end{aligned}$$

and

$$Y_i(\alpha) = - \frac{\bar{\Delta}_i(\alpha)}{\bar{\Delta}(\alpha)}$$

$$\bar{\Delta}(\alpha) = i \cos^2 \alpha \cdot \sin \alpha \{ C_{66} k^2 (C_{12} + C_{66}) - (fs^2 + \frac{C_{66} k^2}{2n}) \cdot (\frac{fs^2}{3} + \frac{\hat{C}_{11} k^2}{6n}$$

$$+ 2nC_{66} + \frac{12 k^2}{6nC_{22}}) \} + i \sin^3 \alpha (\frac{fs^2}{3} + 2nC_{22})$$

$$\times (\frac{C_{66} C_{12} k^2}{6nC_{22}} - \frac{fs^2}{3} - \frac{C_{11} k^2}{6n} - 2nC_{66})$$

$$\bar{\Delta}_1(\alpha) = \cos^3 \alpha (fs^2 + \frac{C_{66}}{2n} k^2)$$

$$+ \sin^2 \alpha \cdot \cos \alpha \{ -(\frac{k}{6n})^2 \frac{C_{12}}{C_{22}} (fs^2 + \frac{C_{66} k^2}{2n}) + \frac{k^2}{6n} C_{66} + (\frac{fs^2}{3} + 2nC_{22}) \}$$

$$\bar{\Delta}_2(\alpha) = k \cdot \cos^2 \alpha \sin \alpha (C_{12} + C_{66}) \quad (II-20)$$

$$+ k \sin^3 \alpha \{ \frac{1}{6n} (\frac{fs^2}{3} + \frac{\hat{C}_{11} k^2}{6n} + 2nC_{66}) - (\frac{k}{6n})^2 \frac{C_{12} C_{66}}{C_{22}} \}$$

$$\bar{\Delta}_3(\alpha) = ik \sin^2 \alpha \cos \alpha \{ \frac{C^2}{6n} k^2 - \frac{1}{6n} (\frac{fs^2}{3} + \frac{\hat{C}_{11} k^2}{6n} + 2nC_{66}) (fs^2 + \frac{C_{66} k^2}{2n})$$

$$+ C_{66} k (\frac{fs^2}{3} + 2nC_{22}) \} + ik \cos^3 \alpha \{ -C_{12} (fs^2 + \frac{C_{66} k^2}{2n}) \}$$

Equations (II-18) with (II-19,20) and the phase shifts  $\alpha$  and  $\beta$  given by (II-16) constitute the final form of the general solutions of the difference equations (II-13).

In Eqs. (II-19,20) we notice that when  $k \rightarrow 0$  we have  $X_1(\beta) = X_3(\beta) = Y_2(\alpha) = Y_3(\alpha) = 0$ . Namely the propagation of the normal stress (with phase shift  $\beta$ ) and the propagation of the shear stress (with phase shift  $\alpha$ ) are completely decoupled. This occurs when the waves are propagating only through the thickness direction [27].

#### Impact Boundary Condition

Boundary conditions for an impact can be described by any two conditions among  $u_o$ ,  $v_o$ ,  $\sigma_o$ , and  $\tau_o$  and another two conditions from  $u_N$ ,  $v_N$ ,  $\sigma_N$  and  $\tau_N$ . For our present problem we have chosen a line impact by a normal stress along the  $x_3$  axis (Figure 1), i. e.,

$$\begin{aligned}\sigma_o &= -\frac{p_o}{4} (1-\cos \frac{2\pi t}{t_o}) (1+\cos \frac{\pi x}{a}) : |x| \leq a \text{ and } 0 \leq t \leq t_o \\ &= 0 : |x| > a \text{ or } t > 0 \text{ or } t > t_o \\ \tau_o &= \sigma_N = \tau_N = 0 .\end{aligned}\tag{II-21}$$

Hence, the boundary conditions for the present impact problem lead to the following equation

$$\begin{bmatrix} 0, X_3(\beta), 1, 0 \\ 1, 0, 0, Y_3(\alpha) \\ iX_3(\beta)\sin 2\beta N, X_3(\beta)\cos 2\beta N, \cos 2\alpha N, i\sin 2\alpha N \\ \cos 2\beta N, i\sin 2\beta N, iY_3(\alpha)\sin 2\alpha N, Y_3(\alpha)\cos 2\alpha N \end{bmatrix} \begin{bmatrix} E_1 \\ E_3 \\ E_3 \\ E_4 \end{bmatrix} = \begin{bmatrix} 0 \\ q \\ 0 \\ 0 \end{bmatrix} \quad (II-22)$$

where  $q$  is the integral transform of the impact function (II-21)\*.

Solving the above equations for  $E_i$ 's we can have

$$\begin{aligned} E_i &= \frac{D_i}{D} q \\ D &= \{1+X_3^2(\beta)Y_3^2(\alpha)\}\sin 2\alpha N \cdot \sin 2\beta N + 2X_3(\beta)Y_3(\alpha)(\cos 2\alpha N \cdot \cos 2\beta N - 1) \\ D_1 &= X_3(\beta)Y_3(\alpha)(\cos 2\alpha N \cdot \cos 2\beta N - 1) + \sin 2\alpha N \cdot \sin 2\beta N \\ D_2 &= i\{\cos 2\beta N \cdot \sin 2\alpha N - X_3(\beta)Y_3(\alpha)\cos 2\alpha N \cdot \sin 2\alpha N\} \\ D_3 &= iX_3(\beta)\{X_3(\beta)Y_3(\alpha)\sin 2\beta N \cdot \cos 2\alpha N - \cos 2\beta N \cdot \sin 2\alpha N\} \\ D_4 &= X_3(\beta)\{X_3(\beta)Y_3(\alpha)\sin 2\alpha N \cdot \sin 2\beta N + \cos 2\beta N \cdot \cos 2\alpha N - 1\} \end{aligned} \quad (II-23)$$

Substituting the  $E_i$ 's into the general solution (II-18) we can find the complete solutions which satisfy the impact boundary conditions given by (II-21). In other words, for given values of  $k$  and  $s$  we first find the phase shift  $\alpha$  and  $\beta$  from (II-15,16) and with these we can find solutions in integral transform from equations (II-18,23) which are the final solutions under impact. After  $\hat{U}_n$ ,  $\hat{V}_n$ ,  $\hat{T}_n$  and  $\hat{\Sigma}_n$  are calculated

\* Allowing the determinant of the coefficient matrix to vanish leads to dispersion relations of an  $N$ -layer plate, namely  $D(\alpha, \beta) = 0$ . Then,  $\alpha$  and  $\beta$  are obtained from (II-15,16) which gives the complete dispersion relationships.

with a given impact function  $q$ , they can be inverted easily by means of the fast Fourier transform routine [3,20] to give the complete displacement and the stress fields after impact.

Tangential Normal Stress

As discussed following Eq. (II-7), the tangential normal stress does not appear explicitly in the approximate equations of motion. Therefore, this component of the stress has to be calculated from the constitutive equation. Namely,

$$\sigma_{11_o} = c_{11} u_{o,1} + \frac{c_{12}}{2b} (v_1 - v_o)$$

$$\sigma_{11_n} = c_{11} u_{n,1} + \frac{c_{12}}{2b} (v_n - v_{n-1}) \quad 1 \leq n \leq N$$

or after normalization and integral transform they are

$$\hat{\sigma}_{11_o} = -ikc_{11} \hat{U}_o + N \cdot c_{12} (\hat{V}_1 - \hat{V}_o) \quad (II-24)$$

$$\hat{\sigma}_{11_n} = -ikc_{11} \hat{U}_n + N \cdot c_{12} (\hat{V}_n - \hat{V}_{n-1}) \quad 1 \leq n \leq N$$

Then once the displacement field is computed the tangential normal stress can be obtained from the above equation and inverted.

#### 4. Some Numerical Results

The analysis discussed in the previous section includes the transient propagation in all directions but suitable choices of impact time, impact radius, sizes of time and distance steps are essential to make good use of the fast Fourier transform. For example, if we take a large time increment with a relatively thin plate propagation through the thickness will not be seen. For this matter we have examined several different cases.

##### Case 1: Longitudinal propagation

Propagation of impact generated waves along the longitudinal direction is examined for an isotropic plate (steel plate:  $\lambda = \mu = 1.2 \times 10^7$  psi) employing a two-layer model. For these calculations we used an impact time  $t_0 = 10 \mu\text{sec}$ , plate thickness  $\Delta = 1 \text{ cm}$ , and impact radius  $a = 4 \text{ cm}$ . Some of the results at a few different time sequences are shown in Fig. 6 a-f.

In these figures we can see two distinct states of propagation and corresponding wave fronts: one for horizontal displacements ( $u$ ) and longitudinal normal stresses ( $\sigma_{11}$ ), and another for vertical displacements ( $v$ ) and shear stresses ( $\tau$ ). In other words, the initial signals of the horizontal displacements and longitudinal normal stresses propagate through the plate with longitudinal wave speed at amplitudes that are relatively small. But the major parts of their signals are due to a bending wave propagating with shear stresses and vertical displacements with a lower velocity. When the group velocities of these waves are calculated from the numerical results, they are about  $5 \text{ mm}/\mu\text{sec}$  and  $3 \text{ mm}/\mu\text{sec}$ , respectively, while the phase velocities of the unbounded

medium of this material are  $C_d = \sqrt{(\lambda+2\mu)/\rho} = 5.61 \text{ mm}/\mu\text{sec}$  and  $C_s = \sqrt{\mu/\rho} = 3.25 \text{ mm}/\mu\text{sec}$ .

#### Case 2: Propagation Through Thickness

To examine the propagation through the thickness it is necessary to have a sufficient number of layers in a plate. It is also essential to make the time step relatively small compared to the layer thickness. To do this we increase the thickness of the plate and the number of layers and reduce the impact time.

In Figs. 7 and 8 propagation of the transverse normal stress in the same plate ( $\Delta = 4 \text{ cm}$ ,  $t_0 = 2\mu\text{sec}$ ,  $a = 40 \text{ cm}$ ; 4-layer model) is shown at different time sequences. As seen in Fig. 7, the transverse normal stress is initially compressive due to the impact and a compression wave propagates through the thickness. But later it becomes a tension wave after reflection from the free surface and the tension wave propagates back to the impact surface. In Fig. 8 we see the change of the transverse normal stress and the interlaminar shear stress with time for the same impact conditions as in Fig. 7.

Similar results are also shown for the case of an anisotropic plate in Fig. 9 (55% graphite fibers-epoxy matrix, layup angle =  $15^\circ$ ;  $\Delta = 1 \text{ cm}$ ,  $t_0 = 2\mu\text{sec}$ ,  $a = 2 \text{ cm}$ ; 8-layer model). Here we again notice a clear delay in time for waves to travel from one layer to the next one. Another important point is that the shape of the impact stress is relatively well preserved during the initial stage of propagation but changes immediately afterwards. The distortion of the shape becomes more serious with further propagation due to reflection, thus, showing the highly dispersive nature of the harmonic waves in the approximate plate theory.

When the group velocities are calculated from these results, we find 6.32 mm/ $\mu$ sec for the dilatation wave and 3.33 mm/ $\mu$ sec for the shear wave in the case of the isotropic plate and 2.5 mm/ $\mu$ sec for the quasi-dilatation wave of the anisotropic plate. Their expected values are, respectively, 5.61, 3.25, and 2.36 mm/ $\mu$ sec. In other words, waves going through the thickness are traveling faster than expected.

### Case 3. Wave Surfaces

In the previous two cases we examined the transient waves propagating dominantly along either the  $x_1$  axis or through the thickness direction by suitable choices of the plate geometry and impact condition. now examine the combined effect, simultaneous propagation in both directions. This effect is shown in Fig. 10 (isotropic plate;  $\Delta = 4$  cm,  $t_0 = 4\mu$ sec,  $a = 4$  cm; 4-layer model) where the transverse normal stress generated from the line source due to impact not only spreads out in all directions but also reflects from the free surface.

When the plate is anisotropic, the situation is more complex in the sense that waves are neither dilatation nor shear but they are coupled together (now called quasi-dilational or quasi-shear waves). Due to the coupling, phase velocities of the anisotropic wave vary from one direction to another, resulting in complicated shapes for the velocity surfaces and wave fronts [2]. For an anisotropic plate (made of 55% graphite fiber-epoxy matrix with layup angle 45°) the velocity surfaces and the wave surfaces are shown in Fig. 11. The stress state at 10  $\mu$ sec after the impact on the same plate ( $\Delta = 4$  cm,  $t_0 = 4\mu$ sec,  $a = 2$  cm; 8-layer model) with the corresponding wave fronts are shown in Fig. 12a. In the

propagation of the quasi-longitudinal wave we notice that the longitudinal propagation is well bounded by the quasi-dilatational wave surface but the transverse propagation is not. The shear wave is not bounded by the quasi-shear wave front in either direction.

This interesting phenomenon of higher propagation speeds through the thickness is related to the dispersion relationship at short wave length limits; it is discussed in the next section.

## 5. Correction Factor and Conclusion

### Correction Factor

According to the present model of a multilayer plate, one of the antisymmetric modes of the dispersion relationships approaches the shear speed when the wave length becomes shorter and shorter, as mentioned in Section 2. It is well understood that such a limit is incorrect, i.e., in the limit of short wave length there should be a Rayleigh wave instead of a shear wave. Such a discrepancy can be eliminated by introduction of proper correction factors, as shown by Mindlin and Medick [18]. Correction factors can be found by examining either the large wave number limit or the cut-off frequencies of both the exact theory and the present approximate theory. Since these two ways lead us to the same results we will find the factors by matching the cut-off frequencies of the two theories.

The cut-off frequencies of the exact theory for an isotropic plate can be obtained from the well-known Rayleigh-Lam's equation. The lowest cut-off frequencies are  $\frac{\pi}{\Delta} \sqrt{(\lambda+2\mu)/\rho}$  for the symmetric mode and  $\frac{\pi}{\Delta} \sqrt{\mu/\rho}$  for the antisymmetric mode. The corresponding cut-off frequencies of our approximate theory are  $\frac{2}{\Delta} \sqrt{3c_{22}/\rho}$  and  $\frac{2}{\Delta} \sqrt{3c_{66}/\rho}$ <sup>\*</sup>. Hence, we notice that replacing  $c_{22}$  by  $c_{22}\pi^2/12$  and  $c_{66}$  by  $c_{66}\pi^2/12$  makes the two theories have the same two lowest cut-off frequencies. Furthermore the shear wave observed in the short wave length limit of the present approximation becomes a wave with a speed of  $\frac{\pi}{\sqrt{12}} \sqrt{\mu/\rho}$ , i.e., the Rayleigh wave.

Another important consequence of the correction factor is to reduce propagation speeds through the thickness, which are related to  $\sqrt{c_{22}/\rho}$

---

\* The lowest two cut-off frequencies are found from Eq. (II-11) and they are independent of the layer number in the plate under investigation.

and  $\sqrt{c_{66}/\rho}$ , with a factor of  $\pi/\sqrt{12}$ . Propagation of the maximum value of the interlaminar normal stress through the thickness is examined with and without correction factors and the results are shown in Fig. 13. Without the correction factor the propagation speed in a composite plate is roughly about 2.60 mm/ $\mu$ sec obtained from the numerical results used in Fig. 12. When the same plate is subjected to identical impact conditions this reduces to about 2.41 mm/ $\mu$ sec with the correction factor. Comparing this with the group velocity in an unbounded composite space ( $= 2.36$  mm/ $\mu$ sec) the agreement of the present approximate theory is remarkable. Similar results are also observed in the case of shear and quasi-shear waves. When these correction factors are introduced in the previous cases, shown in Figs. 8, 9, and 12, all the signals propagating through the thickness are now well bounded within the corresponding wave fronts, as shown in Fig. 12b and from this we can notice the importance of the correction factors.

#### Discussion and Computation Time

It is interesting to compare the computation time of this model with some other methods, such as the finite element method or the finite difference method. In the case of an 8-layer anisotropic plate model, from which Figs. 9 and 12 are produced, we have

9 steps along the thickness: 8-layer model;

32 step along the  $x_1$  direction: 64 points are used in practice but only half of them are useful because of the symmetry of the problem,

32 steps in time;

2 displacement components at each point.

Therefore the total number of the unknowns, which are the basic unknowns either in case of the finite difference or finite element methods, is

18,432. After these primary variables are calculated, 27,648 secondary variables (three stress components at each points) have to be calculated again. According to our present model all these processes require only 200 K of computer space without using magnetic tapes or any kind of additional storage space and only 1 minute 6 seconds for CPU time in the IBM 370-168 model including compiling, linkage editing, I/O and execution.

#### Conclusion

The present theory is a generalization of Mindlin's approximate plate theory applied to a multilayer plate under an impact. By combined use of the finite difference technique in the thickness direction and the fast Fourier transform in the plane of plate and time, this model can be very useful for the study of wave propagation in a composite plate under impact forces. However, reasonable attention in usage of the fast Fourier transform is required to avoid spurious data. From the limited numerical data obtained from this model it appears that the anisotropy in the plate will lead to a considerable interlaminar shear which might lead to ply bonding failures. The model also shows that for short enough impact times, an interlaminar tension can develop as one would expect, which might also account for interlaminar ply failure.

### III. IMPACT OF A COMPOSITE PLATE WITH AN INTERLAMINAR DAMPING LAYER

#### 1. Description of Problem

##### Geometry of Plate

As an extension of the multilayer plate discussed in Chapter II we now examine the impact and the consequent stress wave propagation in a composite plate with viscoelastic damping layers. Possible models for damping mechanisms in plates are shown in Fig. 14. We will formulate a model made of an alternating number of elastic and viscoelastic layers, as shown in Fig. 14-c. As long as the layer structure of the plate is periodic, the main part of the analysis in Chapter II for an elastic plate is valid with additional equations for viscoelastic layers.

##### Viscoelastic Property of Elastomer

The mechanical properties of an elastomer are usually expressed in terms of a complex modulus depending on the frequency, i.e.,

$$G^*(\omega) = G'(\omega) + iG''(\omega) . \quad (\text{III-1})$$

With this the constitutive equation is written as

$$\bar{\sigma}_{ij}(\omega) = G^*(\omega) \bar{\epsilon}_{ij}(\omega) \quad (\text{III-2})$$

in the frequency space where  $\bar{\sigma}_{ij}(\omega)$  and  $\bar{\epsilon}_{ij}(\omega)$  are respectively the Fourier transforms of  $\sigma_{ij}$  and  $\epsilon_{ij}$  in time\* [29].

\* For (III-2) the Fourier transform is defined as

$$\bar{f}(\omega) = \frac{1}{\sqrt{2\pi}} \int_{-\infty}^{\infty} f(t) e^{-i\omega t} dt .$$

The constitutive relation (III-2) with the complex modulus (III-1) implies the following constitutive equation in a time space:

$$\underline{\sigma}(x, t) = \int_{-\infty}^t G(t-\tau) \dot{\underline{\epsilon}}(x, \tau) d\tau \quad (\text{III-3})$$

where the relaxation function  $G(t)$  is related with the complex modulus  $G^*(\omega)$  as

$$G^*(\omega) = \frac{1}{i\omega} \int_0^\infty G(t) e^{-i\omega t} dt. \quad (\text{III-4})$$

Therefore, when the complex modulus  $G^*(\omega)$  is obtained by experiments, usually by means of harmonic excitation of strain, the relaxation function  $G(t)$  can be found by inversion of equation (III-4).

The viscoelastic property of the elastomer under consideration has been extensively investigated (e.g. [19]) and its complex modulus is given in Fig. 15. This complex modulus can be reasonably well described by a three parameter equation as

$$G'(\omega) = a - \frac{6}{\omega^2 + c} . \quad (\text{III-5})$$

These three parameters are obtained from another set of parameters: the maximum values of  $G'(\omega)$  when  $\omega \rightarrow \infty$ , the maximum value of  $G''(\omega)/G'(\omega)$  and the  $\omega_0$  at which  $G''(\omega)/G'(\omega)$  becomes the maximum. Therefore, if we characterize the complex modulus by proper choice of  $G'(\omega)$ ,  $\omega_0$  and the maximum of  $G''(\omega_0)/G'(\omega_0)$ , the relaxation functions are completely described.

## 2. Formulation

### Elastic Layer

In Fig. 16 a typical viscoelastic layer ( $n^{\text{th}}$ ) is shown between two adjacent elastic layers ( $n^{\text{th}}$  and  $(n+1)^{\text{th}}$ ) with appropriate discretization. The approximate equations of motion for the  $n^{\text{th}}$  elastic layer given by Eq. (II-7) are still valid. But remembering the new discretizing notation in Fig. 16 we now have to replace  $(\cdot)_n$  and  $(\cdot)_{n-1}$  by  $(\cdot)_n^-$  and  $(\cdot)_{n-1}^+$ , respectively. The results are

$$\begin{aligned}
 \rho(\ddot{u}_n^- + \dot{u}_{n-1}^+) &= c_{11}(\dot{u}_n^- + \dot{u}_{n-1}^+),_{11} + \frac{c_{12}}{b}(\dot{v}_n^- - \dot{v}_{n-1}^+),_1 + \frac{1}{b}(\tau_n^- - \tau_{n-1}^+) \\
 \rho(\ddot{v}_n^- - \ddot{v}_n^+) &= -\frac{3c_{12}}{b}(\dot{u}_n^- + \dot{u}_{n-1}^+),_1 - \frac{3c_{22}}{b^2}(\dot{v}_n^- - \dot{v}_{n-1}^+)_1 + \frac{3}{b}(\sigma_n^- + \sigma_{n-1}^+) + (\tau_n^- - \tau_{n-1}^+),_1 \\
 \rho(\ddot{u}_n^- - \dot{u}_{n-1}^+) &= \hat{c}_{11}(\dot{u}_n^- - \dot{u}_{n-1}^+),_{11} - \frac{3c_{66}}{b^2}(\dot{u}_n^- - \dot{u}_{n-1}^+)_1 - \frac{3c_{66}}{b}(\dot{v}_n^- + \dot{v}_{n-1}^+),_1 \quad (\text{III-6}) \\
 &\quad + \frac{c_{12}}{c_{22}}(\sigma_n^- - \sigma_{n-1}^+),_1 + \frac{3}{b}(\tau_n^- + \tau_{n-1}^+) \\
 \rho(\ddot{v}_n^- + \dot{v}_{n-1}^+) &= c_{66}\{\frac{1}{b}(\dot{u}_n^- - \dot{u}_{n-1}^+),_1 + (\dot{v}_n^- + \dot{v}_{n-1}^+),_{11}\} + \frac{1}{b}(\sigma_n^- - \sigma_{n-1}^+)
 \end{aligned}$$

### Viscoelastic Layer

Since the thickness of the elastomer is thin compared with the elastic layer, we can assume that the stress field is uniform through the thickness of the elastomer. In other words, we have  $\sigma_n^- = \sigma_n^+ = \sigma_n$  and  $\tau_n^- = \tau_n^+ = \tau_n$  for (III-6). Therefore, the following compatibility conditions for the

elastomer can be obtained immediately:

$$\varepsilon_{12(n)} = \frac{1}{4} \frac{\partial}{\partial x_1} (v_n^+ + v_n^-) + \frac{1}{2D} (u_n^+ - u_n^-) \quad (III-7)$$

$$\varepsilon_{22(n)} = \frac{1}{D} (v_n^+ - v_n^-)$$

where  $D$  is the thickness of the elastomer.

We further assume that the dissipation is mostly due to shear motion, i.e., that the normal component of the continuous traction vector is transmitted through the viscoelastic layer purely elastically. Therefore, by combining (III-7) with (III-3) we find

$$\sigma_n = \frac{E}{D} (v_n^+ - v_n^-) \quad (III-8)$$

$$\tau_n = \int_{-\infty}^t G(t-\tau) \left\{ \frac{1}{2} \frac{\partial}{\partial x_1} (\dot{v}_n^+ + \dot{v}_n^-) + \frac{1}{D} (\dot{u}_n^+ - \dot{u}_n^-) \right\} d\tau .$$

These two equations and four more from Eq. (III-6) are the complete equations needed to solve the impact on a composite plate with elastomer. For a plate made of  $N$  elastic layers and  $(N-1)$  viscoelastic layers Eq. (III-6) provides  $4N$  equations and (III-8) gives  $2(N-1)$  equations. Since the total number of the unknowns are now  $6N+2$  ( $u_o, v_o, \sigma_o, \tau_o; u_1^-, v_1^-, u_1^+, v_1^+, \sigma_1, \tau_1; \dots \dots; u_{N-1}^-, v_{N-1}^-, u_{N-1}^+, v_{N-1}^+, \sigma_{N-1}, \tau_{N-1}; u_N, v_N, \sigma_N, \tau_N$ ) we can solve this system of equations with four additional conditions supplied by the suitable boundary conditions.

Here we notice that the governing equations are now a set of six difference-integro-partial differential equations. These equations can be

reduced to difference equations after appropriate integral transforms and the resulting difference equations can be handled rather simply, as in the previous chapter.

### 3. Numerical Results and Discussion

#### Impact on Plate

For the report we examine the impact on a plate consisting of two elastic layers and a viscoelastic layer, as shown in Fig. 17, with an impact function

$$\begin{aligned}\sigma_0 &= P_0 \left\{ 1 - \left( \frac{x_1}{a} \right)^2 \right\} \sin \frac{\pi t}{t_0} ; \quad |x_1| < a \quad \text{and} \quad 0 < t < t_0 \\ &= 0 \quad ; \quad |x_1| > a \quad \text{or} \quad t > t_0, \text{ or} \quad t < 0\end{aligned}\tag{III-9}$$

with all other stress components vanishing on both surfaces of the plate.

Now by putting  $n = 1$  and  $2$  into Eq. (III-6) we have eight equations and two more equations are obtained from Eq. (III-8). We again normalize these equations and take the integral transform, as in Chapter II. The resulting equations are:

$$\begin{aligned}
 & -\left(\frac{fs^2}{\Delta} + \frac{c_{11}}{\Delta} bk^2\right) (\hat{U}_1^- + \hat{U}_o^-) - c_{12} ik (\hat{V}_1^- - \hat{V}_o^-) + \hat{T}_1^- = 0 \\
 & 3c_{12} ik (\hat{U}_1^- + \hat{U}_o^-) - \left(\frac{fs^2}{b} + \frac{3c_{22}\Delta}{b}\right) (\hat{V}_1^- - \hat{V}_o^-) + 3\hat{\Sigma}_1^- - ik \frac{b\hat{T}_1}{\Delta} = -3\hat{\Sigma}_o^- \\
 & -\left(\frac{fs^2}{\Delta} + \frac{b}{\Delta} c_{66} k^2\right) (\hat{V}_1^- + \hat{V}_o^-) - c_{66} ik (\hat{U}_1^- - \hat{U}_o^-) + \hat{\Sigma}_1^- = \hat{\Sigma}_o^- \\
 & -\left(\frac{fs^2}{\Delta} + \frac{b}{\Delta} c_{11} k^2 + \frac{\Delta}{b} 3c_{66}\right) (\hat{U}_1^- - \hat{U}_o^-) + 3c_{66} ik (\hat{V}_1^- + \hat{V}_o^-) - \frac{c_{12}}{c_{22}} \frac{b}{\Delta} ik \hat{\Sigma}_1^- + 3\hat{T}_1^- = -\frac{c_{12}}{c_{22}} \frac{b}{\Delta} ik \hat{\Sigma}_o^- \\
 & -\left(\frac{fs^2}{\Delta} + \frac{c_{11}}{\Delta} bk^2\right) (\hat{U}_2^- + \hat{U}_1^-) - c_{12} ik (\hat{V}_2^- - \hat{V}_1^-) - \hat{T}_1^- = 0
 \end{aligned}
 \tag{III-10}$$

$$\begin{aligned}
 & 3c_{12} ik (\hat{U}_2^- + \hat{U}_1^-) - \left(\frac{fs^2}{b} + \frac{3c_{22}\Delta}{b}\right) (\hat{V}_2^- - \hat{V}_1^-) + 3\hat{\Sigma}_1^- + \frac{b}{\Delta} ik \hat{T}_1^- = 0 \\
 & -\left(\frac{fs^2}{\Delta} + \frac{b}{\Delta} c_{66} k^2\right) (\hat{V}_2^- + \hat{V}_1^-) - c_{66} ik (\hat{U}_2^- - \hat{U}_1^-) - \hat{\Sigma}_1^- = 0 \\
 & -\left(\frac{fs^2}{\Delta} + \frac{b}{\Delta} c_{11} k^2 + \frac{\Delta}{b} 3c_{66}\right) (\hat{U}_2^- - \hat{U}_1^-) + 3c_{66} ik (\hat{V}_2^- + \hat{V}_1^-) + \frac{c_{12}}{c_{22}} \frac{b}{\Delta} ik \hat{\Sigma}_1^- + 3\hat{T}_1^- = 0
 \end{aligned}$$

$$\hat{\Sigma}_1^- = E \frac{\Delta}{D} (\hat{V}_1^- - \hat{V}_2^-)$$

$$\hat{T}_1^- = \bar{G}(s) \left\{ \frac{\Delta}{D} (\hat{U}_1^- - \hat{U}_2^-) - \frac{ik}{2} (\hat{V}_1^- + \hat{V}_2^-) \right\}$$

where  $\bar{G}(s)$  is the Laplace transform of the relaxation function  $G(t)$

with respect to  $\tau = t/T_o$  and we have used the boundary conditions

$\tau_o = \tau_2 = \sigma_2 = 0$ . From the above 10 equations we can find 10 unknowns  $(\hat{U}_o^-, \hat{V}_o^-, \hat{U}_1^-, \hat{V}_1^-, \hat{U}_1^+, \hat{V}_1^+, \hat{\Sigma}_1^-, \hat{T}_1^-; \hat{U}_2^-, \hat{V}_2^-)$  with given impact function  $\hat{\Sigma}_o^-$  and once these are calculated the displacement and the stress fields can be computed by inversions of the integral transforms by means of the FFT algorithm.

### Numerical Results

For the present computation we have used the Young's modulus  $E = .7*10^4$  psi and the shear modulus  $G'(\omega) = .817*10^4 - \frac{2.41*10^{12}}{3*10^4 + \omega^2}$  for the elastomer where  $\omega$  is given in hertz. The  $G'(\omega)$  in this case implies that  $G'(\infty) = .817*10^4$  psi and  $\max(G''(\omega)/G'(\omega)) = 3.3$  at  $\omega_0 = 800$  Hz.

The propagation of stress wave in this case is quite similar to that of the composite plate without an elastomer layer except the peak values of the interlaminar stress. Values of the peak stress with different thickness of the elastomer layer are plotted with those of the purely elastic plate in Fig. 18. As we can see in this figure the interlaminar shear stress has increased by a small amount while a reduction of the normal stress is considerable when the elastomer layer becomes thicker and thicker. From this result it is obvious that the reduction of the normal component of stress can be achieved by introducing such a soft and energy-dissipating elastomer layer.

### Discussion

In addition to the simple reduction of the normal stress it is also observed that the amount of reduction increases with the value of  $G''(\omega)/G'(\omega)$  and the location of  $\omega_0$  at which  $G''(\omega)/G'(\omega)$  becomes the maximum value. In other words, we can make the dissipation effect more serious by choosing an elastomer whose  $G''(\omega)/G'(\omega)$  becomes maximum at  $\omega_0$  around which the most of the impact energy is carried out.

It is also believed that a further dissipation effect will be possible if we make the transmission of the normal stress viscoelastic across the elastomer layer, which we have assumed is elastic for this report.

#### IV. IMPACT ON A PLATE WITH A CRACK

##### 1. Introduction

When the impact stress is low, the impact is elastic and the stresses in the plate can be described by elastic wave propagation. When the stress is increased beyond a certain limit then the impact damage occurs. Elastic-plastic impact is complicated for two reasons, namely, unloading and loading must be treated differently, and the strain rate effect [30] must be included. If the impact stress is increased further to a certain level where the induced stress is higher than the strength of a target material then penetration begins to occur. In this limit the target material sometimes behaves as a fluid and such a state of impact is known as a hydraulic impact [31]. Another failure mode is the occurrence of interlaminar cracks.

Investigation of the stress state in solids with cracks falls in the category of so-called fracture mechanics and has been under an extensive scrutiny since the famous enunciation by Griffith [32]. Presence of cracks inside a material usually leads us to a mixed boundary value problem and only a limited class of problems can be solved [33,34]. In the case of dynamic loading the problem becomes more difficult due to the scattering of the stress wave by the crack [21-24]. In this report we will formulate the problem of a plate with a crack which is subject to a dynamic loading.

Our original goal was to study the effect of interlaminar cracks in composite plates in response to impact loads. Debugging problems in other parts of this report, however, used valuable time originally set aside for this problem. The following section is an attempt to illustrate the

use of the Mindlin plate theory for the study of interlaminar cracks and to point out the mathematical difficulties that must be overcome in solving the problem.

## 2. Formulation

### Description of Problem

The plate under consideration has a crack on the midplane running from  $x_1 = -h$  to  $+h$  as shown in Fig. 19. Stress can be applied either on the surface of the plate or on the crack surface. In the former case the crack surfaces can be in contact and the boundary conditions become more complex due to the partial continuity of stresses and displacements during the contact. For the present report to illustrate the mathematical difficulties we assume that the crack surface is subject to a known compressive impact.

### Governing Equation and Boundary Conditions

We can formulate this crack problem by assuming that the lower and the upper half plates are made of a number of layers but for simplicity we consider the plate to consist of two identical layers and the crack to be present on the interface of these two layers. Following the notation shown in Fig. 19 we have the governing equations identical to Eq. (III-6) with  $n = 1$  and 2. The boundary condition requires that both plate surfaces remain traction free. The crack surface is subject to a prescribed impact condition while the displacement and stress are continuous along the layer boundary outside the crack. Namely, we have

$$\begin{aligned} \sigma_0 &= \tau_0 = \sigma_2 = \tau_2 = 0 \\ \sigma_1^+ &= \sigma_1^- = -p_0(x_1, t) \\ \tau_1^+ &= \tau_1^- = 0 \end{aligned} \quad \left. \begin{array}{l} \\ \\ \end{array} \right\} |x| < h \quad (IV-1)$$
$$\begin{aligned} u_1^+ &= u_1^- , \quad v_1^+ = v_1^- \\ \sigma_1^+ &= \sigma_1^- , \quad \tau_1^+ = \tau_1^- \end{aligned} \quad \left. \begin{array}{l} \\ \\ \end{array} \right\} |x| > h .$$

Due to the twofold symmetry of the problem we now have  $u_o = u_2$ ,  $v_o = -v_2$ ,  $\tau_1^+ = \tau_1^- = 0$  and we can set  $u_1^+ = u_1^- = u_1$ ,  $-v_1^+ = v_1^- = v_1$ .

Thus, the eight equations obtained from Eq. (III-6) are now reduced to

$$\begin{aligned}
 \rho(\ddot{u}_1 + \ddot{u}_o) &= c_{11}(u_1 + u_o)_{,11} + \frac{c_{12}}{b}(v_1 - v_o)_{,1} \\
 \rho(\ddot{v}_1 - \ddot{v}_o) &= -\frac{3c_{12}}{b}(u_1 + u_o)_{,1} - \frac{3c_{22}}{b^2}(v_1 - v_o) + \frac{3\sigma}{b} \\
 \rho(\ddot{u}_1 - \ddot{u}_o) &= \hat{c}_{11}(u_1 - u_o)_{,11} - \frac{3c_{66}}{b^2}(u_1 - u_o) - \frac{3c_{66}}{b}(v_1 + v_o)_{,1} + \frac{c_{12}\sigma}{c_{22}},_1 \\
 \rho(\ddot{v}_1 + \ddot{v}_o) &= c_{66}\left\{\frac{1}{b}(u_1 - u_o)_{,1} + (v_1 + v_o)_{,11}\right\} + \frac{\sigma}{b}
 \end{aligned} \tag{IV-2}$$

and the boundary condition is now

$$\left. \begin{array}{l} \sigma = -p_o(x_1, t) \quad |x_1| < h \\ v_1 = 0 \quad |x_1| > h \end{array} \right\} \quad \text{along } x_2' = 0 \tag{IV-3}$$

#### Dual Integral Equation

We now normalize the governing equation (IV-2) and take the integral transform. Then we have

$$\begin{bmatrix} (fs^2 + \frac{b}{\Delta}C_{11}k^2), & c_{12}ik, & 0, & 0 \\ -3c_{12}ik, & (fs^2 + \frac{3\Delta}{b}C_{22}), & 0, & 0 \\ 0, & 0, & c_{66}ik, & (fs^2 + \frac{b}{\Delta}C_{66}k^2) \\ 0, & 0, & (fs^2 + \frac{b}{\Delta}\hat{C}_{11}k^2 + \frac{3\Delta}{b}C_{66}), & -3c_{66}ik \end{bmatrix} \begin{bmatrix} \hat{\bar{u}}_1 + \hat{\bar{u}}_o \\ \hat{\bar{v}}_1 - \hat{\bar{v}}_o \\ \hat{\bar{u}}_1 - \hat{\bar{u}}_o \\ \hat{\bar{v}}_1 + \hat{\bar{v}}_o \end{bmatrix} = \begin{bmatrix} 0 \\ 3\hat{\Sigma} \\ \hat{\Sigma} \\ -\frac{c_{12}}{c_{22}} \frac{b}{\Delta} ik \hat{\Sigma} \end{bmatrix} \tag{IV-4}$$

and these can be solved for  $\hat{U}_0$ ,  $\hat{U}_1$ ,  $\hat{V}_0$ , and  $\hat{V}_1$  in terms of  $\hat{\Sigma}$ . Since the mixed boundary conditions are given by  $\sigma$  and  $v_1$  we solve  $\hat{V}_1$  as

$$\hat{V}_1 = K(s, k) \hat{\Sigma} \quad (IV-5)$$

with

$$K(s, k) = \frac{1}{2} \left[ \frac{3}{A} (fs^2 + \frac{b}{\Delta} C_{11} k^2) + \frac{1}{B} \left\{ \frac{C_{12}}{C_{22}} \frac{b}{\Delta} C_{66} k^2 - (fs^2 + \frac{b}{\Delta} \hat{C}_{11} k^2 + \frac{3b}{\Delta} C_{66}) \right\} \right]$$

$$A = \text{Det} \begin{vmatrix} (fs^2 + \frac{b}{\Delta} C_{11} k^2), C_{12} ik \\ -3C_{12} ik, (fs^2 + \frac{3\Delta}{b} C_{22}) \end{vmatrix} \quad (IV-6)$$

$$B = \text{Det} \begin{vmatrix} C_{66} ik, (fs^2 + \frac{b}{\Delta} C_{66} k^2) \\ (fs^2 + \frac{b}{\Delta} \hat{C}_{11} k^2 + \frac{3\Delta}{b} C_{66}), -3C_{66} ik \end{vmatrix}$$

Next we take the inverse transform of  $\hat{\Sigma}$  and  $\hat{V}_1$ , and apply the mixed boundary condition given in Eq. (IV-3). Since the boundary conditions are for all times  $t > 0$  we only take the inverse Fourier transform to apply the boundary conditions, i.e.,

$$\hat{\Sigma}(n, s) = \frac{1}{\sqrt{2\pi}} \int_{-\infty}^{\infty} \hat{\Sigma} e^{-ikn} dk \quad (IV-7)$$

$$\hat{V}_1(n, s) = \frac{1}{\sqrt{2\pi}} \int_{-\infty}^{\infty} K(s, k) \hat{\Sigma} e^{-ikn} dk .$$

Application of the boundary condition given by Eq. (IV-3) results in the following integral equation:

$$\begin{aligned}-\hat{P}_0(\eta, s) &= \frac{1}{\sqrt{2\pi}} \int_{-\infty}^{\infty} \hat{\Sigma} e^{-ik\eta} dk \quad : \quad |\eta| < h/\Delta \\ 0 &= \frac{1}{\sqrt{2\pi}} \int_{-\infty}^{\infty} K(s, k) \hat{\Sigma} e^{-ik\eta} dk \quad : \quad |\eta| > h/\Delta\end{aligned}\tag{IV-8}$$

for an unknown function  $\hat{\Sigma}$ .

### 3. Discussion

The integral equations of the type given in Eq. (IV-8) are known as dual integral equations, each of which has its own region of application and occur in mixed boundary value problems [35]. There are a number of ways to solve this type of integral equations, such as by reduction to a single Fredholm integral equation or by using the Wiener-Hopf technique [36]. Finding the solution depends on the kernel and in general it is rather difficult to do except for some special cases such as for Bessel kernels or trigonometric kernels.

Once the unknown function  $\hat{\Sigma}$  is determined the other variables  $(\hat{U}_0, \hat{U}_1, \hat{V}_0, \hat{V}_1)$  can be computed by solving the algebraic equation (IV-4) and the complete displacement can be found by inversions of the integral transform.

The problem formulated in this chapter is the simplest impact problem in that the contact of the crack surface does not occur and that it has a twofold symmetry. But it is expected that the critical response of the plate, particularly the stress field near the crack, can be a guideline for a more complex problem.

## V. CONCLUSION AND RECOMMENDED RESEARCH

The present theory is a generalization of Mindlin's approximate theory of plate applied to a multilayer plate under impact. By combined use of the finite difference technique in the thickness direction and integral transforms this model has been shown to be very effective for wave propagation analyses.

This model is extended to examine the effects of an elastomer layer between elastic layers of the plate. The reduction of interlaminar normal stress is significant due to the damping layer but further investigation seems necessary to determine the nature of the reduction.

The presence of a crack in the plate has been formulated. The resulting equations are given by dual integral equations which, as in many cases, are rather difficult to solve.

The basic idea of the periodic structure of the multilayer plate, where the governing equations are derived for each layer and given by a set of difference-differential equations, may be useful to handle different types of problems, such as heat conduction and thermoelastic problems in composite plates.

### References

- [1] Mindlin, R.D., - "High Frequency Vibrations of Crystal Plates", Quart. Appl. Math., Vol. 19, p. 51-61 (1961).
- [2] Moon, F.C., - "Wave Surfaces Due to Impact on Anisotropic Plates", J. Composite Materials, Vol. 6, p. 62 (1972).
- [3] Moon, F.C. and Kang, C.K., - "Analysis of Edge Impact Stresses in Composite Plates", TR to NASA Lewis Research Center, Princeton University (1974).
- [4] Moon, F.C., - "One Dimensional Transient Waves in Anisotropic Plate", J. Appl. Mech., Trans. ASME, p. 485 (1973).
- [5] Moon, F.C., Kim, B.S. and Fang - Landau, S.R., - "Impact of Composite Plates: Analysis of Stresses and Forces", TR to NASA Lewis Research Center, Princeton University (1976).
- [6] White, J.E. and Angona, F.A., - "Elastic Wave Velocities in Laminated Media", J. Acoust. Soc. Am., Vol. 27, p. 310 (1955).
- [7] Sun, C.T., Achenbach, J.D. and Herrmann, G., - "Continuum Theory for a Laminated Media", J. Appl. Mech., Trans. ASME, p. 467 (1968).
- [8] Nayfeh, A.H. and Gurtman, G.A., - "A Continuum Approach to the Propagation of Shear Waves in Laminated Wave Guides", J. Appl. Mech., Trans. ASME, p. 106 (1974).
- [9] Hegemier, G.A., Gurtman, G.A. and Nayfeh, A.M., - "A Continuum Mixture Theory of Wave Propagation in Laminated and Fiber Reinforced Composites", Int. J. Solids Struc., Vol. 9, p. 395 (1973).
- [10] Chao, T. and Lee, P.C.Y., - "Discrete Continuum Theory for Periodically Layered Composite Materials", J. Acoust. Soc. Am., Vol. 57, p. 78 (1975).
- [11] Lee, P.Y.C. and Nikodem, Z., - "An Approximate Theory for High Frequency Vibrations of Elastic Plates", Int. J. Solids Struc., Vol. 8, p. 581 (1972).
- [12] Dong, S.B. and Nelson, R.B., - "On Natural Vibrations and Waves in Laminated Orthotropic Plates", J. Appl. Mech., Trans. ASME, p. 739 (1972).
- [13] Hegemier, G.A. and Nayfeh, A.H., - "A Continuum Theory for Wave Propagation in Laminated Composites, Case 1: Propagation Normal to the Laminates", J. Appl. Mech., Trans. ASME, p. 503 (1973).
- [14] Hegemier, G.A. and Nayfeh, A.H., - "A Continuum Theory for Wave Propagation in Laminated Composites, Case 2: Propagation Parallel to the Laminates" J. Elasticity, Vol. 3, p. 125-140 (1973).

- [15] Cooley, J.W., Lewis, P.A.W. and Welch, P.D., - "The Fast Fourier Transform Algorithm: Programming Considerations in the Calculation of sine, cosine and Laplace Transforms", J. Sound Vib., Vol. 12, p. 315-337 (1970).
- [16] Brillouin, L. - Wave Propagation in Periodic Structures, Dover, N.Y. (1946).
- [17] Thomson, W.T., - Vibration Theory and Application, Prentice Hall, N.J. (1965).
- [18] Mindlin, R.D. and Medick, M.A., - "Extensional Vibrations of Elastic Plates", J. Appl. Mech., Trans. ASME, p. 561 (1959).
- [19] Yan, M.J. and Dowell, E.H., - "High Damping Measurements and Preliminary Evaluation of an Equation for Constrained Layer Damping", AIAA Journal, Vol. 11, p. 388 (1973).
- [20] Nakra, B.C. and Grootenhuis, P., - "Structural Damping Using a Four Layer Sandwich", J. Eng. Ind., Trans. ASME, p. 81 (1972).
- [21] Achenback, J.D., - "Crack Propagation Generated By a Horizontally Polarized Shear Wave", J. Mech. Phys. Solids, Vol. 18, p. 245 (1970).
- [22] Achenback, J.D. and Nuismer, R., - "Fracture Generated by a Dilatational Wave", Int. J. Frac. Mech., Vol. 7, p. 77 (1971).
- [23] Nuismer, R.J. and Achenback, J.D., - "Dynamically Induced Fracture", J. Mech. Phys. Solids, Vol. 20, p. 203 (1972).
- [24] Keer, L.M. and Luong, W.C., - "Diffraction of Waves and Stress Intensity Factors in a Cracked Layered Composite", J. Acoust. Soc. Am., Vol. 56, p. 1681 (1974).
- [25] Levy, H. and Lessman, F., - Finite Difference Equations, MacMillan Co. (1961).
- [26] Kim, B.S. and Moon, F., - "Impact on a Laminated Half Space", to be published.
- [27] Premont, E.J. and Stubenrauch, K.R., - "Impact Resistance of Composite Fan Blades", Tech. Rep. to NASA Lewis Research Center, NASA CR-134515, Pratt and Whitney Aircraft (1973).
- [28] Novak, R.C., - "Multi-Fiber Composites", Tech. Rep. to NASA Lewis Research Center, NASA OR-135062, United Technology (1976).
- [29] Christensen, R.M., - Theory of Viscoelasticity, Academic Press, N.Y. (1971).
- [30] Christescu, N., - Dynamic Plasticity, North-Holland, New York (1967).
- [31] Birkhoff, A. et al, - "Explosives with Lined Cavities", J. Appl. Phys. Vol. 19, p. 563 (1948).

- [32] Griffith, A., - "Phenomenon of Rupture and Flaw in the Solids", Phil. Trans. Roy. Soc. (London), Vol. A221, p. 163 (1921).
- [33] Liebowitz, H., (Ed.) - Fracture, Vol. 2, Academic Press, N.Y. (1968).
- [34] Sneddon, I.N. and Lowengrub, M. - Crack Problems in the Classical Theory of Elasticity, John Wiley and Sons, New York (1969).
- [35] Sneddon, I.N., - Mixed Boundary Value Problems in Potential Theory, North-Holland, Amsterdam (1966).
- [36] Noble, B., - Method Based On the Wiener-Hopf Technique, Pergamon Press, New York (1958).

## Figures

1. Composite Plate and Layer
- 2 a,b. Dispersion Relationship and Phase Velocity for Isotropic Plate: One-layer Model ( $\lambda = \mu$ ).
- 3 a,b. Dispersion Relationship and Phase Velocity for Composite Plate: One-layer Model (55% Graphite Fiber-Epoxy Matrix, Layup Angle  $45^\circ$ ).
- 4 a,b. Dispersion Relationship and Phase Velocity for Isotropic Plate: Two-layer Model ( $\lambda = \mu$ ).
- 5 a,b. Dispersion Relationship and Phase Velocity for Composite Plate: Two-layer Model (55% Graphite Fiber-Epoxy Matrix, Layup Angle  $45^\circ$ ).
- 6 a-f. Longitudinal Propagation Impact Stress in Isotropic Plate: Two-layer Model ( $\lambda = \mu = 1.2 \times 10^7$  psi;  $\Delta = 1$  cm,  $t_0 = 10$   $\mu$ sec,  $a = 4$  cm).
7. Transverse Propagation of Normal Stress in Isotropic Plate: 4-layer Model ( $\lambda = \mu = 1.2 \times 10^7$  psi;  $\Delta = 4$  cm,  $t_0 = 2$   $\mu$ sec,  $a = 40$  cm).
8. Transverse Propagation of Normal and Shear Stress in Isotropic Plate: (Same as in Fig. 7).
9. Transverse Propagation of Normal Stress in Composite Plate: 8-layer Model (55% Graphite Epoxy-Fiber Matrix, Layup Angle  $15^\circ$ ;  $\Delta = 1$  cm,  $t_0 = 2$   $\mu$ sec,  $a = 2$  cm).
10. Two Dimensional Propagation of Normal Stress in Isotropic Plate: 4-layer Model ( $\lambda = \mu = 1.2 \times 10^7$  psi;  $\Delta = 4$  cm,  $t_0 = 4$   $\mu$ sec,  $a = 4$  cm).
11. Velocity Surface and Wave Surface of Composite Plate (55% Graphite Fiber-Epoxy Matrix, Layup Angle  $45^\circ$ ).
- 12a,b. Comparison of Theoretical Wave Front and Numerical Wave Front of Composite Plate 10  $\mu$ sec after Impact: 55% Graphite Fiber-Epoxy Matrix (For Numerical Results; 8-layer Model,  $\Delta = 4$  cm,  $t_0 = 4$   $\mu$ sec,  $a = 2$  cm). Without and with Correction Factors.
13. Effect of Correction Factor on Transverse Propagation of Peak Value of Normal Stress: 8-layer Model (55% Graphite Fiber-Epoxy Matrix, Layup Angle  $45^\circ$ ;  $\Delta = 4$  cm,  $t_0 = 4$   $\mu$ sec,  $a = 2$  cm).
14. Viscoelastic Impact Energy Absorbing Models.
- 15a,b. Complex Modulus of Elastomer.
16. Plate with Viscoelastic Layers.
17. Impact of Plate Made of 2 Elastic Layers and a Viscoelastic Layer.

18. Peak Value of Interlaminar Stress Vs Elastomer thickness (Two Elastic Layers and a Viscoelastic Layer: ( $\Delta = 1$  cm,  $t_0 = 10$   $\mu$ sec,  $a = 4$  cm)).
19. Composite Plate with Crack.

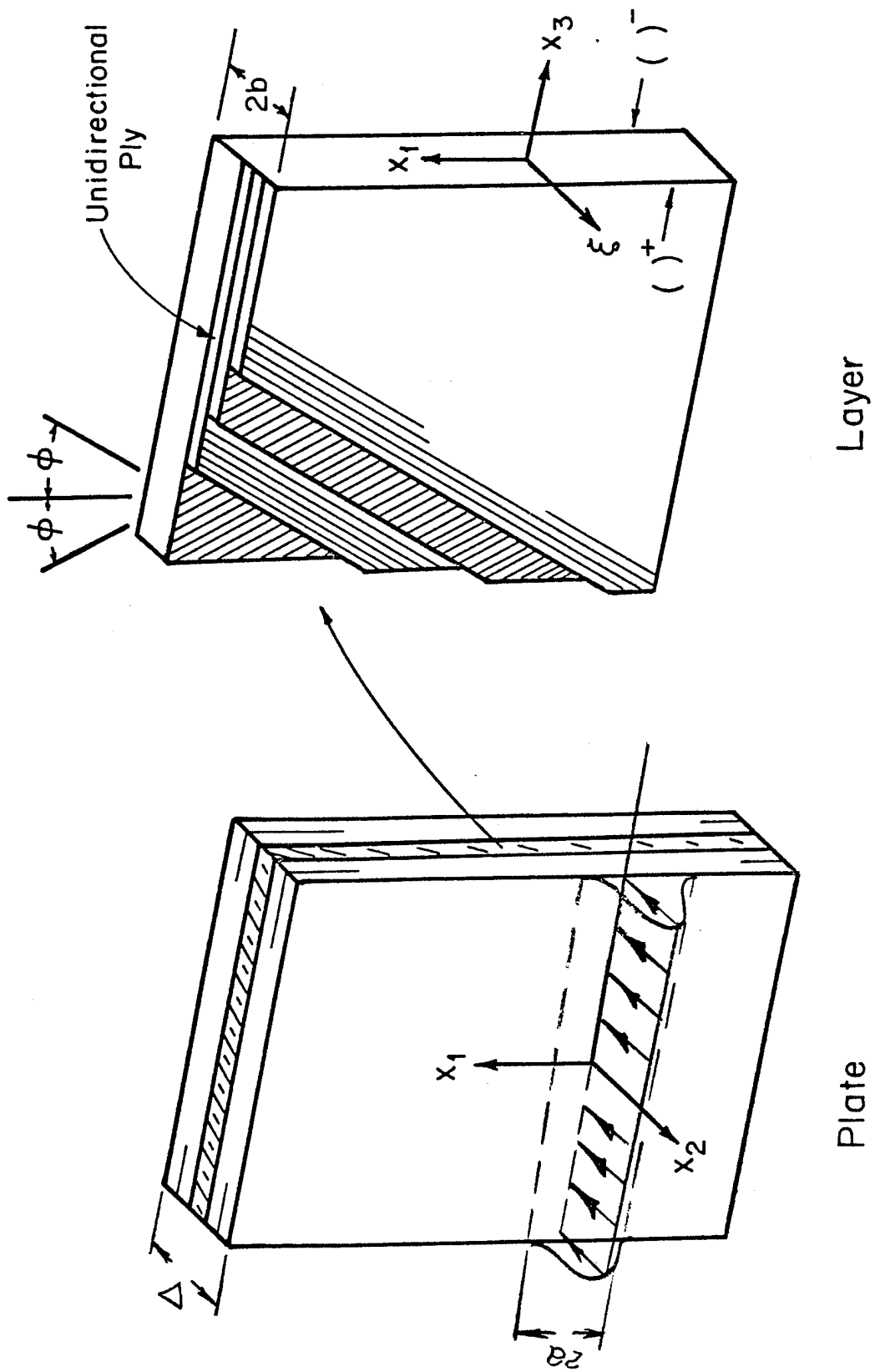


Figure 1. Multilayered Composite Plate and Layer

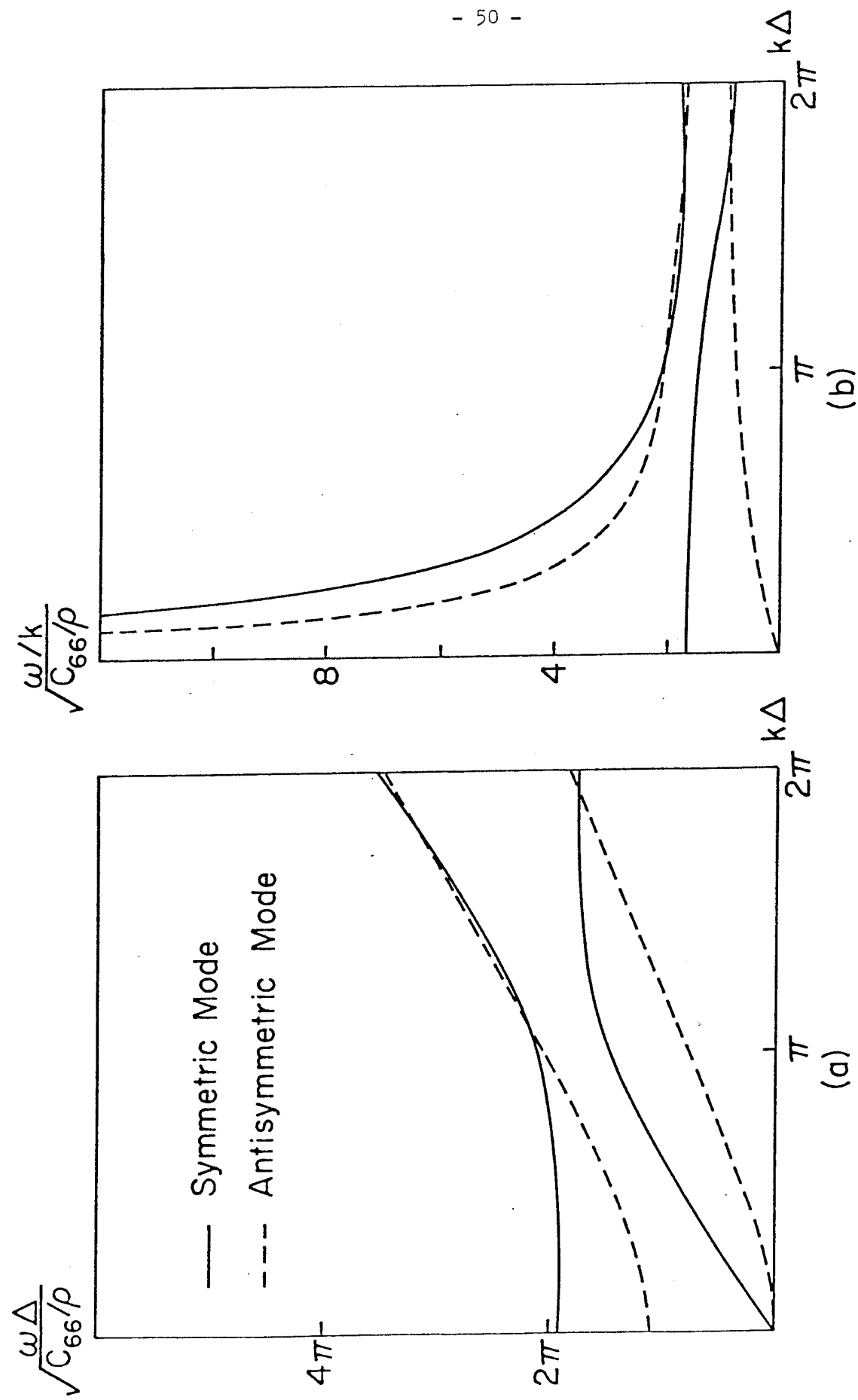


Figure 2. Dispersion Relationship and Phase Velocity of Isotropic Plate:  
One-Layer Model ( $\lambda = \mu$ , Poisson's Ratio =  $1/4$ )

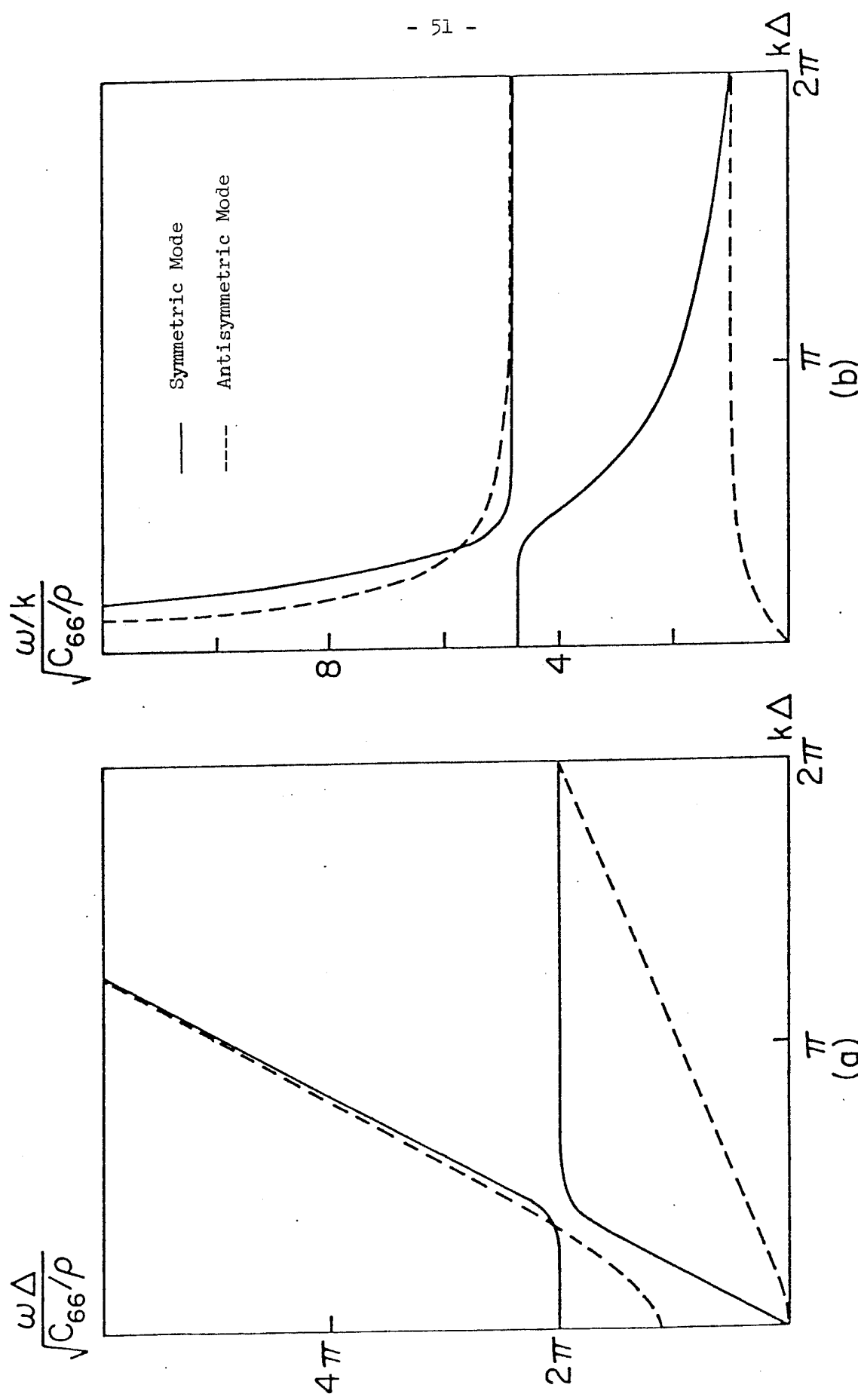


Figure 3. Dispersion Relationship and Phase Velocity of Composite Plate:  
One-Layer Model (55% Graphite Fiber - Epoxy Matrix; Layup Angle = 45°)

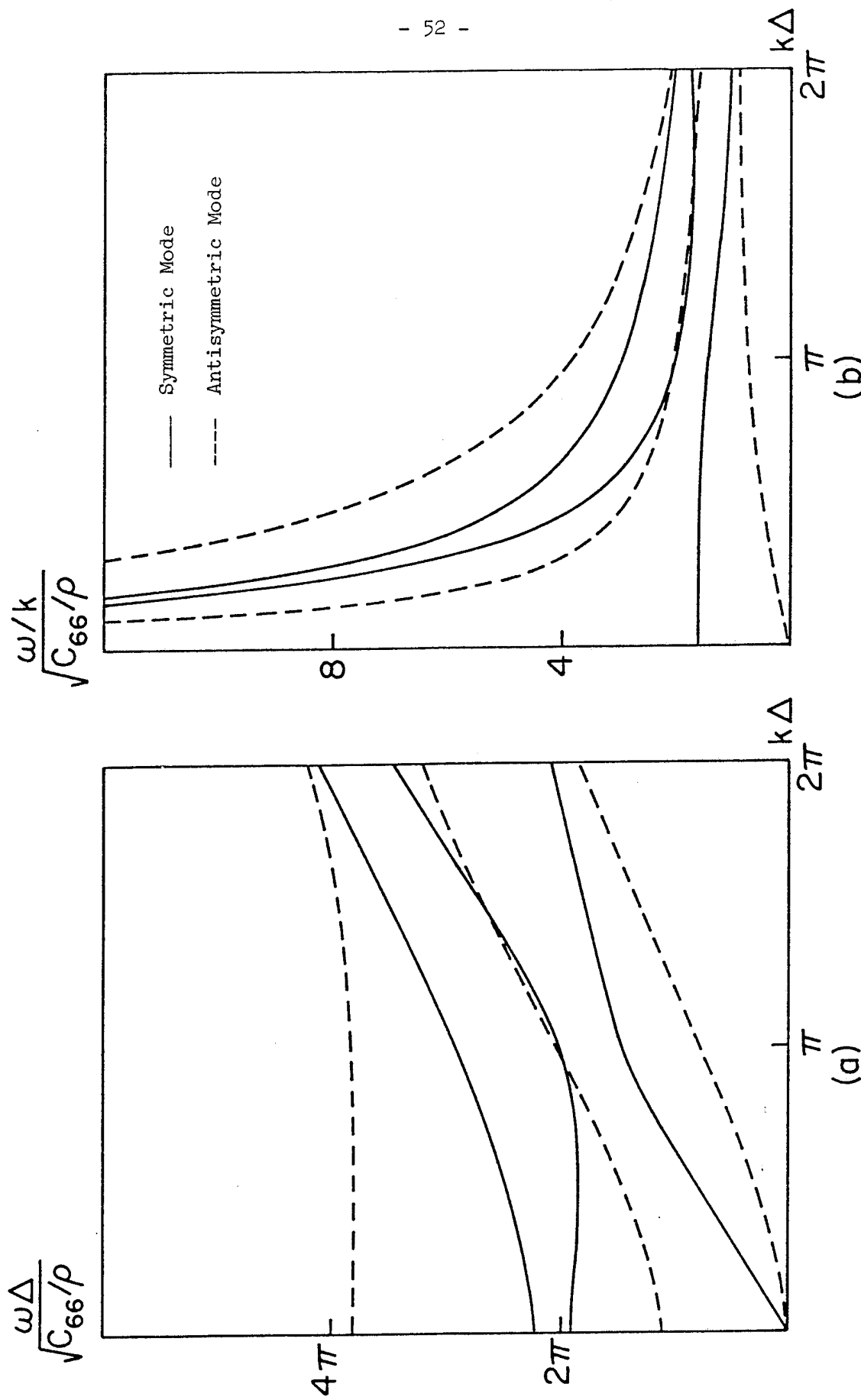


Figure 4. Dispersion Relationship and Phase Velocity of Isotropic Plate:  
Two-layer Model ( $\lambda = \mu$ , Poisson's Ratio = 1/4)

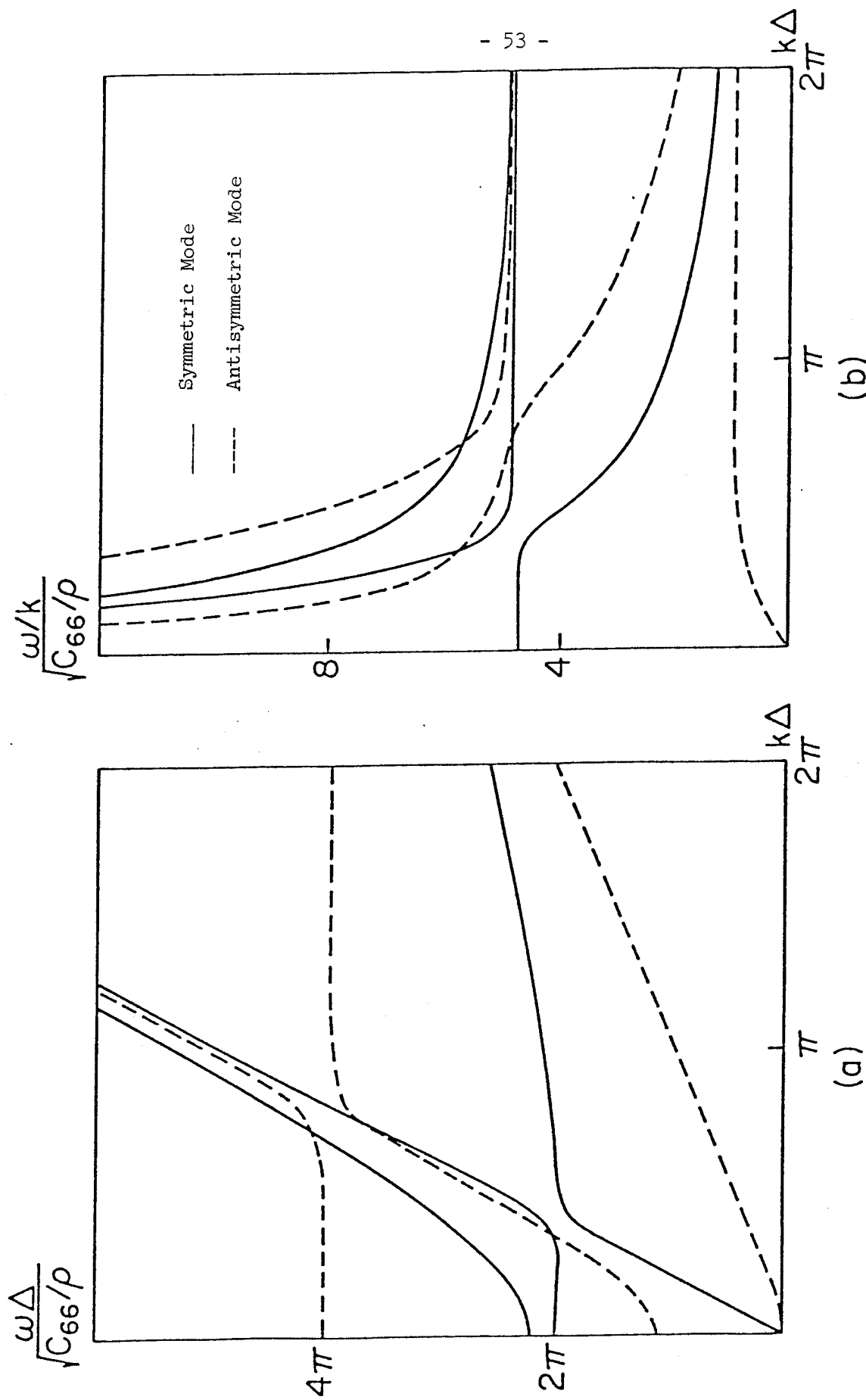


Figure 5. Dispersion Relationship and Phase Velocity of Composite Plate:  
Two-Layer Model (55% Graphite Fiber - Epoxy Matrix, Layup Angle = 45°)

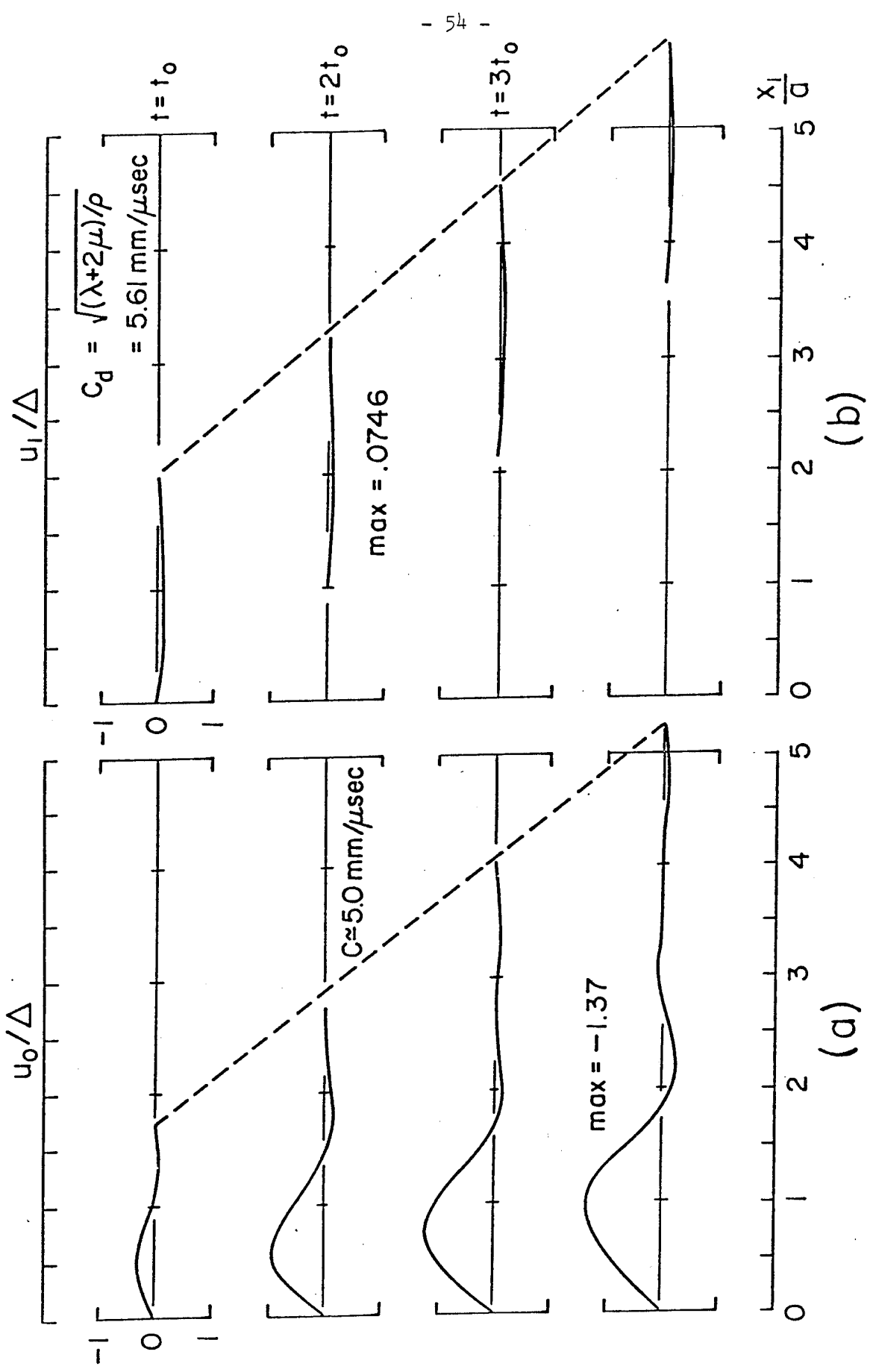


Figure 6 Longitudinal Propagation in Isotropic Plate; 2-layer Model  
 $(\lambda = \mu = 1.2 \times 10^7 \text{ psi}; \Delta = 1 \text{ cm}, t_0 = 10 \text{ usec}, a = 4 \text{ cm})$

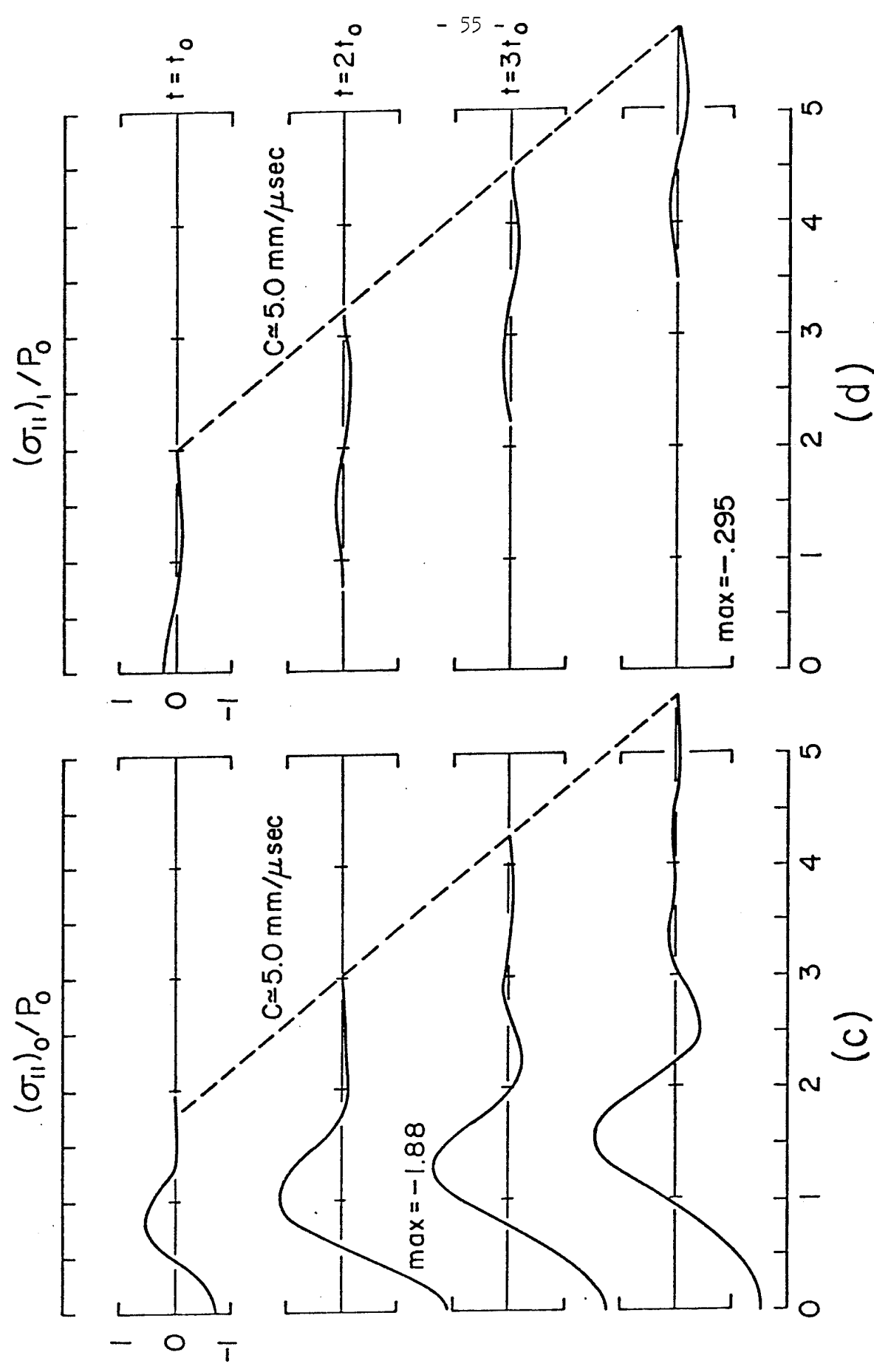


Figure 6 Continued

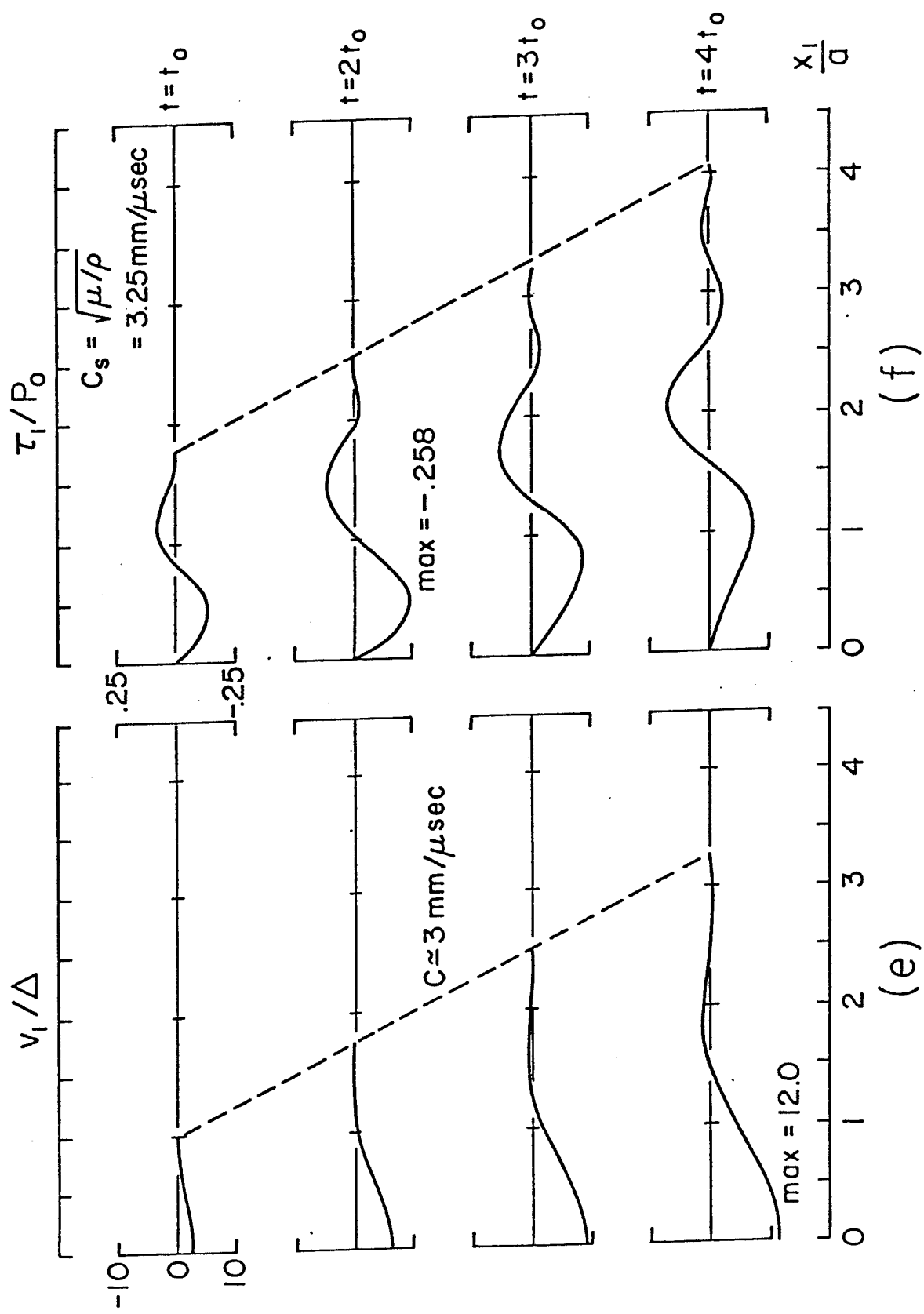


Figure 6 Continued

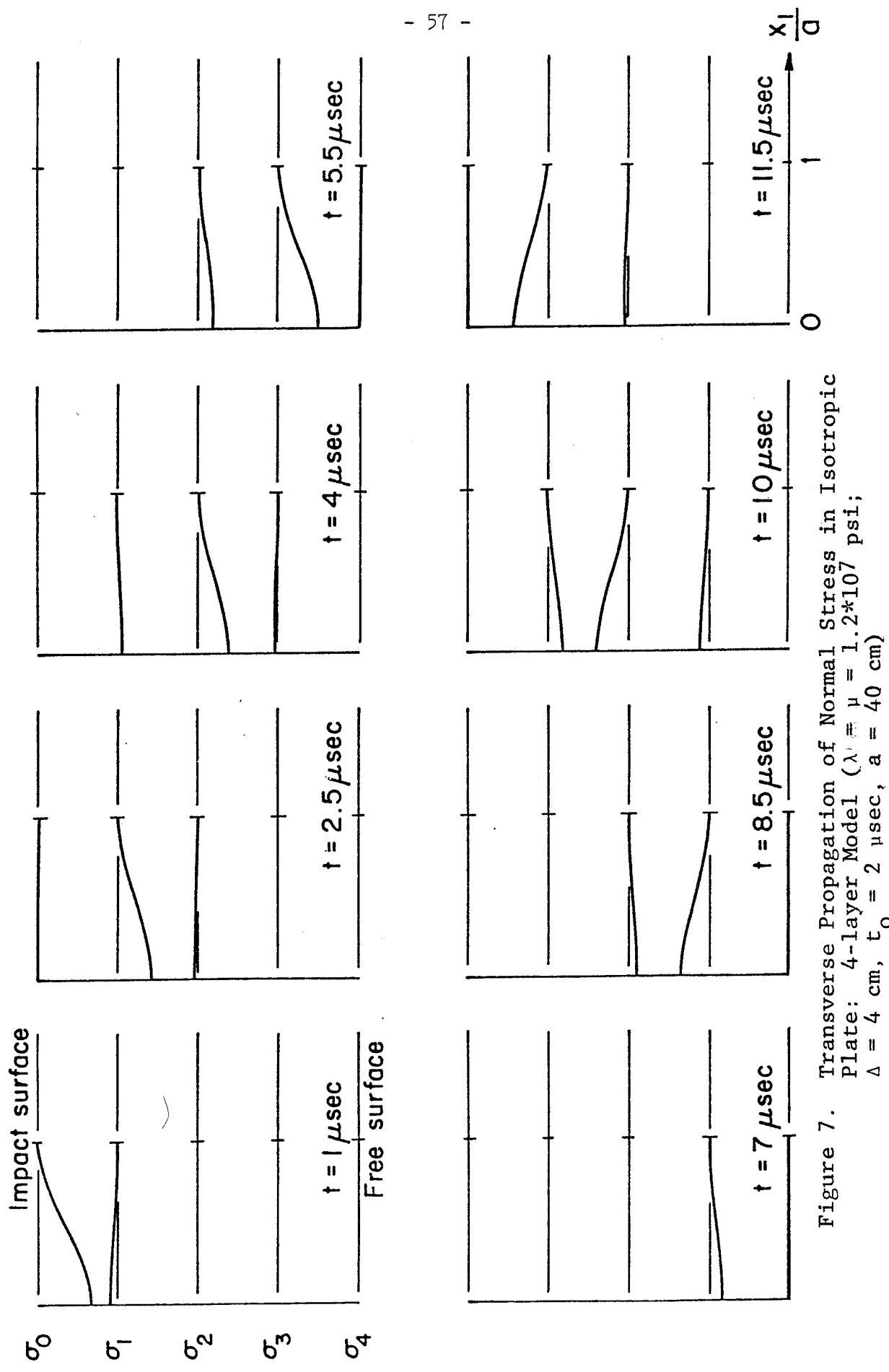


Figure 7. Transverse Propagation of Normal Stress in Isotropic Plate: 4-layer Model ( $\lambda = \mu = 1.2 \times 10^7$  psi;  
 $\Delta = 4$  cm,  $t_0 = 2 \mu\text{sec}$ ,  $a = 40$  cm)

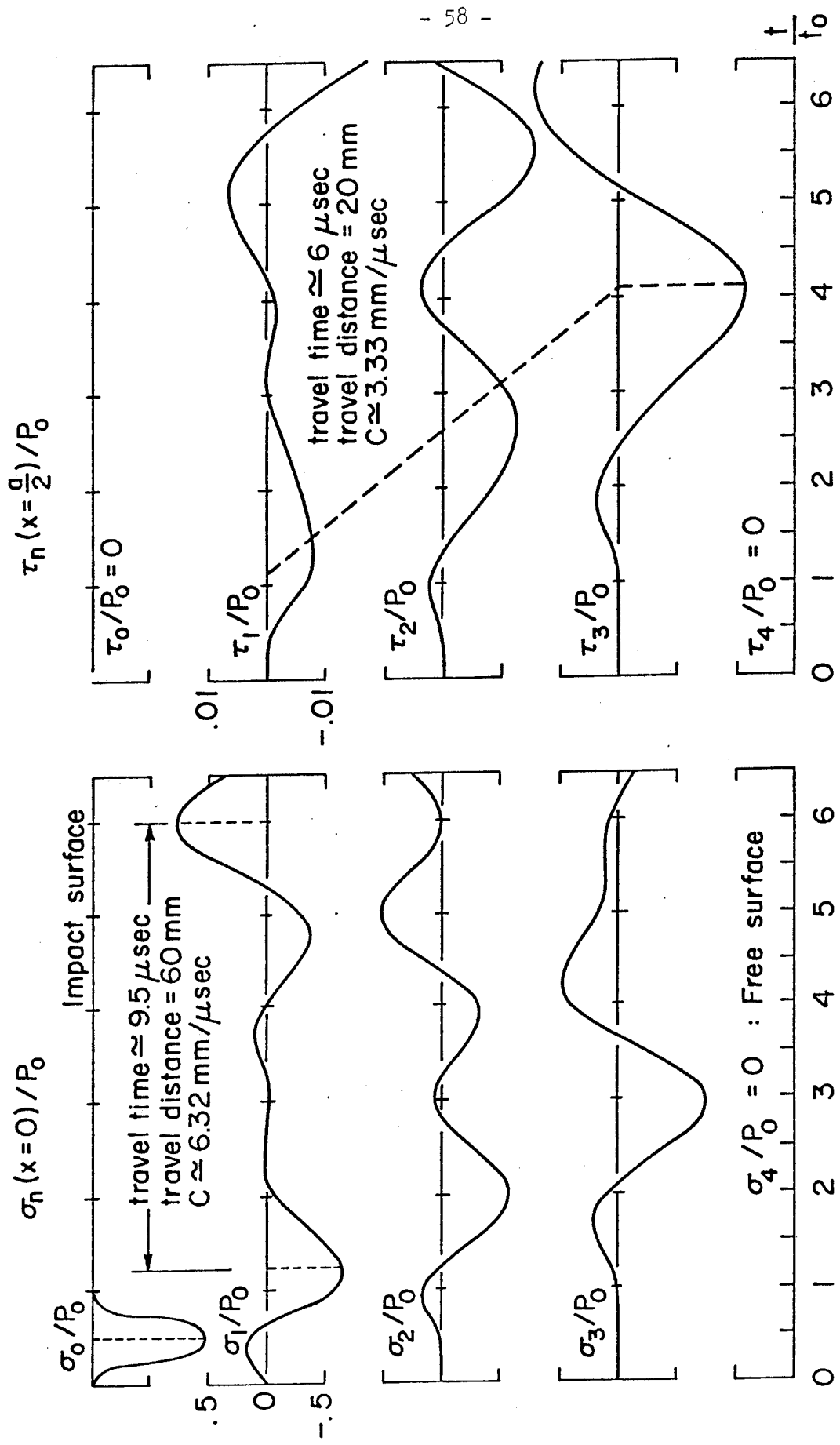


Figure 8. Transverse Propagation of Normal and Shear Stress  
(Same as in Figure 7)

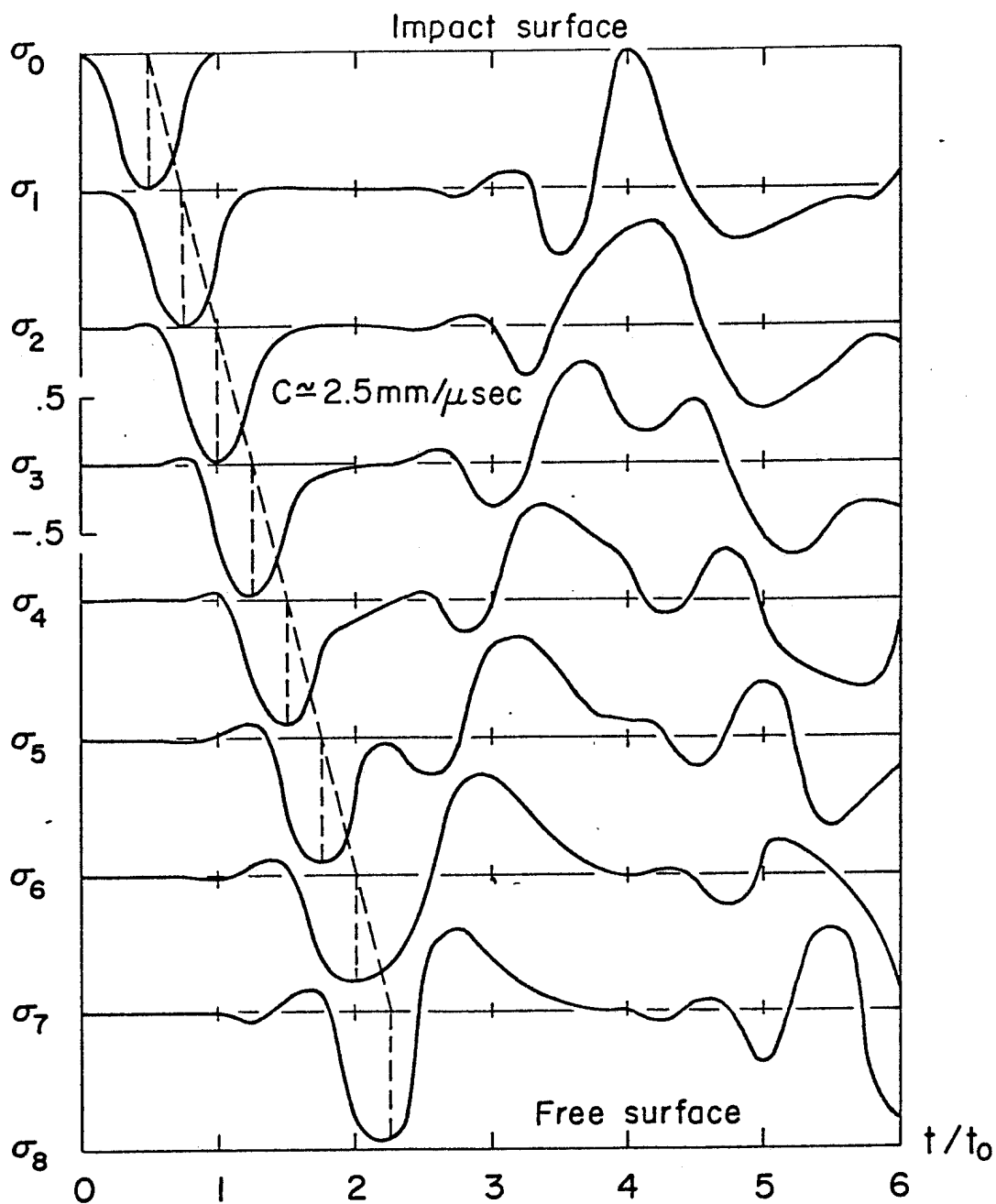


Figure 9 Transverse propagation of normal stress in composite plate; 8-layer Model (55% Graphite Fiber - Epoxy Matrix,  $\pm 15^\circ$  Layup;  $\Delta = 1 \text{ cm}$ ,  $t_0 = 2 \mu\text{sec}$ ,  $a = 2 \text{ cm}$ )

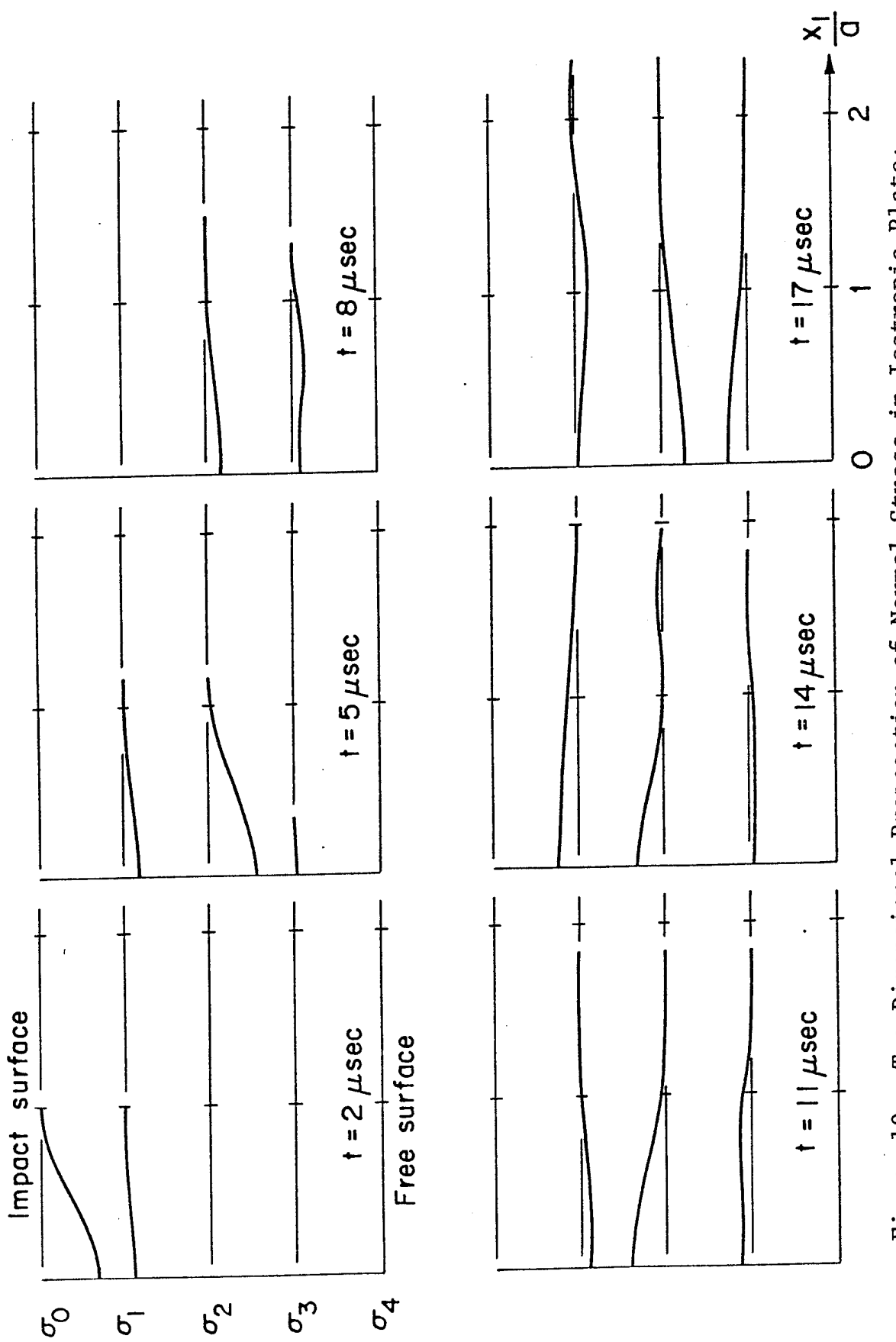


Figure 10. Two Dimensional Propagation of Normal Stress in Isotropic Plate:  
4-layer Model ( $\lambda = \mu = 1.2 \times 10^7$  psi;  $\Delta = 4$  cm,  $t_0 = 4 \mu\text{sec}$ ,  $a = 4$  cm)

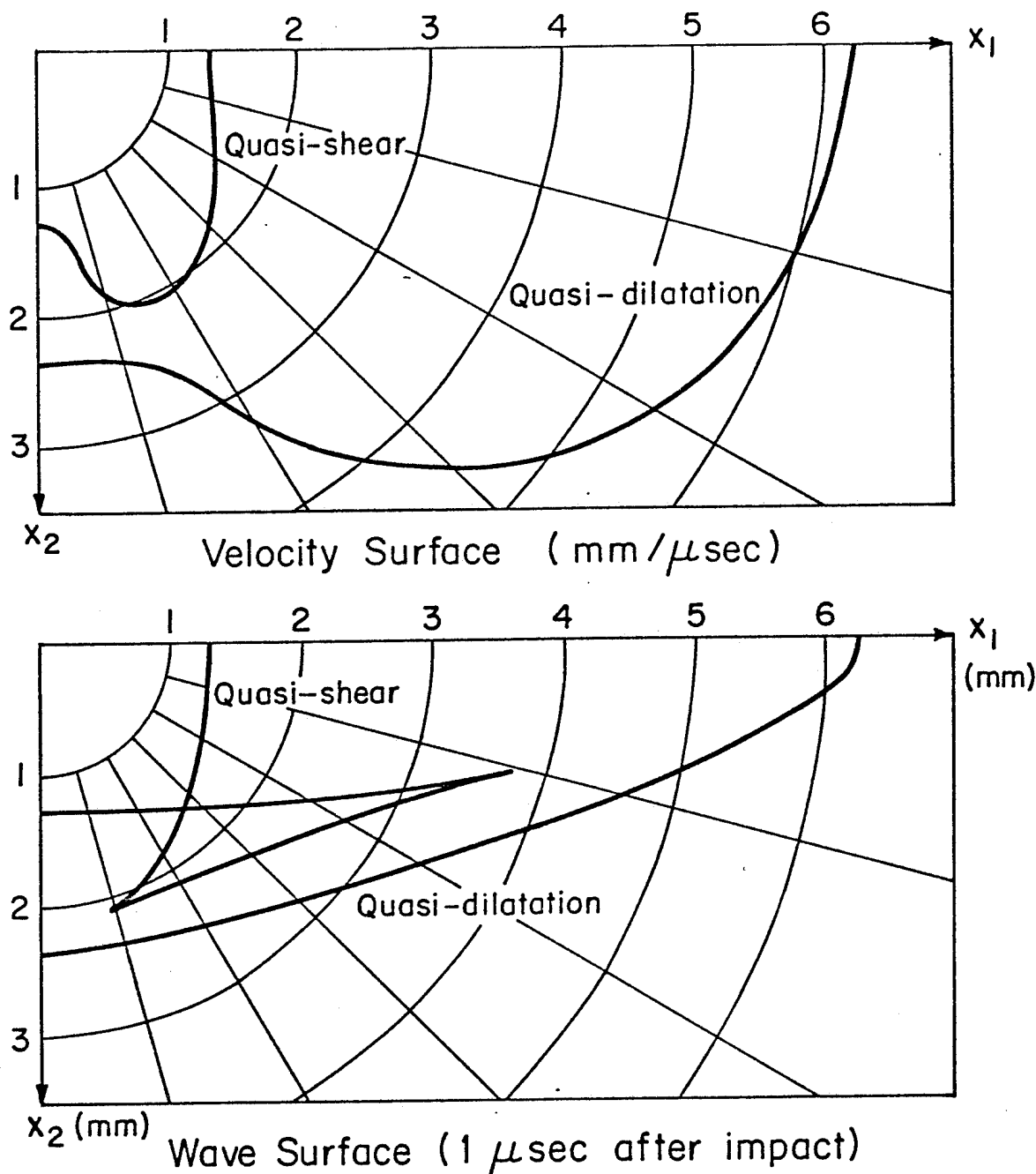


Figure 11. Velocity Surface and Wave Surface of Composite Plate (55% Graphite Fiber-Epoxy Matrix, Layup Angle 45°)

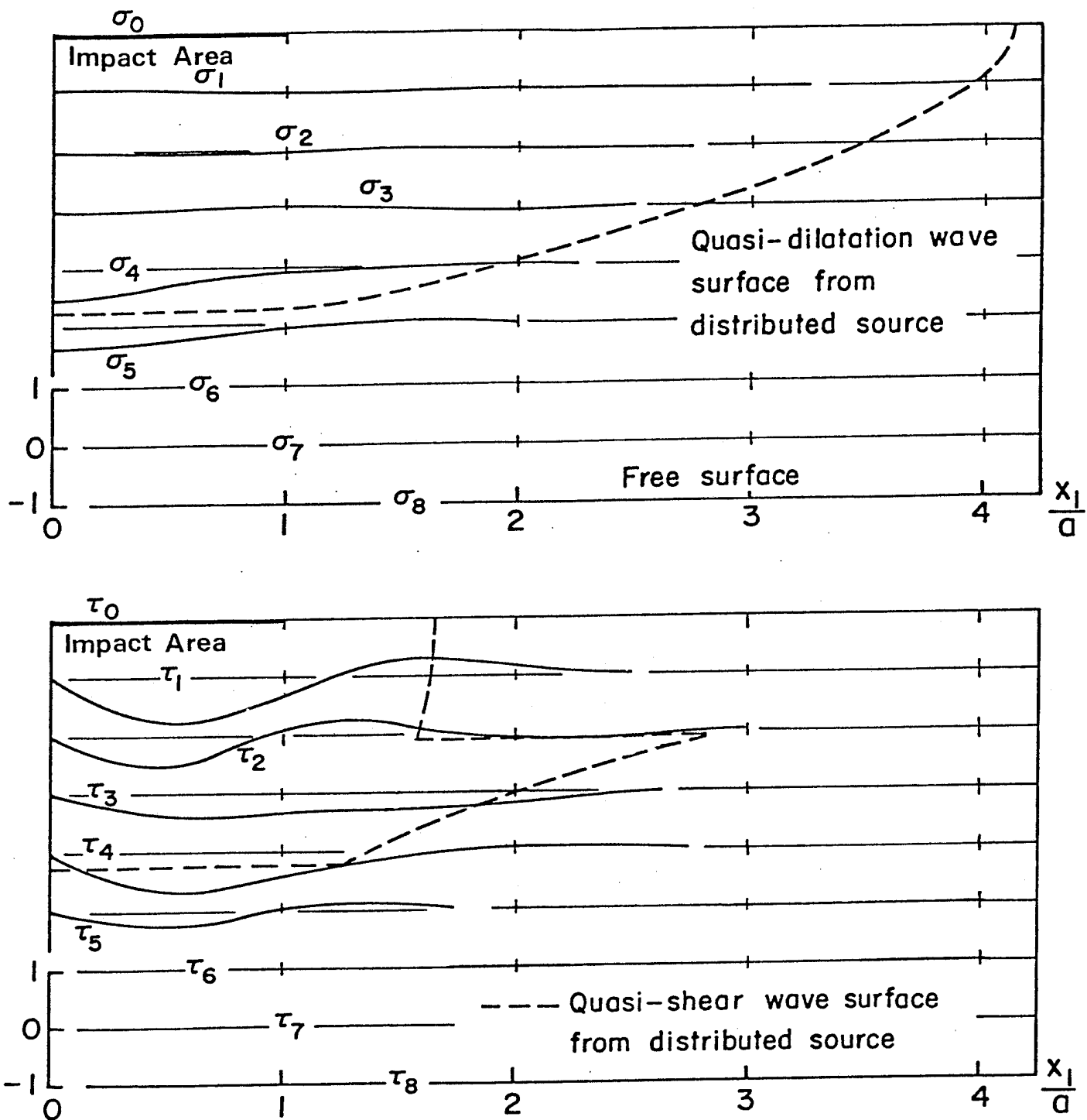


Figure 12a. Wave front 10  $\mu$ sec after impact (without correction factor)  
(55% Graphite Fiber-Epoxy Matrix,  $\pm 45^\circ$  Layup;  $\Delta = 4$  cm,  
8-layer Model;  $t_0 = 4 \mu$ sec,  $a = 2$  cm)

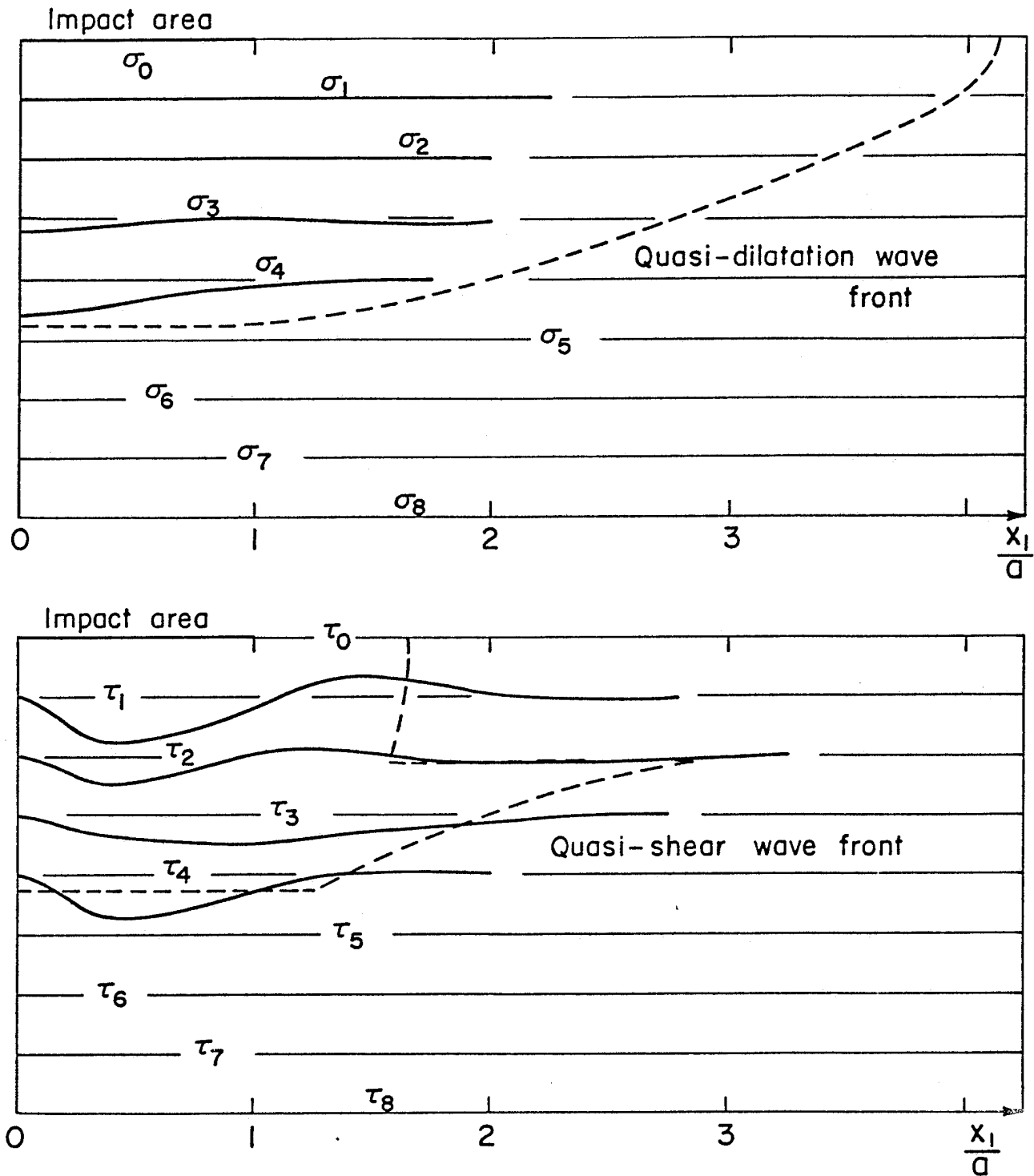


Figure 12b. Wave front 10  $\mu$ sec after impact (with correction factor)  
(55% Graphite Fiber-Epoxy Matrix,  $\pm 45^\circ$  Layup;  $\Delta = 4$  cm,  
8-layer Model;  $t = 4 \mu$ sec,  $a = 2$  cm)

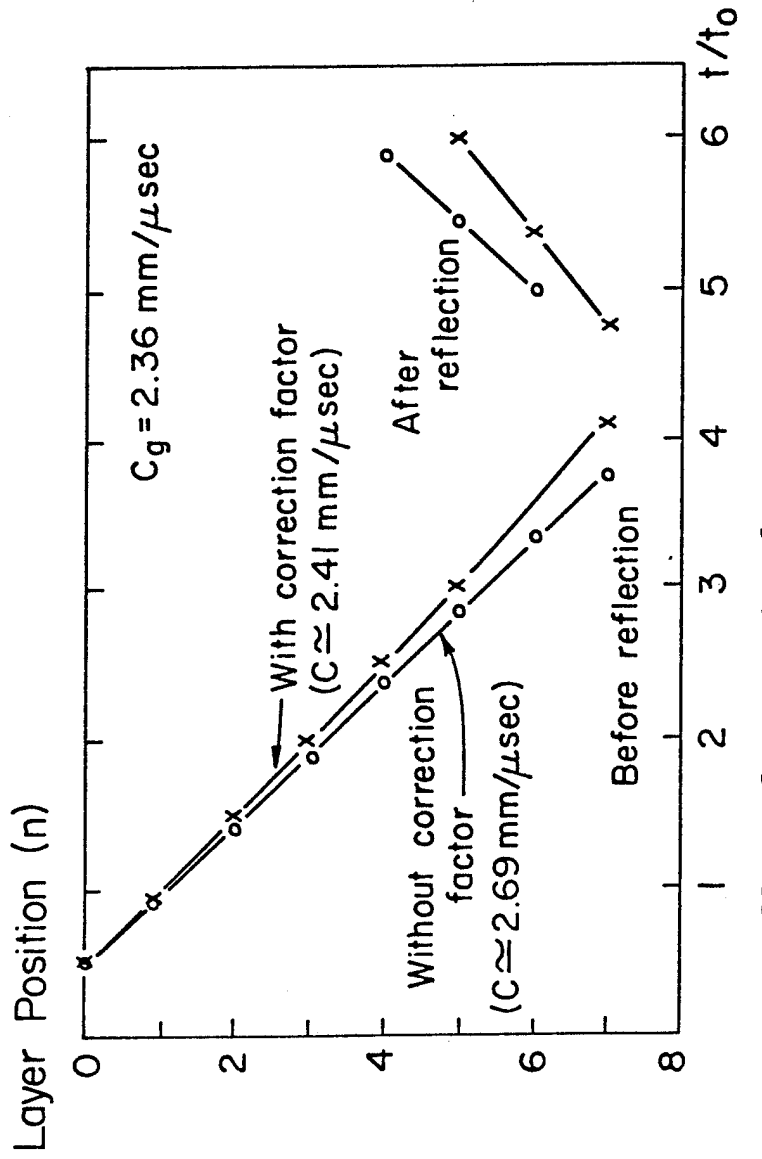


Figure 13 Effect of correction factors on transverse propagation of  $\max \sigma_n (x_1 = 0)$ ; 8-layer Model. (55% Graphite Fiber-Epoxy Matrix,  $\pm 45^\circ$  Layup;  $\Delta = 4$  cm,  $t_0 = 4 \mu\text{sec}$ ,  $a = 2$  cm)

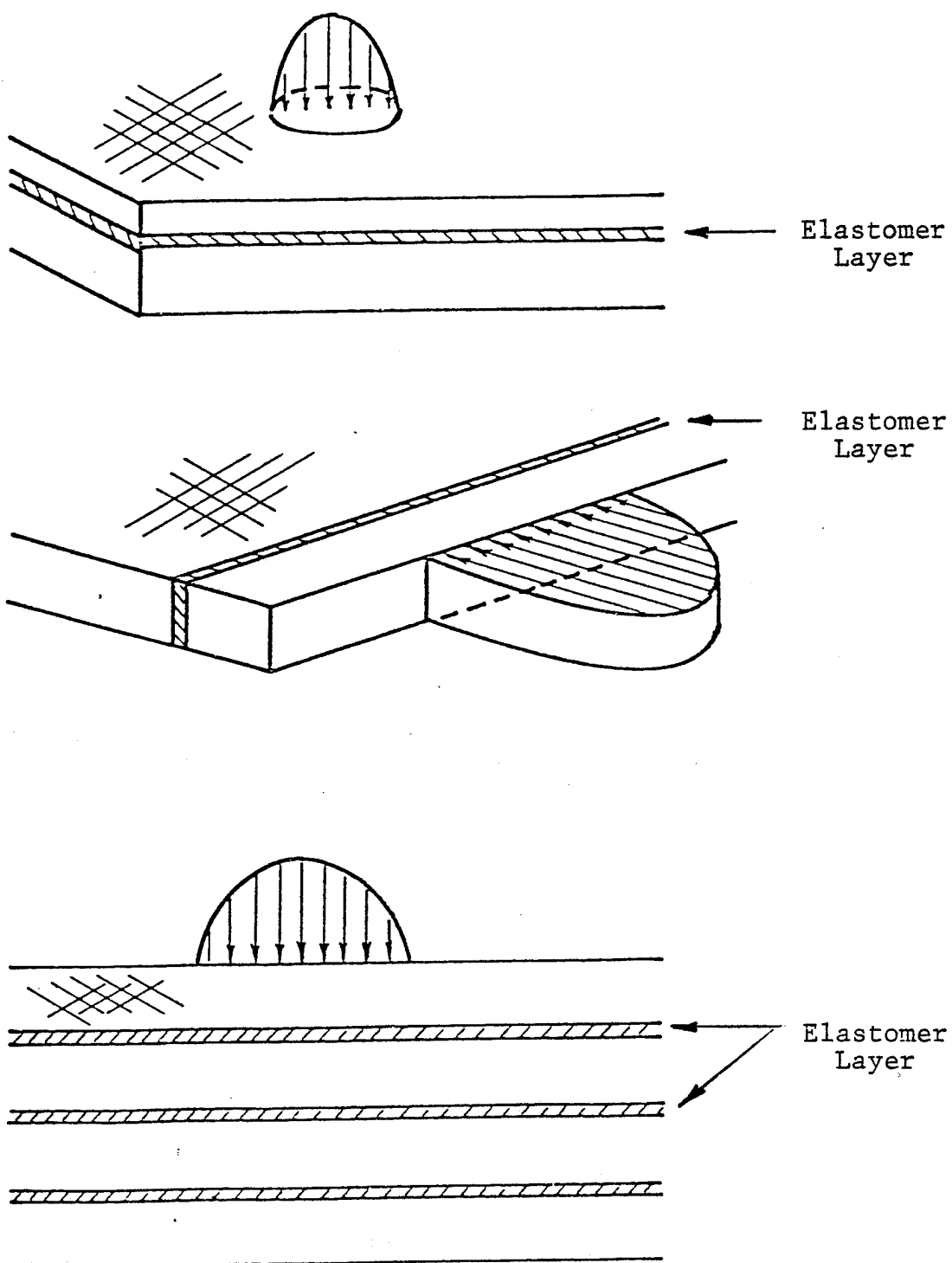


Figure 14. Viscoelastic Impact Energy Absorbing Models

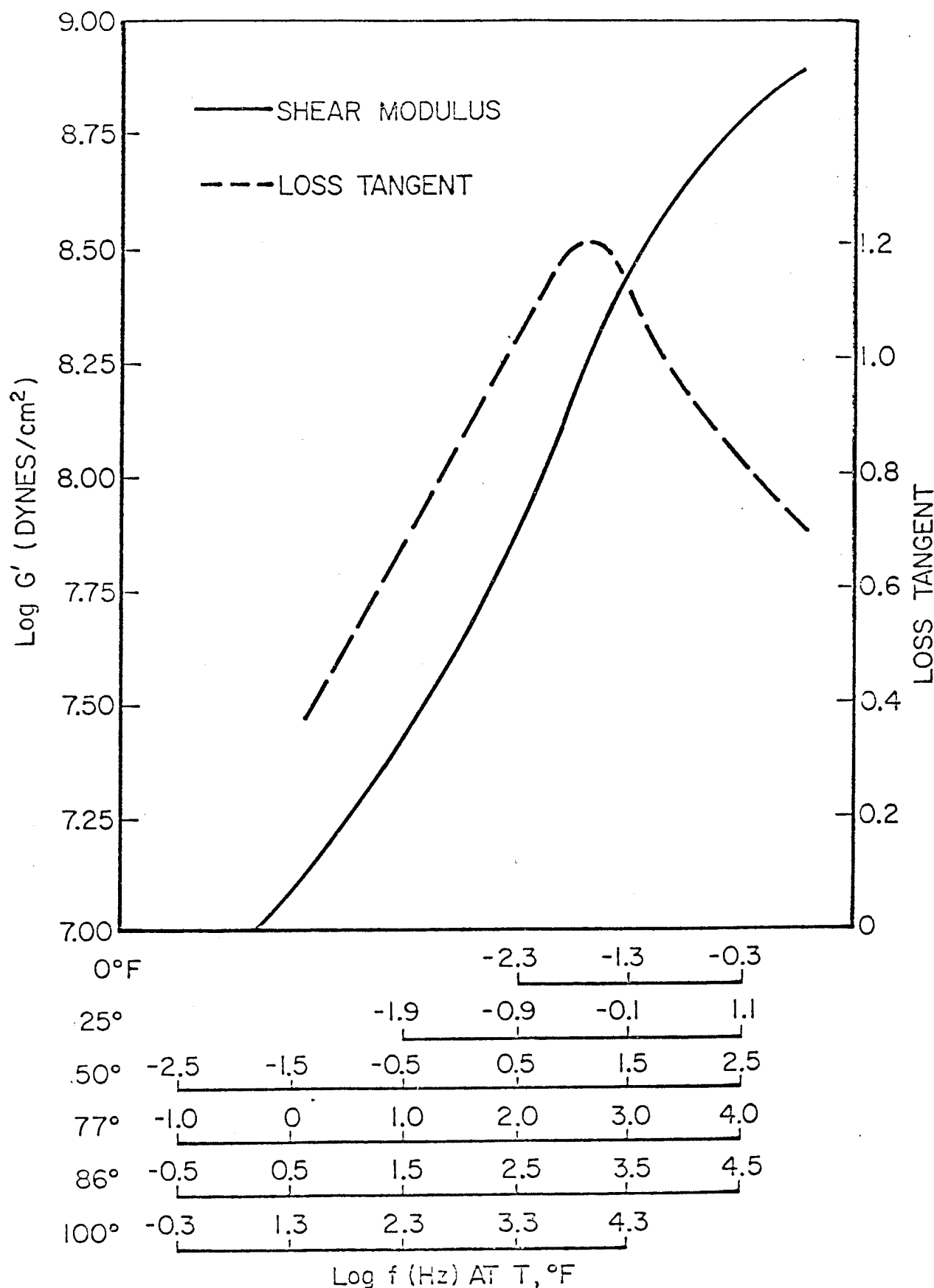


FIGURE 15a SHEAR MODULUS AND LOSS TANGENT AT  $T$  °F VS FREQUENCY FOR DUPONT LR3-604

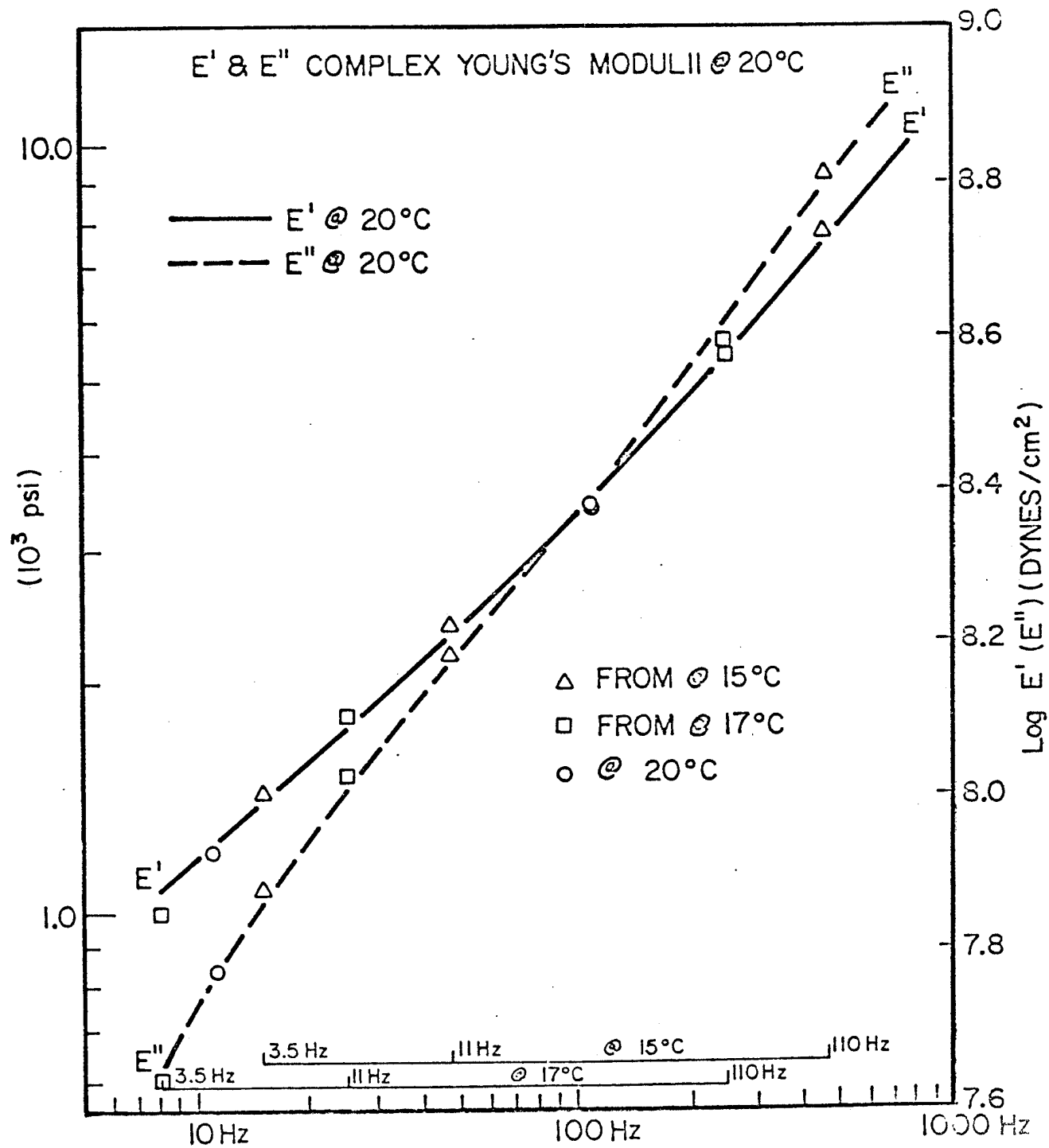


FIGURE 15b. THE COMPLEX YOUNG'S MODULUS OF LR3-604 MEASURED

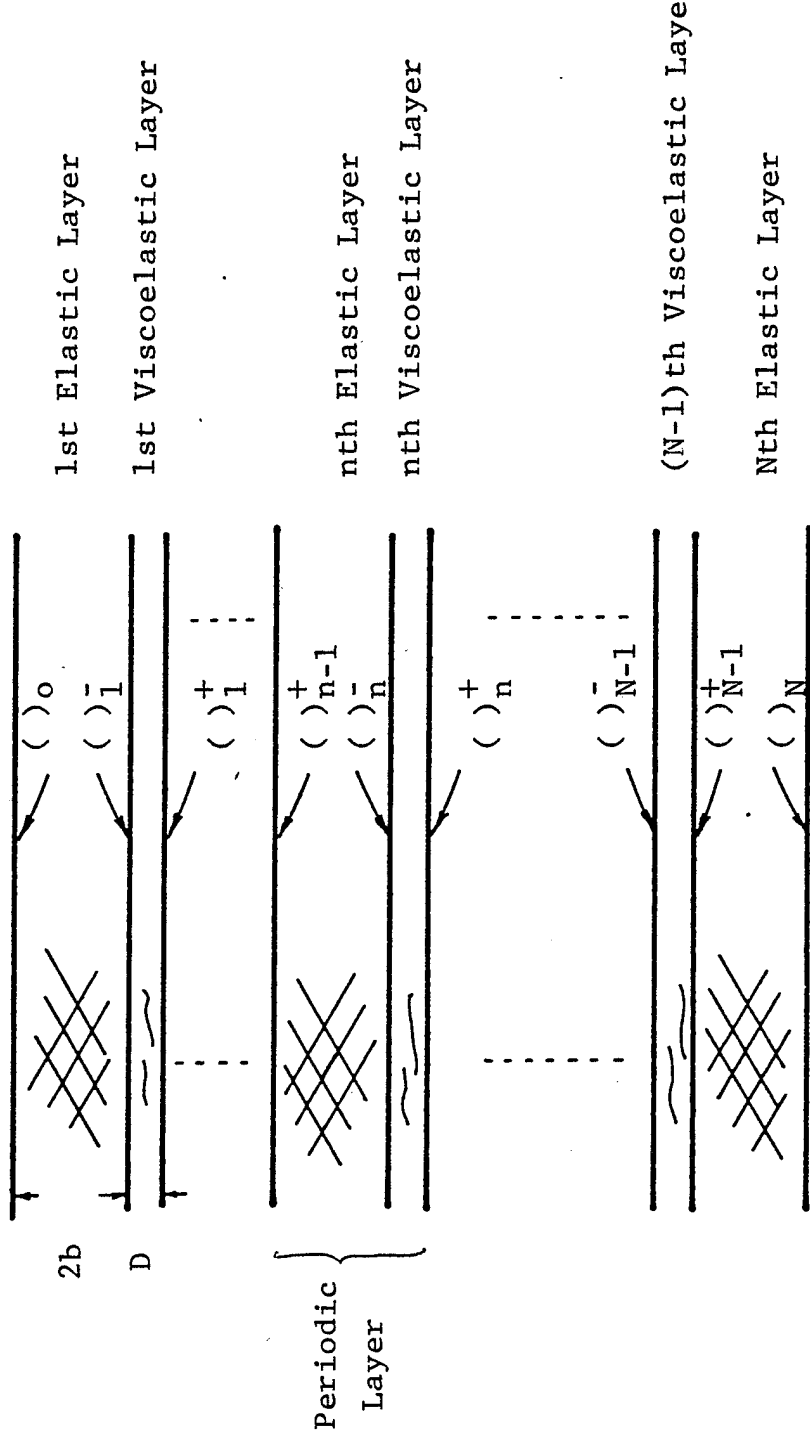


Figure 16. Plate with Viscoelastic Layers

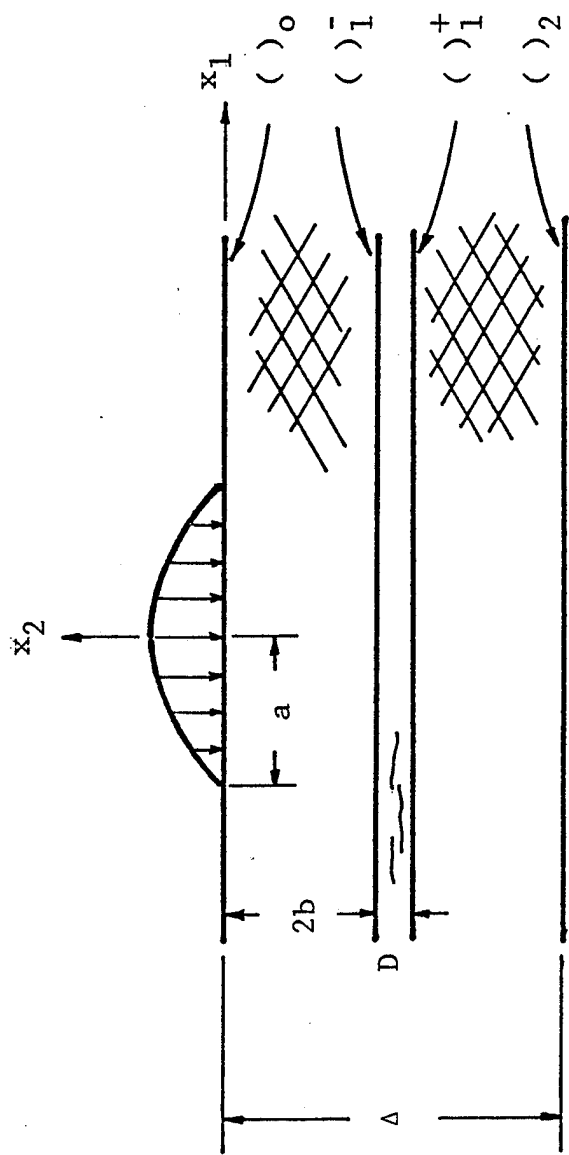


Figure 17. Impact of Plate Made of 2 Elastic Layers and a Viscoelastic Layer

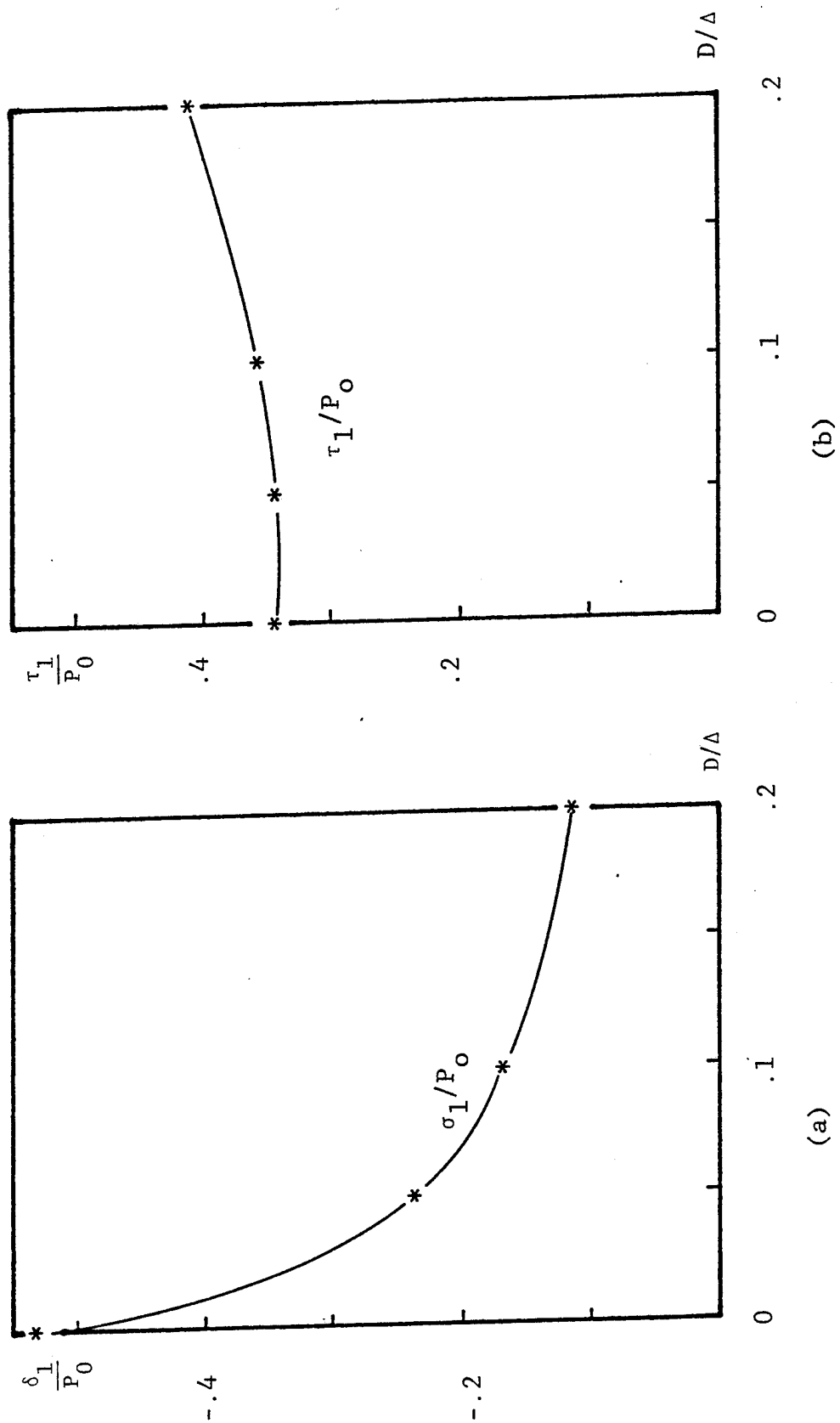


Figure 18. Peak Value of Interlaminar Stress Vs. Elastomer Thickness (two elastic layers and a viscoelastic layer;  $\Delta = 1$  cm,  $t_o = 10 \mu\text{sec}$ ,  $a = 4$  cm)

\*Calculated values

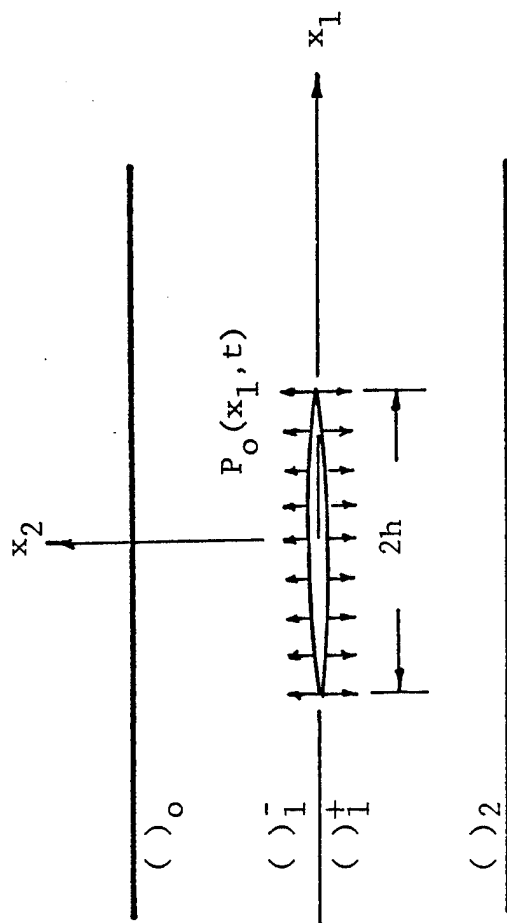
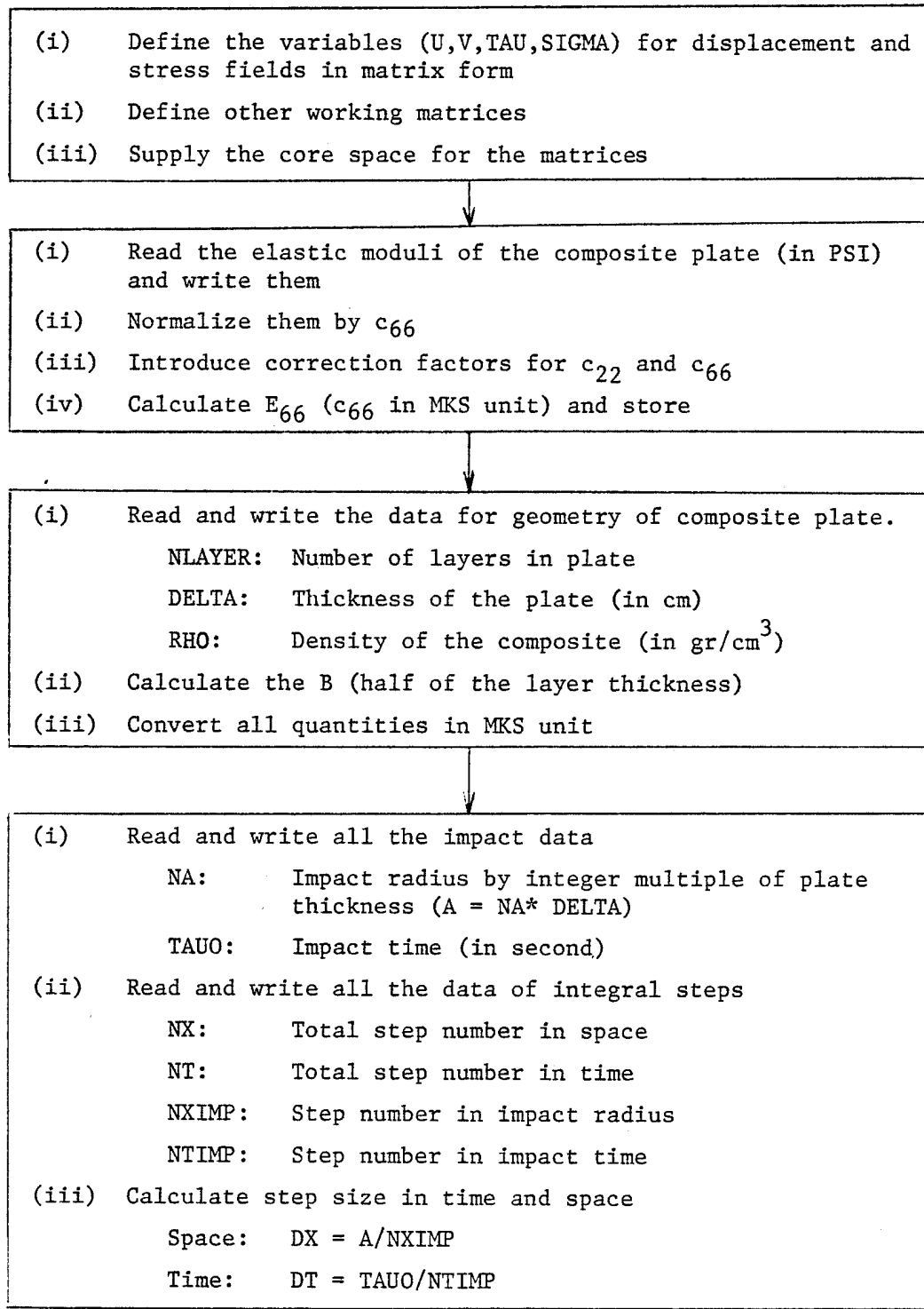


Figure 19. Composite Plate with Crack

## APPENDIX A FLOW CHART

In this flow chart and program,  $U(I,J)$ ,  $V(I,J)$ ,  $TAU(I,J)$ ,  $SIGMA(I,J)$  and  $SIGMA1(I,J)$  represent  $\hat{U}$ ,  $\hat{V}$ ,  $\hat{T}$  and  $\hat{\Sigma}$  in Eq. (II-17,18) and integral transform of  $\sigma_{11}$





(i) Calculate normalization units

Space: UNITX = DELTA (Thickness of the plate)

Time: UNITT =  $A/\sqrt{E_{66}/\rho}$  (Time required for the quasi-shear wave to travel the impact radius)

(ii) Normalized all quantities by UNITT and UNITX

(iii) Calculate integral limits ( $\omega_0$  and  $k_0$ ) in Fast Fourier Transform



Calculate  $Q_0(I,J)$ ,  $CBX(I,J)$ ,  $CAX(I,J)$ ,  $XIBX(I,J)$ ,  $YIAX(I,J)$  ....  $Y3AX(I,J)$ , over a half of the range of integration ( $I = 1 \sim NT$ ,  $J = 1, NX/2$ ).

$Q_0$ : Impact function given in Eq. (II-22)

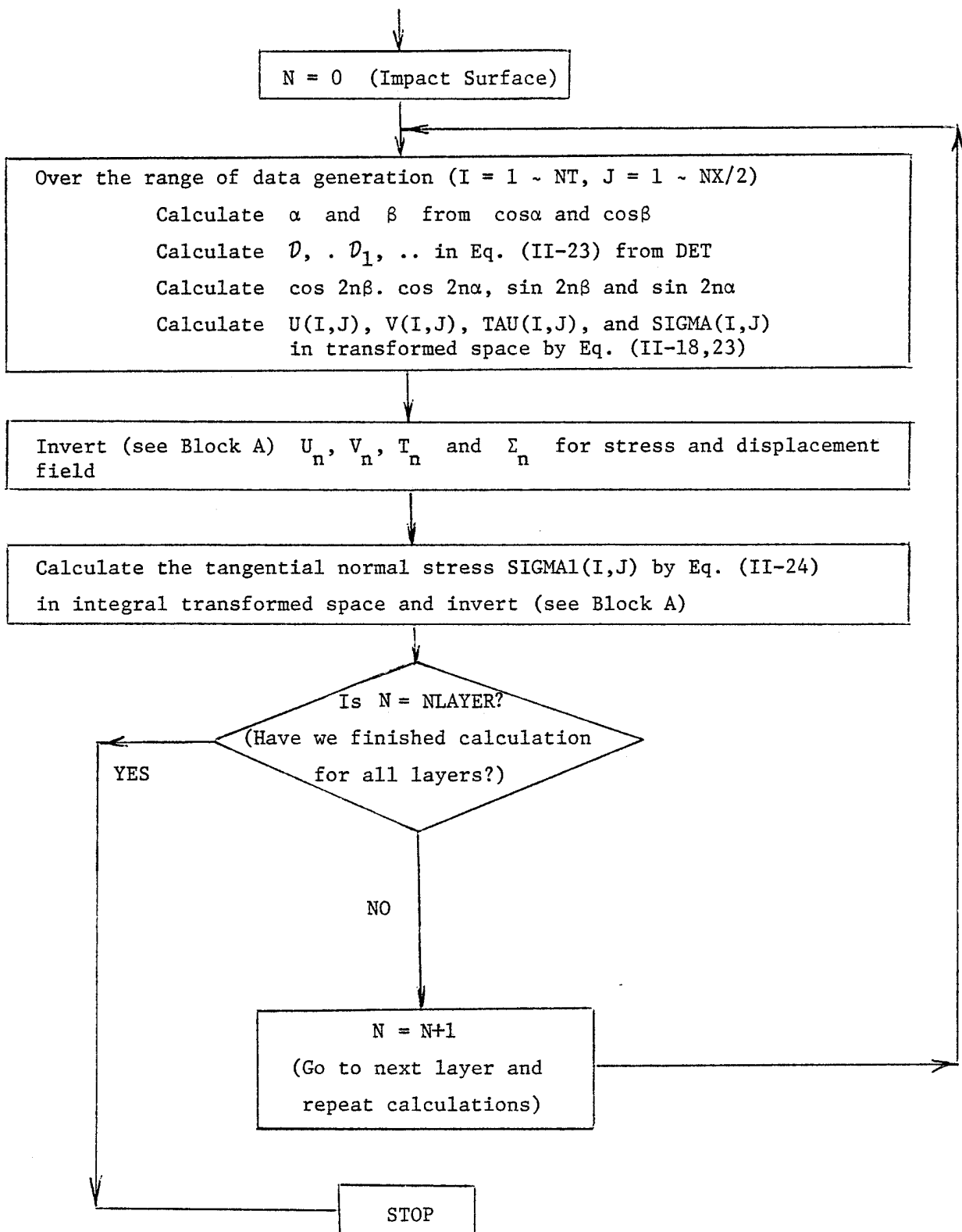
$CBX$ ,  $CAX$ :  $\cos\beta$  and  $\cos\alpha$  in Eq. (II-16,17) by DPHASE

$X1BX$ ,  $X2BX$  ...:  $X_1(\beta)$ ,  $X_2(\beta)$  in Eq. (II-18,19) by DELL

$Y1AX$ ,  $Y2AX$  ...:  $Y_1(\alpha)$ ,  $Y_2(\alpha)$  in Eq. (II-18,19) by DELL



Invert (see Block A) and check the impact function  $\sigma_0$  with  $Q_0$



Block A Inversion

- (i) Data  $xx(I,J)$  in integral transformed space are generated for a half of the inverse transform range:  $I = 1 \sim NT$ ,  $J = 1 \sim NX/2$
- (ii) Generate full data over  $J = 1 \sim NX$  by FLIP
  - Symmetric flip:  $V(I,J)$ ,  $SIGMA(I,J)$ ,  $SIGMA1(I,J)$ ,  $Q0(I,J)$
  - Antisymmetric flip:  $U(I,J)$ ,  $TAU(I,J)$
- (iii) Invert them for displacement and stress fields by FOURT
- (iv) Take care of the coordinate shifts and multiplication factors in FOURT by FACT
- (v) Print out by MAP

## APPENDIX B SAMPLE COMPUTER DECK

64	32	8	24	Data Card 4
2	6.E-06			Data Card 3
8	1.	1.44		Data Card 2
15	0.2456E 08	0.4000E 06	0.1170E 07	0.3552E 06

11 GO. SYSIN DD \*  
12

PROGRAM IN SOURCE DECK (see Appendix C)

EXEC FORTGOLG

\*LIMITS REGION=207K, LINES=5K, CLASS=0

JOB CARD

APPENDIX C LISTING OF PROGRAM AND SAMPLE OUTPUT

51 RELEASE 2.0

MAIN

DATE = 77139

21/11/39

\*\*\*\*\*

C

C

C THIS PROGRAM CALCULATES THE TRANSIENT PROPAGATION OF STRESS WAVE  
C IN A LAMINATED COMPOSITE PLATE DUE TO A NORMAL IMPACT.

C

C

C

C THE PRESENT PROGRAM IS A PART OF THE RESEARCH PROJECT OF  
C PROFESSOR FRANCIS C. MOON  
C DEPARTMENT OF THEORETICAL AND APPLIED MECHANICS  
C CORNELL UNIVERSITY  
C AND SUPPORTED BY NASA-LEWIS RESEARCH CENTER.

C

C

C

C FOLLOWING USER'S GUIDES ARE PROVIDED BY DR. B.S.KIM AND ALL THE EQUATION  
C NUMERS CORRESPOND EQUATIONS IN THE ACCOMPANYING TECHNICAL REPORT

C

C

C

C 1. DATA TO BE SUPPLIED BY 4 DATA CARDS (IN THE ORDER OF READING)

C

C

C IANGLE: FIBER LAYUP ANGLE IN COMPOSITES  
C C11,C12.. : ELASTIC MODULI OF COMPOSITE LAYER(IN PSI)

C

C NLAYER: NUMBER OF THE LAYERS IN THE GIVEN PLATE

C D,DELTA: THICKNESS OF COMPOSITE PLATE(IN CM)

C RHO: MASS DENSITY OF COMPOSITE LAYER(IN GR/CM\*\*3)

C

C NA: RADIUS OF THE IMPACT AS A MULTIPLE OF THE PLATE THICKNESS

C TAU0: IMPACT TIME(IN SECOND)

C

C NX: NUMBER OF INTEGRATION STEPS IN SPACE

C NT: NUMBER OF INTEGRATION STEPS IN TIME DOMAIN

C NXIMP: NUMBER OF SPACE STEPS IN IMPACT RADIUS

C NTIMP: NUMBER OF TIME STEPS IN IMPACT TIME

C

C

C

C

C

C

C

C

C

C

C

C

1 RELEASE 2.0

MAIN

DATE = 77139

21/11/39

C B: A HALF OF THE LAYER THICKNESS  
C  
C K: WAVE NUMBER FOR FOURIER TRANSFORM  
C S: LAPLACE TRANSFORM VARIABLE  
C  
C KO: LIMIT OF INTEGRATION FOR INVERSE FOURIER TRANSFORM FOR X  
C OMEGA0: LIMIT OF INTEGRATION FOR INVERSE TRANSFORM IN TIME  
C CO: LAPLACE TRANSFORM PARAMETER  
C  
C  
C  
C  
C

---

C 3. DISPLACEMENT AND STRESS FIELDS ARE CALCULATED IN TRANSFORMED SPACE  
C AND BY INVERSIONS THESE BECOME DISPLACEMENTS AND STRESSES.  
C THEY ARE GIVEN IN A MATRIX FORM AS XX(I,J) REPRESENTING QUANTITY AT  
C ITH TIME STEP AND JTH SPACE STEP IN X

C U(I,J): HORIZONTAL DISPLACEMENT  
C V(I,J): VERTICAL DISPLACEMENT  
C SIGMA(I,J): NORMAL STRESS  
C TAU(I,J): SHEAR STRESS  
C SIGMA1(I,J): TANGENTIAL NORMAL STRESS  
C  
C  
C

---

C 4. FOLLOWINGS ARE WORKING MATRICES FOR THIS PROGRAM

C  
C DATA(I,J), SUB(I,J): WORKING MATRICES FOR SUBROUTINE FOURT  
C Q0(I,J): INTEGRAL TRANSFORM OF IMPACT FUCTION GIVEN IN EQ(II-22)  
C  
C CAX(I,J), CBX(I,J): COS(ALPHA) AND COS(BETA) IN EQ(II-16)  
C X1BX(I,J), Y1AX(I,J),..: X1(BETA), Y1(ALPHA),.. IN EQ(II-18)  
C  
C

---

C 5. FOLLOWING SUBROUTINE ARE SUPPLIED IN THE PRESENT PROGLAM

C  
C DPHASE: CALCULATES COS(BETA) AND COS(ALPHA) IN EQ(II-16) WITH GIVEN  
C VALUES OF WAVE NUMBER K AND LAPLACE TRANSFORM VARIABLE S  
C  
C DELL: CALCULATES X1(BETA), Y1(ALPHA),.. IN EQ (II-19,20)

51 RELEASE 2.0

MAIN

DATE = 77139

21/11/39

C  
C DET: CALCULATE D,D1,... IN EQ(II-23)  
C  
C FLIP: THIS PROGRAM GENERATES ONLY A HALF OF THE DATA (X>0) DUE  
C TO SYMMETRY AND FLIP THEM TO FIND FULL DATA ALONG X AXIS  
C  
C MAP: CONTROLS THE PRINTOUT FORMAT  
C  
C FACT: TAKES CARES OF THE COORDINATE SHIFT AND MULTIPLICATION FACTORS  
C IN FOURIER-LAPLACE DOUBLE INTEGRAL TRANSFORMS  
C  
C FOURT: IS FAST FOURIER TRANSFORM ROUTINE SUPPLIED BY IBM  
C  
C  
C\*\*\*\*\*  
C  
C IMPLICIT REAL\*8(K)  
COMPLEX DATA(32,64),SUB(32,32),CAX(32,32),CBX(32,32),Q0(32,32)  
COMPLEX SIGMA(32,32),SIGMA1(32,32),TAU(32,32)  
COMPLEX U(32,32),V(32,32),VX(32,32)  
COMPLEX Y1AX(32,32),Y2AX(32,32),Y3AX(32,32)  
COMPLEX X1BX(32,32),X2BX(32,32),X3BX(32,32)  
DIMENSION NN(2),MM(32)  
C  
REAL\*8 C11,C12,C22,C66,CHAT,E66,V66,PI,P2  
REAL\*8 DCOS,DSIN,DBLE,DSQRT,DFLOAT,DLOG  
REAL\*8 DELTA,D,RHO,FN,F,KX(32),B,TAU0,A,DX,DT,UNITT,UNITX  
REAL\*8 Q,OMEGA0,BL,CO  
C  
COMPLEX\*16 CDEXP,CDLOG,CDSQRT,CDCOS,CDSIN  
COMPLEX\*16 BETA,ALPHA,CB,CA,SB,SA,C2NB,C2NA,S2NB,S2NA  
COMPLEX\*16 S,SI,S2,D1,D2,D3,D4  
COMPLEX\*16 Y1A,Y2A,Y3A,X1B,X2B,X3B  
C  
COMMON Y1A,Y2A,Y3A,X1B,X2B,X3B,D1,D2,D3,D4,C11,C12,C22,C66,CHAT  
EQUIVALENCE (DELTA,D)  
EQUIVALENCE (DATA(1,1),SUB(1,1))  
C  
SI=(0.D 00,1.D 00)  
PI=3.1415926536D 00  
P2=PI\*2.D 00  
INDEX=0  
INDEX=1  
C  
4 WRITE(6,4)  
FORMAT('1'//////////20X,'\*\*\* WAVE PROPAGATION IN COMPOSITE P  
LATE \*\*\*')

61 RELEASE 2.0

MAIN

DATE = 77139

21/11/39

```
      WRITE(6,5)
5      FORMAT(22X,'GRAPHITE FIBER(55%)-EPOXY MATRIX COMPOSITE')
C
C***** ****
C
C      INPUT DATA FOR ELASTIC PROPERTIES OF COMPOSITE PLATE
C      ALL THE DATA ARE SUPPLIED IN PSI UNIT BUT NORMALIZED BY C66
C      WHICH IS CONSTANT REGARDLESS THE LAYUP ANGLE
C
C
101     READ (5,101) IANGLE,C11,C12,C22,C66
      FORMAT(I10,4D15.7)
      CHAT=C11-C12**2/C22
      IF (IANGLE.EQ.100) GO TO 200
      WRITE(6,102) IANGLE,C11,C12,C22,C66
102     FORMAT(// 20X,'LAYUP ANGLE=',I3,3X,'DEGREE'
      $ /20X,'C(1,1)=',D12.5,' PSI',10X,'C(1,2)=',D12.5,' PSI'
      $ /20X,'C(2,2)=',D12.5,' PSI',10X,'C(6,6)=',D12.5,' PSI'//)
      GO TO 201
200     CONTINUE
      WRITE(6,210) C11,C12,C22,C66
210     FORMAT(/20X,' PLATE IS ISOTROPIC WITH POISSON''S RATIO 1/4'
      $ /20X,'C(1,1)=',D12.5,' PSI',10X,'C(1,2)=',D12.5,' PSI'
      $ /20X,'C(2,2)=',D12.5,' PSI',10X,'C(6,6)=',D12.5,' PSI'//)
201     CONTINUE
C
      E66=C66*6892.2D 00
      C11=C11/C66
      C12=C12/C66
      C22=C22/C66
      CHAT=CHAT/C66
      C66=1.D 00
C
C***** WITH CORRECTION FACTOR
C
      C66=PI**2/12.D 00
      C22=C22*C66
C
C-----
```

C

C INPUT DATA FOR GEOMETRY OF COMPOSITE PLATE

C ALL THE DATA ARE FIRST SUPPLIED IN CGS UNIT BUT CONVERTED INTO MKS UNIT

C

C

120 READ(5,120) NLAYER,DELTA,RHO
 FORMAT(I10,2D20.10)

61 RELEASE 2.0

MAIN

DATE = 77139

21/11/39

```
NL1=NAYER+1
FN=DFLOAT(NAYER)
B=DELTA/FN
121 WRITE(6,121) DELTA,RHO,NAYER,B
  FORMAT(20X,'TOTAL THICKNESS OF COMPOSITE PLATE ; DELTA=',F10.5,
  $ ' CM'
  $ 20X,'DENSITY OF COMPOSITE ; RHO=',F10.5,' GR/CM**3'
  $ 20X,'PLATE IS MADE OF ',I3,3X,'IDENTICAL LAYERS'
  $ 20X,'LAYER THICKNESS ; 2B=',F10.5,' CM'//)
C
C   DELTA=DELTA/100.D 00
C   RHO=RHO*1000.D 00
C   B=B/200.D 00
C
C
C   -----
C
C   INPUT DATA FOR IMPACT
C
C
60  READ(5,60) NA,TAU0
  FORMAT(I10,D20.10)
111 READ(5,111) NX,NT,NXIMP,NTIMP
  FORMAT(4I10)
C
112 WRITE(6,112) NX,NXIMP,NT,NTIMP
  FORMAT(20X,'TOTAL SPACE STEPS; NX=',I3,5X,'WITH',I3,2X,'STEPS FOR
  $ CONTACT RADIUS'
  $ 20X,'TOTAL TIME STEPS ; NT=',I3,5X,'WITH',I3,2X,'STEPS FOR CONTACT
  $ TIME'//)
C
A=DFLOAT(NA)*DELTA
DX=A/DFLOAT(NXIMP)
DT=TAU0/DFLOAT(NTIMP)
C
61  WRITE(6,61) A,DX,TAU0,DT
  FORMAT(20X,'CONTACT RADIUS ; A=',D12.5,' M'
  $ 20X,'SPACE STEP ; DX=',D12.5,' M'
  $ 20X,'CONTACT TIME ; TAU0=',D12.5,' SECOND'
  $ 20X,'TIME STEP ; DT=',D12.5,' SECOND'//)
C
C
C   -----
C
C   NORMALIZE ALL THE INPUT DATA
C
C
V66=DSQRT(E66/RHO)
```

G1 RELEASE 2.0

MAIN

DATE = 77139

21/11/39

```
UNITT=A/V66
UNITX=DELTA
F=D*D*RHO/(E66*UNITT**2)/2.D 00/FN
```

```
C
NX2=NX/2
NN(1)=NT
NN(2)=NX
DX=DX/UNITX
DT=DT/UNITT
KO=PI/DX
OMEGA0=PI/DT
BL=A/D
CO=DLOG(1.D 06*2.D 00*DT)/(3.D 00*DT*DFLOAT(NT))
```

```
C
C
C
C*****CALCULATE THE IMPACT INPUT FUNCTION Q0(I,J) IN EQ(II-22)
C*****CALCULATE COS(BETA) AND COS(ALPHA) IN EQ(II-16) BY SUBROUTINE DPHASE
C*****CALCULATE X1(BETA), Y1(ALPHA) ,.. BY SUBROUTINE DELL
C
C
```

```
DO 30 J=1,NX2
K=2.D 00*K0*(DFLOAT(J)-.5)/DFLOAT(NX)-KO
K2=K**2
KX(J)=K
Q=PI**2/DSQRT(P2)*DSIN(K*BL)/K/((K*BL)**2-PI**2)
C
DO 30 I=1,NT
S=CO+SI*OMEGA0*(1.D 00-(DFLOAT(I)-.5D 00)*2.D 00/DFLOAT(NT))
S2=S**2*F
Q0(I,J)=Q/2./S*(1.D 00-CDEXP(-S*TAU0/UNITT))*(P2*UNITT)**2
$ /((S*TAU0)**2+(P2*UNITT)**2)
C
CALL DPHASE (K,S2,CB,CA,NLAYER)
CBX(I,J)=CB
CAX(I,J)=CA
C
CALL DELL(K,S2,CB,CA,SI,NLAYER)
Y1AX(I,J)=Y1A
Y2AX(I,J)=Y2A
Y3AX(I,J)=Y3A
X1BX(I,J)=X1B
X2BX(I,J)=X2B
X3BX(I,J)=X3B
C
```

61 RELEASE 2.0

MAIN

DATE = 77139

21/11/39

30 CONTINUE

C

C

C

C\*\*\*\*\* REPRODUCE THE IMPACT FUNCTION TO CHECK INPUT  
C

DO 300 I=1,NT

DO 300 J=1,NX2

300 SUB(I,J)=Q0(I,J)

CALL FLIP(DATA,NX,NX2,NT,+1)

CALL FOURT(DATA,NN,2,-1,1,0)

CALL FACT(DATA,NX,NT,CO,OMEGAO,K0,PI,SI)

WRITE(6,301)

301 FORMAT('1'//////////20X, '\*\*\* REPRODUCTION OF IMPACT FUNCTIO  
N \*\*\*')

CALL MAP(DATA,NX,NT,NX2,MM,INDEX)

C

C

C

C\*\*\*\*\* THIS IS THE MAIN PART OF THE PROGRAM.

C

C CALCULATE D(BETA),DBAR(ALPHA),.. IN EQ(II-19,20) BY SUBROUTINE DET

C NEXT CALCULATE 1,V,.. IN EQ(II-18) IN TRANSFORMED SPACE

C AND FLIP TO FIND FULL DATA AND INVERT THEM BY MEANS OF FOURT.

C REPEAT THIS PROCESS FROM N=0 TO NLAYER

C

DO 11 N=1,NL1

NY=N-1

NYY=NY-1

C

C

C

C-----  
C GENERATION OF DATA FOR DISPLACEMENTS AND STRESS IN TRANSFORMED SPACE

C

DO 100 J=1,NX2

DO 100 I=1,NT

CB=CBX(I,J)

CA=CAX(I,J)

X1B=X1BX(I,J)

X2B=X2BX(I,J)

X3B=X3BX(I,J)

```

G1 RELEASE 2.0          MAIN          DATE = 77139        21/11/39

      Y1A=Y1AX(I,J)
      Y2A=Y2AX(I,J)
      Y3A=Y3AX(I,J)

C
      SB=CDSQRT(1.D 00-CB**2)
      SA=CDSQRT(1.D 00-CA**2)
      BETA=CB+SI*SB
      ALPHA=CA+SI*SA
      BETA=CDLOG(BETA)/SI
      ALPHA=CDLOG(ALPHA)/SI

C
      CALL DET(ALPHA,BETA,SI,FN)
      C2NB=CDCOS(2.D 00*BETA*DFLOAT(NY))
      S2NB=CDSIN(2.D 00*BETA*DFLOAT(NY))
      C2NA=CDCOS(2.D 00*ALPHA*DFLOAT(NY))
      S2NA=CDSIN(2.D 00*ALPHA*DFLOAT(NY))

C
      U(I,J)=(X1B*(D1*C2NB+SI*D2*S2NB)+Y1A*(D4*C2NA+SI*D3*S2NA))*Q0(I,J)
      V(I,J)=(X2B*(D2*C2NB+SI*D1*S2NB)+Y2A*(D3*C2NA+SI*D4*S2NA))*Q0(I,J)
      TAU(I,J)=(X3B*(D2*C2NB+SI*D1*S2NB)+(D3*C2NA+SI*D4*S2NA))*Q0(I,J)
      SIGMA(I,J)=((D1*C2NB+SI*D2*S2NB)+Y3A*(D4*C2NA+SI*D3*S2NA))*Q0(I,J)

100  CONTINUE

C
C
C
C
C-----
```

C INVERSION AND PRINTOUT OF HORIZONTAL DISPLACEMENT UN(I,J)

C

DO 10 I=1,NT

DO 10 J=1,NX2

10 SUB(I,J)=U(I,J)

CALL FLIP(DATA,NX,NX2,NT,-1)

CALL FOURT(DATA,NN,2,-1,1,0)

CALL FACT(DATA,NX,NT,CO,OMEGAO,KO,PI,SI)

WRITE(6,981) NY

981 FORMAT('1'//////////20X,'U',I3)

CALL MAP(DATA,NX,NT,NX2,MM,INDEX)

C

C

C-----

C INVERSION AND PRINTOUT OF VERTICAL DISPLACEMENT VN(I,J)

C

DO 20 I=1,NT

DO 20 J=1,NX2

20 SUB(I,J)=V(I,J)

CALL FLIP(DATA,NX,NX2,NT,+1)

CALL FOURT(DATA,NN,2,-1,1,0)

31 RELEASE 2.0

MAIN

DATE = 77139

21/11/39

```
CALL FACT(DATA,NX,NT,CO,OMEGAO,KO,PI,SI)
WRITE(6,982) NY
982 FORMAT('1'//////////20X,'V',I3)
CALL MAP(DATA,NX,NT,NX2,MM,INDEX)

C
C
C
C
C-----  
C INVERSION AND PRINTOUT OF SHEAR STRESS TAU(I,J)
C
DO 35 I=1,NT
DO 35 J=1,NX2
35 SUB(I,J)=TAU(I,J)
CALL FLIP(DATA,NX,NX2,NT,-1)
CALL FOURT(DATA,NN,2,-1,1,0)
CALL FACT(DATA,NX,NT,CO,OMEGAO,KO,PI,SI)
WRITE(6,983) NY
983 FORMAT('1'//////////20X,'TAU',I3)
CALL MAP(DATA,NX,NT,NX2,MM,INDEX)

C
C
C
C
C-----  
C INVERSION AND PRINTOUT OF NORMAL STRESS SIGMA(I,J)
C
DO 40 I=1,NT
DO 40 J=1,NX2
40 SUB(I,J)=SIGMA(I,J)
CALL FLIP(DATA,NX,NX2,NT,+1)
CALL FOURT(DATA,NN,2,-1,1,0)
CALL FACT(DATA,NX,NT,CO,OMEGAO,KO,PI,SI)
WRITE(6,984) NY
984 FORMAT('1'//////////20X,'SIGMA',I3)
CALL MAP(DATA,NX,NT,NX2,MM,INDEX)

C
C
C
C
C-----  
C INVERSION AND PRINTOUT OF TANGENTIAL NORMAL STRESS SIGMA1(I,J)
C
IF (NY.EQ.0) GO TO 160
DO 50 I=1,NT
DO 50 J=1,NX2
50 SUB(I,J)=SIGMA1(I,J)+FN*C12*V(I,J)
CALL FLIP(DATA,NX,NX2,NT,+1)
CALL FOURT(DATA,NN,2,-1,1,0)
CALL FACT(DATA,NX,NT,CO,OMEGAO,KO,PI,SI)
WRITE(6,985) NY
```

G1 RELEASE 2.0

MAIN

DATE = 77139

21/11/39

```
985  FORMAT('1'//////////20X,'SIGMA1',I3)
      CALL MAP(DATA,NX,NT,NX2,MM,INDEX)
C
      IF (NY.EQ.NLAYER) GO TO 70
      DO 51 I=1,NT
      DO 51 J=1,NX2
  51  SIGMA1(I,J)=-SI*KX(J)*C11*U(I,J)-FN*C12*VX(I,J)
      GO TO 80
C
 160  CONTINUE
      DO 161 I=1,NT
      DO 161 J=1,NT
 161  SIGMA1(I,J)=-SI*KX(J)*C11*U(I,J)-FN*C12*V(I,J)
      GO TO 80
C
 70   CONTINUE
      DO 71 I=1,NT
      DO 71 J=1,NX2
 71   SUB(I,J)=-SI*KX(J)*C11*U(I,J)+FN*C12*(V(I,J)-VX(I,J))
      CALL FLIP(DATA,NX,NX2,NT,+1)
      CALL FOURT(DATA,NN,2,-1,1,0)
      CALL FACT(DATA,NX,NT,CO,OMEGA0,K0,PI,SI)
      WRITE(6,985) NY
      CALL MAP(DATA,NX,NT,NX2,MM,INDEX)
      GO TO 90
C
 80   CONTINUE
      DO 81 I=1,NT
      DO 81 J=1,NX2
 81   VX(I,J)=V(I,J)
C
 90   CONTINUE
C
C
 11   CONTINUE
C
C
C
C
C
C
      STOP
      END
```

/ G1 RELEASE 2.0

MAIN

DATE = 77139

21/11/39

```
C
C
C*****THIS SUBROUTINE CALCULATES THE PHASE SHIFT BETA AND ALPHA FROM
C      EQ(II-15,16) OF THE PRESENT REPORT WITH GIVEN VALUES OF
C      WAVE NUMBER K AND LAPLACE TRANSFORM VARIABLE S
C
C      CA=COS(ALPHA)
C      CB=COS(BETA)
C
C*****SUBROUTINE DPHASE(K,S ,CB,CA,NLAYER)
C      IMPLICIT COMPLEX*16(A,X,Y)
C      COMPLEX*16 ROOTP,ROOTM,S,CDSQRT,DCMPLX,DCB,DCA
C      COMPLEX*16 D1,D2,D3,D4
C      COMPLEX*16 CB,CA
C      REAL*8 C11,C12,C22,C66,CHAT,N,K2,DFLOAT,DBLE,K
C
C      COMMON Y1A,Y2A,Y3A,X1B,X2B,X3B,D1,D2,D3,D4,C11,C12,C22,C66,CHAT
C      ROOTP(AA,AB,AC)=(-AB+CDSQRT(AB**2-4.D 00*AA*AC))/(2.D 00*AA)
C      ROOTM(AA,AB,AC)=(-AB-CDSQRT(AB**2-4.D 00*AA*AC))/(2.D 00*AA)
C
C      N=DFLOAT(NLAYER)*2.D 00
C      K2=K**2
C
C      A1=(K2*C11/N+S)*(K2*C66/N+S)
C      A2=K2*CHAT/(3.D 00*N)+N*C66+S/3.D 00-C12*C66*K2/(3.D 00*N*C22)
C      A2=A2*(-C12*K2/(3.D 00*N)+N*C22+S/3.D 00)
C      A3=N*C22+S/3.D 00-K2*C12*(C66*K2/N+S)/(9.D 00*N**2*C22)+C66*K2/
C      $ (3.D 00*N)
C      A3=A3*(C11*K2/N+S)-K2*(C12+C66)**2
C      A3=A3+(C66*K2/N+S)*(CHAT*K2/(3.D 00*N)+N*C66+S/3.+C12**2*K2/
C      $ (3.D 00*C22))
C
C      AA=A1+A2-A3
C      AB=A3-2.D 00*A2
C      AC=A2
C      DCB=ROOTP(AA,AB,AC)
C      DCA=ROOTM(AA,AB,AC)
C
C      CB=CDSQRT(DCB)
C      CA=CDSQRT(DCA)
C      RETURN
C      END
```

/ G1 RELEASE 2.0

MAIN

DATE = 77139

21/11/39

```
C
C
C*****THIS SUBROUTINE CALCULATES DELTA(BETA),DELTABAR(ALPHA),DELTA1(BETA),...
C      IN EQ(II-19,20) AND X1(BETA),Y1(ALPHA) IN EQ(II-18,19,20)
C
C      X1B=X1(BETA),  Y1A=Y1(ALPHA)
C      .
C      .
C
C*****SUBROUTINE DELL (K,S,CB,CA,SI,NLAYER)
C      IMPLICIT REAL*8(K),COMPLEX*16(S,X,D,Y)
C      COMPLEX*16 SB,CB,CDSQRT,SA,CA
C      REAL*8 N,DFLOAT
C      REAL*8 C11,C12,C22,C66,CHAT
C
C      COMMON Y1A,Y2A,Y3A,X1B,X2B,X3E,D1,D2,D3,D4,C11,C12,C22,C66,CHAT
C
C      K2=K**2
C      N=DFLOAT(NLAYER)
C
C      S11=S+C11*K2/2.D 00/N
C      S66=S+C66*K2/2.D 00/N
C      SA=CDSQRT(1.D 00-CA**2)
C      SB=CDSQRT(1.D 00-CB**2)
C
C      DELTAB=CB**3*S11*S66+SB**2*CB*(-C66*(C66+C12)*K2
C      $ +S66*(S/3.D 00+CHAT*K2/6.D 00/N+2.D 00*N*C66))
C      DEL1B=SI*K*SB**2*CB*(-C66-C12+C12*S66/6.D 00/N/C22)
C      DEL2B=SI*SB**3*(C12*C66*K2/6.D 00/N/C22-S/3.D 00
C      $ -CHAT*K2/6.D 00/N-2.D 00*N*C66)-SI*CB**2*SB*S11
C      DEL3B=CB**2*SB*(C12*K*S11*S66/6.D 00/N/C22-C66*K*S11)
C      $ +SB**3*(C12*K*(S/3.D 00+CHAT*K2/6.D 00/N+2.D 00*N*C66)
C      $ -C12**2*C66*K*K2/6.D 00/N/C22)
C
C      DELTAA=SI*CA**2*SA*((C12+C66)*C66*K2-S66*(S/3.D 00+CHAT*K2
C      $ /6.D 00/N+2.D 00*N*C66+C12**2*K2/6.D 00/N/C22))
C      $ +SI*SA**3*(S/3.D 00+2.D 00*N*C22)*(C66*C12*K2/6.D 00/N/C22
C      $ -S/3.D 00-CHAT*K2/6.D 00/N-2.D 00*N*C66)
C      DEL1A=SA**2*CA*(-K2*C12*S66/6.D 00/6.D 00/N**2/C22+C66*K2/6.D 00/N
C      $ +S/3.D 00+2.D 00*N*C22)+CA**3*S66
C      DEL2A=CA**2*SA*K*(C12+C66)
```

V G1 RELEASE 2.0

DELL

DATE = 77139

21/11/39

```
$ +SA**3*(K/6.D 00/N*(S/3.D 00+CHAT*K2/6.D 00/N+2.D 00*N*C66)
$ -C66*C12*K**3/36.D 00/C22/N**2)
DEL3A=-SI*CA**3*C12*K*S66+SI*SA**2*CA*(C66*K*(S/3.D 00+2.D 00*N
$ *C22+C66*K2/6.D 00/N)-K/6.D 00/N*S66*(S/3.D 00+CHAT*K2/6.D 00
$ /N+2.D 00*N*C66))
```

C

C

```
X1B=-DEL1B/DELTAB
X2B=-DEL2B/DELTAB
X3B=-DEL3B/DELTAB
Y1A=-DEL1A/DELTAA
Y2A=-DEL2A/DELTAA
Y3A=-DEL3A/DELTAA
```

C

```
RETURN
END
```

/ G1 RELEASE 2.0

MAIN

DATE = 77139

21/11/39

```
C
C
C***** THIS SUBROUTINE CALCUALTES D,D1,.. IN EQ(II-23) OF THE PRESENT REPORT
C***** THIS SUBROUTINE CALCUALTES D,D1,.. IN EQ(II-23) OF THE PRESENT REPORT
C
C
C
SUBROUTINE DET(ALPHA,BETA,SI,FN)
IMPLICIT COMPLEX*16(D,X,Y)
COMPLEX*16 ALPHA,BETA
COMPLEX*16 C2NB,C2NA,S2NA,S2NB,CDSQRT,SI
REAL*8 FN
REAL*8 C11,C12,C22,C66,CHAT
C
COMMON Y1A,Y2A,Y3A,X1B,X2B,X3B,D1,D2,D3,D4,C11,C12,C22,C66,CHAT
C
C2NA=CDCOS(2.D 00*ALPHA*FN)
S2NA=CDSIN(2.D 00*ALPHA*FN)
C2NB=CDCOS(2.D 00*BETA*FN)
S2NB=CDSIN(2.D 00*BETA*FN)
C
X=Y3A*X3B*(1.D 00-C2NA*C2NB)
Y=X3B*Y3A*S2NB*C2NA-S2NA*C2NB
C
D=-2.D 00*X+(1.D 00+X3B**2*Y3A**2)*S2NA*S2NB
D1=-(X-S2NA*S2NB)
D2=-SI*Y
D3=SI*Y*X3B
D4=X3B*(X3B*Y3A*S2NB*S2NA+C2NA*C2NB-1.D 00)
C
D1=D1/D
D2=D2/D
D3=D3/D
D4=D4/D
C
RETURN
END
```

V G1 RELEASE 2.0

MAIN

DATE = 77139

21/11/39

C  
C  
C\*\*\*\*\*  
C  
C  
C ALL THE DATA IN THE MAIN PROGRAM ARE GENERATED FOR ONLY HALF OF THE  
C PLATE WHEN X>0. DUE TO SYMMETRY OF THE PROBLEM WE CAN GENERATE  
C THE FULL DATA BY FLIPPING THE HALF OF THE DATA.  
C  
C  
C\*\*\*\*\*  
C  
C  
SUBROUTINE FLIP(DATA,NX,NX2,NT,INDEX)  
COMPLEX DATA(NT,NX)  
DO 10 J=1,NX2  
JJ=NX+1-J  
DO 10 I=1,NT  
DATA(I,JJ)=FLOAT(INDEX)\*DATA(I,J)  
10 CONTINUE  
RETURN  
END

V G1 RELEASE 2.0

MAIN

DATE = 77139

21/11/39

```
C
C
C*****THIS SUBROUTINE TAKES CARE OF THE COORDINATE SHIFT IN
C      LAPLACE AND FOURIER TRANSFORM IN THE PROCESS OF APPLYING
C      FAST FOURIER TRANSFORM ALGORITHM
C
C
C*****SUBROUTINE FACT(DATA,NX,NT,CO,W0,K0,PI,SI)
COMPLEX DATA(NT,NX)
COMPLEX*16 CDEXP,SI
REAL*8 DEXP,DSQRT,DFLOAT
REAL*8 CO,W0,PI,K0,FT,FX
FX=DFLOAT(NX)
FT=DFLOAT(NT)
NX2=NX/2
C
DO 10 L=1,NX2
DO 10 M=1,NT
DATA(M,L)=DATA(M,L)*4.D 00*K0*W0/(DSQRT(2.D 00*PI)**3*FT*FX)
$ *DEXP(CO*PI*DFLOAT(M-1)/W0)*CDEXP(SI*PI*(1.D 00-1.D 00/FT)
$ *DFLOAT(L-1))*CDEXP(SI*PI*(1.D 00-1.D 00/FT)*DFLOAT(M-1))
10  CONTINUE
RETURN
END
```

V G1 RELEASE 2.0

MAIN

DATE = 77139

21/11/39

```
C
C***** THIS SUBROUTINE CONTROLS THE FORMAT OF THE PRINTOUT OF THE FINAL RESULTS
C
C      IF INDEX=0: ALL THE NUMERICAL VALUES ARE PRINTED
C                  =1: THE MAXIMUM AND NORMALIZED VALUES ARE PRINTED
C
C
C***** SUBROUTINE MAP(DATA,NX,NT,NX2,MM,INDEX)
COMPLEX DATA(NT,NX),S
DIMENSION MM(NX2)
IF (INDEX.EQ.1) GO TO 200
DO 44 IQ=1,NT
44  WRITE(6,15) IQ,(DATA(IQ,I),I=1,NX2)
15  FORMAT(I5,2E14.5,2X,2E14.5,2X,2E14.5,2X,2E14.5/
$      3(5X,2E14.5,2X,2E14.5,2X,2E14.5,2X,2E14.5)/
$      4(5X,2E14.5,2X,2E14.5,2X,2E14.5,2X,2E14.5)/)
200 CONTINUE
C*** FIND THE MAXIMUM VALUE
RS= 1.E-3
NT5=NT-5
NX5=NX2-5
DO 114 I=1,NT5
DO 114 J= 1,NX5
S= DATA(I,J)
TP= REAL(S)/RS
IF (ABS(TP).LT.1.) GO TO 114
RS= REAL(S)
114 CONTINUE
WRITE (6,516) RS
516 FORMAT(20X,'***  MAXIMUM VALUE =',E12.5,' ***//)
DO 119 I=1,NT5
DO 113 J=1,NX5
S= DATA(I,J)
113 MM(J)= REAL(S)/RS*100
WRITE(6,515) (MM(KIM),KIM=1,27)
119 CONTINUE
515 FORMAT(10X,27I3)
RETURN
END
```

1 RELEASE 2.0

FOURT

DATE = 77139

21/11/39

SUBROUTINE FOURT(DATA,NN,NDIM,ISIGN,IFORM,WORK)  
DIMENSION DATA(1),NN(1),IFACT(32),WORK(1)

FFTT000  
FFT0770

TWOPI=6.283185307

FFTT0780

IF(NDIM-1)920,1,1

FFTT0790

1 NTOT=2

FFTT0800

DO 2 IDIM=1,NDIM

FFTT0810

IF(NN(IDIM))920,920,2

FFTT0820

2 NTOT=NTOT\*NN(IDIM)

FFTT0830

C

C MAIN LOOP FOR EACH DIMENSION

C

NP1=2

FFTT0840

DO 910 IDIM=1,NDIM

FFTT0850

N=NN(IDIM)

FFTT0860

NP2=NP1\*N

FFTT0870

IF(N-1)920,900,5

FFTT0880

C

C FACTOR N

C

5 M=N

FFTT0950

NTWO=NP1

FFTT0960

IF=1

FFTT0970

IDIV=2

FFTT0980

10 IQUOT=M/IDIV

FFTT0990

IREM=M-IDIV\*IQUOT

FFTT1000

IF(IQUOT-IDIV)50,11,11

FFTT1010

11 IF(IREM)20,12,20

FFTT1020

12 NTWO=NTWO+NTWO

FFTT1030

M=IQUOT

FFTT1040

GO TO 10

FFTT1050

20 IDIV=3

FFTT1060

30 IQUOT=M/IDIV

FFTT1070

IREM=M-IDIV\*IQUOT

FFTT1080

IF(IQUOT-IDIV)60,31,31

FFTT1090

31 IF(IREM)40,32,40

FFTT1100

32 IFACT(IF)=IDIV

FFTT1110

IF=IF+1

FFTT1120

M=IQUOT

FFTT1130

GO TO 30

FFTT1140

40 IDIV=IDIV+2

FFTT1150

GO TO 30

FFTT1160

50 IF(IREM)60,51,60

FFTT1170

51 NTWO=NTWO+NTWO

FFTT1180

GO TO 70

FFTT1190

60 IFACT(IF)=M

FFTT1200

C

C SEPARATE FOUR CASES--

FFTT1210

1. COMPLEX TRANSFORM OR REAL TRANSFORM FOR THE 4TH, 5TH, ETC.

FFTT1220

FFTT1230

1 RELEASE 2.0

FOUR

DATE = 77139

21/11/39

1 RELEASE 2.0

FOURT

DATE = 77139

21/11/39

```
DATA(I3)=DATA(J3)          FFTT172
DATA(I3+1)=DATA(J3+1)       FFTT173
DATA(J3)=TEMPI             FFTT174
125  DATA(J3+1)=TEMPI       FFTT175
130  M=NP2HF                FFTT176
140  IF(J-M)150,150,145     FFTT177
145  J=J-M                  FFTT178
     M=M/2                  FFTT179
     IF(M-NON2)150,140,140   FFTT180
150  J=J+M                  FFTT181
C
C  MAIN LOOP FOR FACTORS OF TWO.  PERFORM FOURIER TRANSFORMS OF   FFTT182
C  LENGTH FOUR, WITH ONE OF LENGTH TWO IF NEEDED.  THE TWIDDLE FACTOR FFTT183
C  W=EXP(ISIGN*2*PI*SQRT(-1)*M/(4*MMAX)).  CHECK FOR W=ISIGN*SQRT(-1) FFTT184
C  AND REPEAT FOR W=ISIGN*SQRT(-1)*CONJUGATE(W).                 FFTT185
C
NON2T=NON2+NON2            FFTT186
IPAR=NTWO/NP1               FFTT187
310  IF(IPAR-2)350,330,320   FFTT188
320  IPAR=IPAR/4             FFTT189
     GO TO 310               FFTT190
330  DO 340 I1=1,I1RNG,2     FFTT191
     DO 340 J3=I1,NON2,NP1   FFTT192
     DO 340 K1=J3,NTOT,NON2T FFTT193
     K2=K1+NON2               FFTT194
     TEMPI=DATA(K2)
     TEMPR=DATA(K2+1)
     DATA(K2)=DATA(K1)-TEMPI
     DATA(K2+1)=DATA(K1+1)-TEMPI
     DATA(K1)=DATA(K1)+TEMPI
340  DATA(K1+1)=DATA(K1+1)+TEMPI
350  MMAX=NCN2
360  IF(MMAX-NP2HF)370,600,600
370  LMAX=MAX0(NON2T,MMAX/2)
     IF(MMAX-NON2)405,405,380
380  THETA=-TWOPI*FLOAT(NON2)/FLOAT(4*MMAX)
     IF(ISIGN)400,390,390
390  THETA=-THETA
400  WR=COS(THETA)
     WI=SIN(THETA)
     WSTPR=-2.*WI*WI
     WSTPI=2.*WR*WI
405  DO 570 L=NON2,LMAX,NON2T
     M=L
     IF(MMAX-NON2)420,420,410
410  W2R=WR*WR-WI*WI
     W2I=2.*WR*WI
     W3R=W2R*WR-W2I*WI
                                FFTT195
                                FFTT196
                                FFTT197
                                FFTT198
                                FFTT199
                                FFTT200
                                FFTT201
                                FFTT202
                                FFTT203
                                FFTT204
                                FFTT205
                                FFTT206
                                FFTT207
                                FFTT208
                                FFTT209
                                FFTT210
                                FFTT211
                                FFTT212
                                FFTT213
                                FFTT214
                                FFTT215
                                FFTT216
                                FFTT217
                                FFTT218
                                FFTT219
```

1 RELEASE 2.0

FOURT

DATE = 77139

21/11/39

	W3I=W2R*WI+W2I*WR	FFTT220
420	DO 530 I1=1,I1RNG,2	FFTT221
	DO 530 J3=I1,NON2,NP1	FFTT222
	KMIN=J3+IPAR*M	FFTT223
	IF(MMAX-NON2)430,430,440	FFTT224
430	KMIN=J3	FFTT225
440	KDIF=IPAR*MMAX	FFTT226
450	KSTEP=4*KDIF	FFTT227
	DO 520 K1=KMIN,NTOT,KSTEP	FFTT228
	K2=K1+KDIF	FFTT229
	K3=K2+KDIF	FFTT230
	K4=K3+KDIF	FFTT231
	IF(MMAX-NON2)460,460,480	FFTT232
460	U1R=DATA(K1)+DATA(K2)	FFTT233
	U1I=DATA(K1+1)+DATA(K2+1)	FFTT234
	U2R=DATA(K3)+DATA(K4)	FFTT235
	U2I=DATA(K3+1)+DATA(K4+1)	FFTT236
	U3R=DATA(K1)-DATA(K2)	FFTT237
	U3I=DATA(K1+1)-DATA(K2+1)	FFTT238
	IF(ISIGN)470,475,475	FFTT239
470	U4R=DATA(K3+1)-DATA(K4+1)	FFTT240
	U4I=DATA(K4)-DATA(K3)	FFTT241
	GO TO 510	FFTT242
475	U4R=DATA(K4+1)-DATA(K3+1)	FFTT243
	U4I=DATA(K3)-DATA(K4)	FFTT244
	GO TO 510	FFTT245
480	T2R=W2R*DATA(K2)-W2I*DATA(K2+1)	FFTT246
	T2I=W2R*DATA(K2+1)+W2I*DATA(K2)	FFTT247
	T3R=WR*DATA(K3)-WI*DATA(K3+1)	FFTT248
	T3I=WR*DATA(K3+1)+WI*DATA(K3)	FFTT249
	T4R=W3R*DATA(K4)-W3I*DATA(K4+1)	FFTT250
	T4I=W3R*DATA(K4+1)+W3I*DATA(K4)	FFTT251
	U1R=DATA(K1)+T2R	FFTT252
	U1I=DATA(K1+1)+T2I	FFTT253
	U2R=T3R+T4R	FFTT254
	U2I=T3I+T4I	FFTT255
	U3R=DATA(K1)-T2R	FFTT256
	U3I=DATA(K1+1)-T2I	FFTT257
	IF(ISIGN)490,500,500	FFTT258
490	U4R=T3I-T4I	FFTT259
	U4I=T4R-T3R	FFTT260
	GO TO 510	FFTT261
500	U4R=T4I-T3I	FFTT262
	U4I=T3R-T4R	FFTT263
510	DATA(K1)=U1R+U2R	FFTT264
	DATA(K1+1)=U1I+U2I	FFTT265
	DATA(K2)=U3R+U4R	FFTT266
	DATA(K2+1)=U3I+U4I	FFTT267

1 RELEASE 2.0

FOURT

DATE = 77139

21/11/39

```
DATA(K3)=U1R-U2R          FFTT268
DATA(K3+1)=U1I-U2I          FFTT269
DATA(K4)=U3R-U4R          FFTT270
520  DATA(K4+1)=U3I-U4I          FFTT271
      KMIN=4*(KMIN-J3)+J3          FFTT272
      KDIF=KSTEP          FFTT273
      IF(KDIF-NP2)450,530,530          FFTT274
530  CONTINUE          FFTT275
      M=MMAX-M          FFTT276
      IF(ISIGN)540,550,550          FFTT277
540  TEMPR=WR          FFTT278
      WR=-WI          FFTT279
      WI=-TEMPR          FFTT280
      GO TO 560          FFTT281
550  TEMPR=WR          FFTT282
      WR=WI          FFTT283
      WI=TEMPR          FFTT284
560  IF(M-LMAX)565,565,410          FFTT285
565  TEMPR=WR          FFTT286
      WR=WR*WSTPR-WI*WSTPI+WR          FFTT287
570  WI=WI*WSTPR+TEMPR*WSTPI+WI          FFTT288
      IPAR=3-IPAR          FFTT289
      MMAX=MMAX+MMAX          FFTT290
      GO TO 360          FFTT291
C
C      MAIN LOOP FOR FACTORS NOT EQUAL TO TWO.  APPLY THE TWIDDLE FACTOR
C      W=EXP(ISIGN*2*PI*SQRT(-1)*(J2-1)*(J1-J2)/(NP2*IFP1)), THEN
C      PERFORM A FOURIER TRANSFORM OF LENGTH IFACT(IF), MAKING USE OF
C      CONJUGATE SYMMETRIES.
C
600  IF(NTWO-NP2)605,700,700          FFTT292
605  IFP1=NON2          FFTT293
      IF=1          FFTT294
      NP1HF=NP1/2          FFTT295
610  IFP2=IFP1/IFACT(IF)          FFTT296
      J1RNG=NP2          FFTT297
      IF(ICASE-3)612,611,612          FFTT298
611  J1RNG=(NP2+IFP1)/2          FFTT299
      J2STP=NP2/IFACT(IF)          FFTT300
      J1RG2=(J2STP+IFP2)/2          FFTT301
612  J2MIN=1+IFP2          FFTT302
      IF(IFP1-NP2)615,640,640          FFTT303
615  DO 635 J2=J2MIN,IFP1,IFP2          FFTT304
      THETA=-TWOPI*FLOAT(J2-1)/FLOAT(NP2)
      IF(ISIGN)625,620,620          FFTT305
620  THETA=-THETA          FFTT306
625  SINH=SIN(THETA/2.)          FFTT307
      WSTPR=-2.*SINH*SINH          FFTT308
                                         FFTT309
                                         FFTT310
                                         FFTT311
                                         FFTT312
                                         FFTT313
                                         FFTT314
                                         FFTT315
```

RELEASE 2.0

FOURT

DATE = 77139

21/11/39

```
WSTPI=SIN(THETA)          FFFT3160
WR=WSTPR+1.               FFFT3170
WI=WSTPI                 FFFT3180
J1MIN=J2+IFP1             FFFT3190
DO 635 J1=J1MIN,J1RNG,IFP1 FFFT3200
I1MAX=J1+I1RNG-2          FFFT3210
DO 630 I1=J1,I1MAX,2      FFFT3220
DO 630 I3=I1,NTOT,NP2     FFFT3230
J3MAX=I3+IFP2-NP1          FFFT3240
DO 630 J3=I3,J3MAX,NP1     FFFT3250
TEMPIR=DATA(J3)            FFFT3260
DATA(J3)=DATA(J3)*WR-DATA(J3+1)*WI
630 DATA(J3+1)=TEMPIR*WI+DATA(J3+1)*WR
TEMPIR=WR
WR=WR*WSTPR-WI*WSTPI+WR
635 WI=TEMPIR*WSTPI+WI*WSTPR+WI
640 THETA=-TWOPI/FLOAT(IFACT(IF))
IF(ISIGN)650,645,645
645 THETA=-THETA
650 SINH=SIN(THETA/2.)
WSTPR=-2.*SINH*SINH
WSTPI=SIN(THETA)
KSTEP=2*N/IFACT(IF)
KRANG=KSTEP*(IFACT(IF)/2)+1
DO 698 I1=1,I1RNG,2
DO 698 I3=I1,NTOT,NP2
DO 690 KMIN=1,KRANG,KSTEP
J1MAX=I3+J1RNG-IFP1
DO 680 J1=I3,J1MAX,IFP1
J3MAX=J1+IFP2-NP1
DO 680 J3=J1,J3MAX,NP1
J2MAX=J3+IFP1-IFP2
K=KMIN+(J3-J1+(J1-I3)/IFACT(IF))/NP1HF
IF(KMIN-1)655,655,665
655 SUMR=0.
SUMI=0.
DO 660 J2=J3,J2MAX,IFP2
SUMR=SUMR+DATA(J2)
660 SUMI=SUMI+DATA(J2+1)
WORK(K)=SUMR
WORK(K+1)=SUMI
GO TO 680
665 KCONJ=K+2*(N-KMIN+1)
J2=J2MAX
SUMR=DATA(J2)
SUMI=DATA(J2+1)
OLDSR=0.
OLDSI=0.
```

1 RELEASE 2.0

FOURT

DATE = 77139

21/11/39

J2=J2-IFP2 FFTT364  
670 TEMPR=SUMR FFTT365  
TEMPI=SUMI FFTT366  
SUMR=TWOWR\*SUMR-OLDSR+DATA(J2) FFTT367  
SUMI=TWOWR\*SUMI-OLDSI+DATA(J2+1) FFTT368  
OLDSR=TEMPR FFTT369  
OLDSI=TEMPI FFTT370  
J2=J2-IFP2 FFTT371  
IF(J2-J3)675,675,670 FFTT372  
675 TEMPR=WR\*SUMR-OLDSR+DATA(J2) FFTT373  
TEMPI=WI\*SUMI FFTT374  
WORK(K)=TEMPR-TEMPI FFTT375  
WORK(KCONJ)=TEMPR+TEMPI FFTT376  
TEMPR=WR\*SUMI-OLDSI+DATA(J2+1) FFTT377  
TEMPI=WI\*SUMR FFTT378  
WORK(K+1)=TEMPR+TEMPI FFTT379  
WORK(KCONJ+1)=TEMPR-TEMPI FFTT380  
680 CONTINUE FFTT381  
IF(KMIN-1)685,685,686 FFTT382  
685 WR=WSTPR+1. FFTT383  
WI=WSTPI FFTT384  
GO TO 690 FFTT385  
686 TEMPR=WR FFTT386  
WR=WR\*WSTPR-WI\*WSTPI+WR FFTT387  
WI=TEMPR\*WSTPI+WI\*WSTPR+WI FFTT388  
690 TWOWR=WR+WR FFTT389  
IF(ICASE-3)692,691,692 FFTT390  
691 IF(IFP1-NP2)695,692,692 FFTT391  
692 K=1 FFTT392  
I2MAX=I3+NP2-NP1 FFTT393  
DO 693 I2=I3,I2MAX,NP1 FFTT394  
DATA(I2)=WORK(K) FFTT395  
DATA(I2+1)=WORK(K+1) FFTT396  
693 K=K+2 FFTT397  
GO TO 698 FFTT398  
C FFTT399  
C COMPLETE A REAL TRANSFORM IN THE 1ST DIMENSION, N ODD, BY CON- FFTT400  
C JUGATE SYMMETRIES AT EACH STAGE. FFTT401  
C FFTT402  
695 J3MAX=I3+IFP2-NP1 FFTT403  
DO 697 J3=I3,J3MAX,NP1 FFTT404  
J2MAX=J3+NP2-J2STP FFTT405  
DO 697 J2=J3,J2MAX,J2STP FFTT406  
J1MAX=J2+J1RG2-IFP2 FFTT407  
J1CNJ=J3+J2MAX+J2STP-J2 FFTT408  
DO 697 J1=J2,J1MAX,IFP2 FFTT409  
K=1+J1-I3 FFTT410  
DATA(J1)=WORK(K) FFTT411

RELEASE 2.0

FOURT

DATE = 77139

21/11/39

```
DATA(J1+1)=WORK(K+1)          FFTT4120
IF(J1-J2)697,697,696          FFTT4130
696 DATA(J1CNJ)=WORK(K)        FFTT4140
DATA(J1CNJ+1)=-WORK(K+1)      FFTT4150
J1CNJ=J1CNJ-IFP2             FFTT4160
697 CONTINUE                  FFTT4170
698 IF=IF+1                    FFTT4180
IFP1=IFP2                    FFTT4190
IF(IFP1-NP1)700,700,610      FFTT4200
C
C COMPLETE A REAL TRANSFORM IN THE 1ST DIMENSION, N EVEN, BY CON-
C JUGATE SYMMETRIES.          FFTT4210
C
700 GO TO (900,800,900,701),ICASE FFTT4220
701 NHALF=N                    FFTT4230
N=N+N
THETA=-TWOPI/FLOAT(N)        FFTT4240
IF(ISIGN)703,702,702          FFTT4250
702 THETA=-THETA             FFTT4260
703 SINTH=SIN(THETA/2.)        FFTT4270
WSTPR=-2.*SINTH*SINTH        FFTT4280
WSTPI=SIN(THETA)             FFTT4290
WR=WSTPR+1.                  FFTT4300
WI=WSTPI                      FFTT4310
IMIN=3                        FFTT4320
JMIN=2*NHALF-1               FFTT4330
GO TO 725                      FFTT4340
710 J=JMIN                      FFTT4350
DO 720 I=IMIN,NTOT,NP2        FFTT4360
SUMR=(DATA(I)+DATA(J))/2.      FFTT4370
SUMI=(DATA(I+1)+DATA(J+1))/2. FFTT4380
DIFR=(DATA(I)-DATA(J))/2.      FFTT4390
DIFI=(DATA(I+1)-DATA(J+1))/2. FFTT4400
TEMPR=WR*SUMI+WI*DIFR        FFTT4410
TEMPI=WI*SUMI-WR*DIFR        FFTT4420
DATA(I)=SUMR+TEMPR            FFTT4430
DATA(I+1)=DIFI+TEMPI          FFTT4440
DATA(J)=SUMR-TEMPR            FFTT4450
DATA(J+1)=-DIFI+TEMPI          FFTT4460
720 J=J+NP2                      FFTT4470
IMIN=IMIN+2                    FFTT4480
JMIN=JMIN-2                    FFTT4490
TEMPR=WR                      FFTT4500
WR=WR*WSTPR-WI*WSTPI+WR       FFTT4510
WI=TEMPR*WSTPI+WI*WSTPR+WI   FFTT4520
725 IF(IMIN-JMIN)710,730,740   FFTT4530
730 IF(ISIGN)731,740,740       FFTT4540
731 DO 735 I=IMIN,NTOT,NP2   FFTT4550
                                FFTT4560
                                FFTT4570
                                FFTT4580
                                FFTT4590
```

1	PELEASE 2.0	FOURT	DATE = 77139	21/11/39
735	DATA(I+1)=-DATA(I+1)			FFTT460C
740	NP2=NP2+NP2			FFTT461C
	NTOT=NTOT+NTOT			FFTT462C
	J=NTOT+1			FFTT463C
745	IMAX=NTOT/2+1			FFTT464C
	IMIN=IMAX-2*NHALF			FFTT465C
	I=IMIN			FFTT466C
	GO TO 755			FFTT467C
750	DATA(J)=DATA(I)			FFTT468C
	DATA(J+1)=-DATA(I+1)			FFTT469C
755	I=I+2			FFTT470C
	J=J-2			FFTT471C
	IF(I-IMAX)750,760,760			FFTT472C
760	DATA(J)=DATA(IMIN)-DATA(IMIN+1)			FFTT473C
	DATA(J+1)=0.			FFTT474C
	IF(I-J)770,780,780			FFTT475C
765	DATA(J)=DATA(I)			FFTT476C
	DATA(J+1)=DATA(I+1)			FFTT477C
770	I=I-2			FFTT478C
	J=J-2			FFTT479C
	IF(I-IMIN)775,775,765			FFTT480C
775	DATA(J)=DATA(IMIN)+DATA(IMIN+1)			FFTT481C
	DATA(J+1)=0.			FFTT482C
	IMAX=IMIN			FFTT483C
	GO TO 745			FFTT484C
780	DATA(1)=DATA(1)+DATA(2)			FFTT485C
	DATA(2)=0.			FFTT486C
	GO TO 900			FFTT487C
C				FFTT488C
C	COMPLETE A REAL TRANSFORM FOR THE 2ND OR 3RD DIMENSION BY			FFTT489C
C	CONJUGATE SYMMETRIES.			FFTT490C
C				FFTT491C
800	IF(I1RNG-NP1)805,900,900			FFTT492C
805	DO 860 I3=1,NTOT,NP2			FFTT493C
	I2MAX=I3+NP2-NP1			FFTT494C
	DO 860 I2=I3,I2MAX,NP1			FFTT495C
	IMIN=I2+I1RNG			FFTT496C
	IMAX=I2+NP1-2			FFTT497C
	JMAX=2*I3+NP1-IMIN			FFTT498C
	IF(I2-I3)820,820,810			FFTT499C
810	JMAX=JMAX+NP2			FFTT500C
820	IF(IDIM-2)850,850,830			FFTT501C
830	J=JMAX+NP0			FFTT502C
	DO 840 I=IMIN,IMAX,2			FFTT503C
	DATA(I)=DATA(J)			FFTT504C
	DATA(I+1)=-DATA(J+1)			FFTT505C
840	J=J-2			FFTT506C
850	J=JMAX			FFTT507C

1 RELEASE 2.0

FOURT

DATE = 77139

21/11/39

```
DO 860 I=IMIN,IMAX,NPO          FFTT5080
DATA(I)=DATA(J)                FFTT5090
DATA(I+1)=-DATA(J+1)          FFTT5100
860  J=J-NPO                  FFTT5110
C                                     FFTT5120
C                                     FFTT5130
C                                     FFTT5140
900  NPO=NP1                  FFTT5150
NP1=NP2                      FFTT5160
910  NPREV=N                  FFTT5170
920  RETURN                   FFTT5180
      END                      FFTT5190
```

\*\*\* WAVE PROPAGATION IN COMPOSITE PLATE \*\*\*  
GRAPHITE FIBER (55%)-EPOXY MATRIX COMPOSITE

LAYUP ANGLE= 15 DEGREE  
C(1,1)= 0.24560D+08 PSI  
C(2,2)= 0.11700D+07 PSI

C(1,2)= 0.40000D+06 PSI  
C(6,6)= 0.35520D+06 PSI

TOTAL THICKNESS OF COMPOSITE PLATE ; DELTA= 1.00000 CM  
DENSITY OF COMPOSITE ; RHO= 1.44000 GR/CM\*\*3  
PLATE IS MADE OF 8 IDENTICAL LAYERS  
LAYER THICKNESS ; 2B= 0.12500 CM

TOTAL SPACE STEPS; NX= 64 WITH 8 STEPS FOR CONTACT RADIUS  
TOTAL TIME STEPS; NT= 32 WITH 24 STEPS FOR CONTACT TIME

CONTACT RADIUS ; A= 0.20000D-01 M  
SPACE STEP ; DX= 0.25000D-02 M  
CONTACT TIME ; TAU0= 0.60000D-05 SECOND  
TIME STEP ; DT= 0.25000D-06 SECOND

REPRODUCTION OF IMPACT FUNCTION \*\*\*  
MAXIMUM VALUE = -0.10003E+01 \*\*\*

\*\*\*\*\* SIGMA 1 MAXIMUM VALUE = -0.10067E+01 \*\*\*\*\*

\*\*\*  
SIGMA<sup>3</sup> MAXIMUM VALUE = -0.96697E+00 \*\*\*

\*\*\*\*\* SIGMA 5 MAXIMUM VALUE =-0.98567E+00 \*\*\*\*

\*\*\*\*\*  
SIGMA 7 MAXIMUM VALUE = -0.53190E+00  
\*\*\*\*\*

U 4 \*\*\*\*\* MAXIMUM VALUE = 3.86667E-02 \*\*\*

\*\*\*\*\*  
V 4 MAXIMUM VALUE = 0.18017E+00 \*\*\*\*

```
***  
SIGMA 4 MAXIMUM VALUE = -0.94195E+00 ***
```

TAU<sub>4</sub> MAXIMUM VALUE = -0.10045E+00 \*\*\*

\*\*\*\*\* SIGMA1 4 MAXIMUM VALUE =-0.34042E+00 \*\*\*\*\*